Functional renormalization group and its application in nonperturbative QCD

Wei-jie Fu

Dalian University of Technology

强子质量的非微扰起源

CCAST, Beijing, April 17-28, 2023

Based on :

WF, Xiaofeng Luo, Jan M. Pawlowski, Fabian Rennecke, Shi Yin, in preparation;

WF, Jan M. Pawlowski, Fabian Rennecke, Rui Wen, Shi Yin, in preparation;

WF, Chuang Huang, Jan M. Pawlowski, Yang-yang Tan, *SciPost Phys.* 14 (2023) 069, arXiv:2209.13120;

WF, *CTP* 74 (2022) 097304, arXiv:2205.00468

QCD phase structure

Skewness and kurtosis of net-proton distributions:

QCD phase diagram

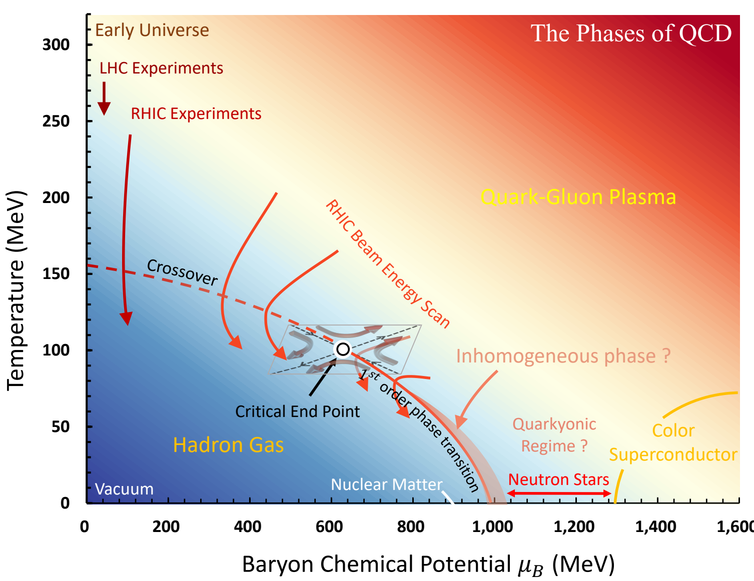

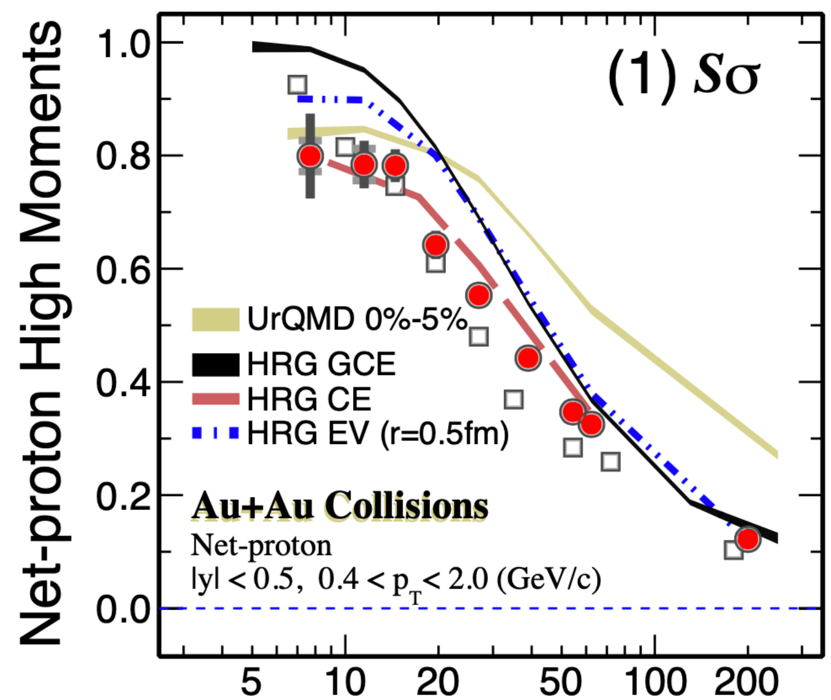

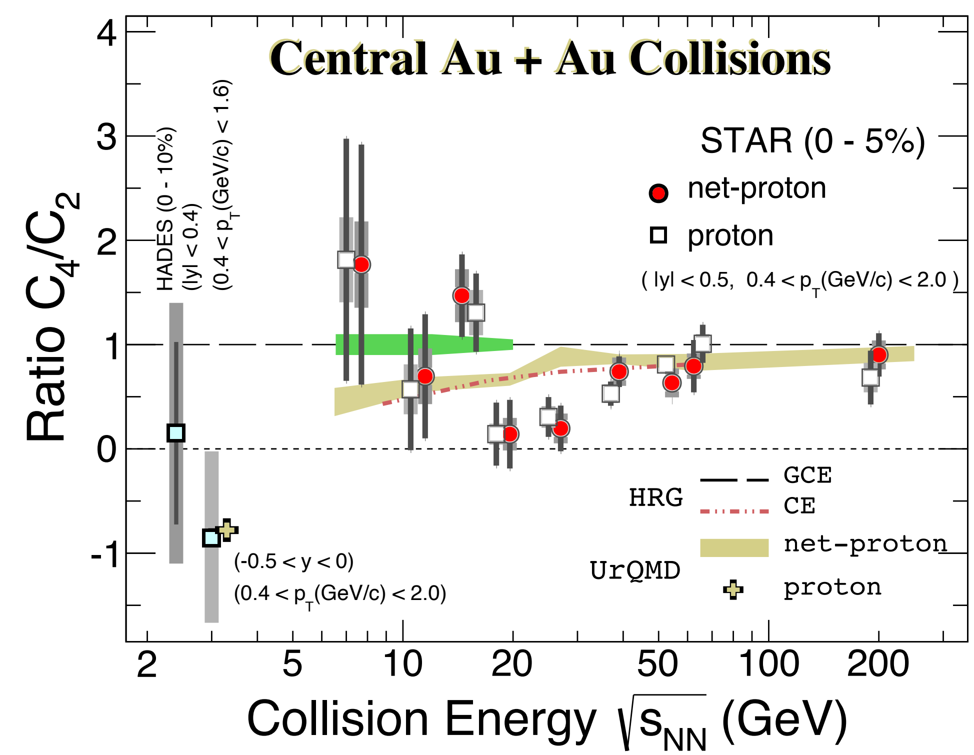

J. Adam *et al.* (STAR), *PRL* 126 (2021), 092301;
M. Abdallah *et al.* (STAR), *PRC* 104 (2021), 024902;
M. Abdallah *et al.* (STAR), *PRL* 128 (2022) 20, 202303

- The non-monotonicity of the kurtosis is observed with 3.1σ significance.
- Is there a "peak" structure in the regime of low colliding energy?

QCD phase structure

Skewness and kurtosis of net-proton distributions:

QCD phase diagram

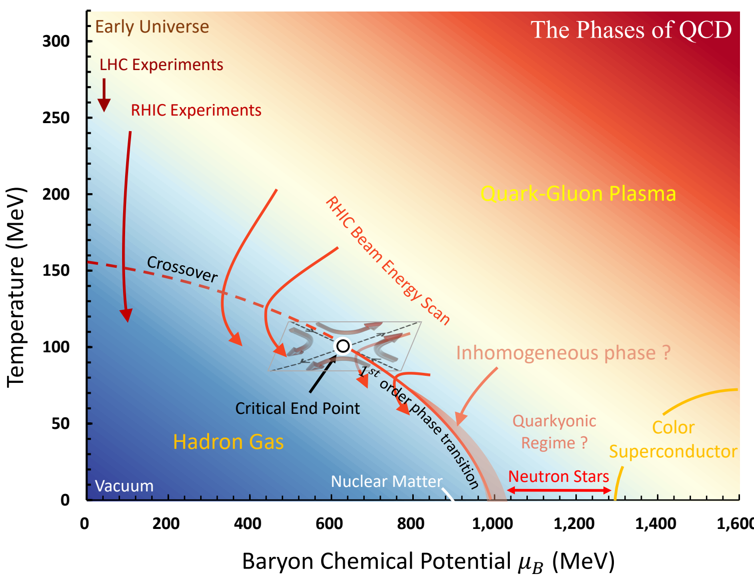

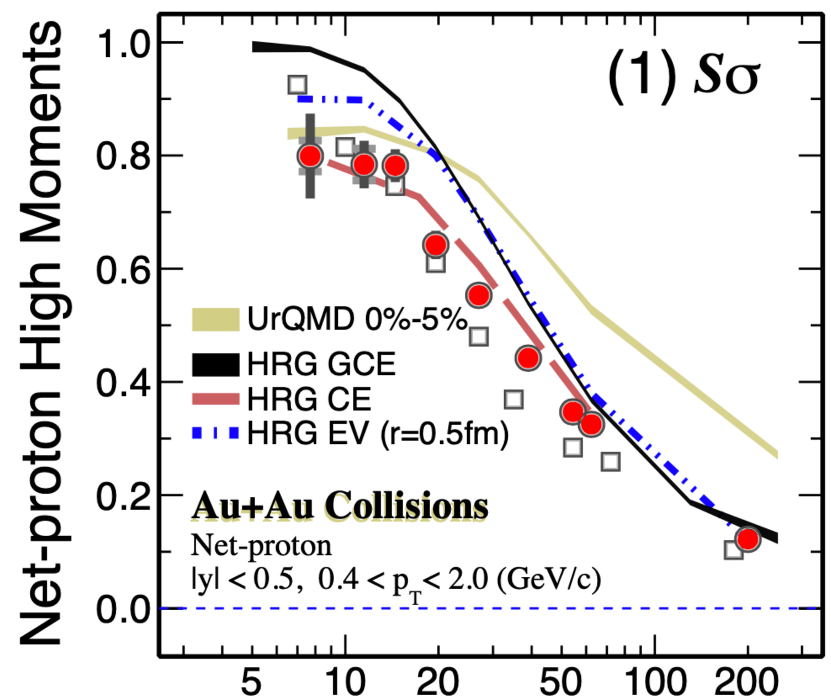

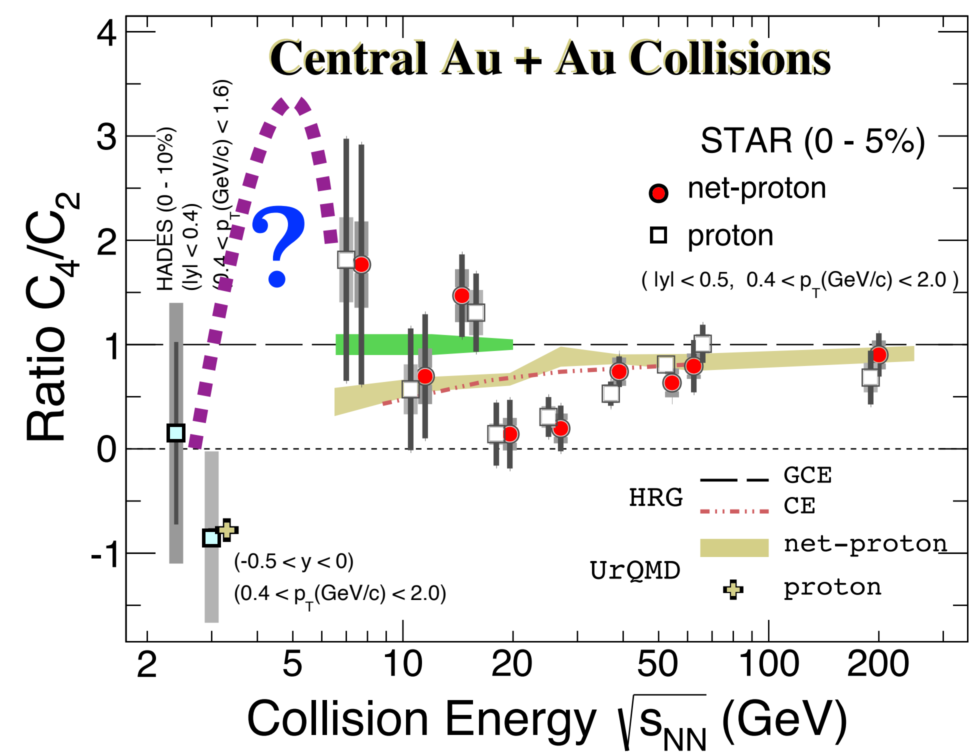

J. Adam *et al.* (STAR), *PRL* 126 (2021), 092301;
M. Abdallah *et al.* (STAR), *PRC* 104 (2021), 024902;
M. Abdallah *et al.* (STAR), *PRL* 128 (2022) 20, 202303

- The non-monotonicity of the kurtosis is observed with 3.1σ significance.
- Is there a "peak" structure in the regime of low colliding energy?

Outline

- Introduction
- Brief review about (f)RG
- QCD in vacuum
- QCD phase structure
- Baryon number fluctuations
- Summary

Functional renormalization group

Functional integral with an IR regulator

$$Z_k[J] = \int (\mathscr{D}\hat{\Phi}) \exp\left\{ -S[\hat{\Phi}] - \Delta S_k[\hat{\Phi}] + J^a \hat{\Phi}_a \right\}$$

$$W_k[J] = \ln Z_k[J]$$

regulator:

$$\Delta S_k[\varphi] = \frac{1}{2}\int \frac{d^4 q}{(2\pi)^4} \varphi(-q) R_k(q) \varphi(q)$$

flow of the Schwinger function:

$$\partial_t W_k[J] = -\frac{1}{2}\mathrm{STr}\left[\left(\partial_t R_k\right) G_k\right] - \frac{1}{2}\Phi_a \partial_t R_k^{ab} \Phi_b$$

Legendre transformation:

$$\Gamma_k[\Phi] = -W_k[J] + J^a \Phi_a - \Delta S_k[\Phi]$$

flow of the effective action:

$$\partial_t \Gamma_k[\Phi] = \frac{1}{2}\mathrm{STr}\left[\left(\partial_t R_k\right) G_k\right] = \frac{1}{2}$$

Wetterich formula

C. Wetterich, *PLB*, 301 (1993) 90

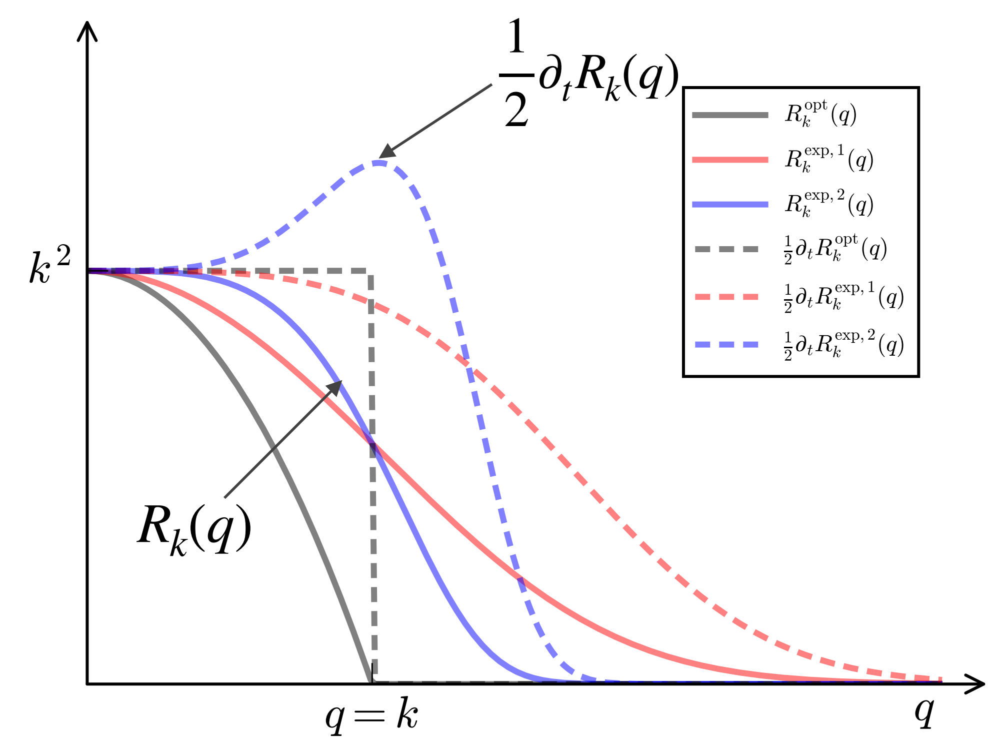

$$G_{k,ab} = \gamma^c{}_a \left(\Gamma_k^{(2)}[\Phi] + \Delta S_k^{(2)}[\Phi]\right)^{-1}_{cb},$$

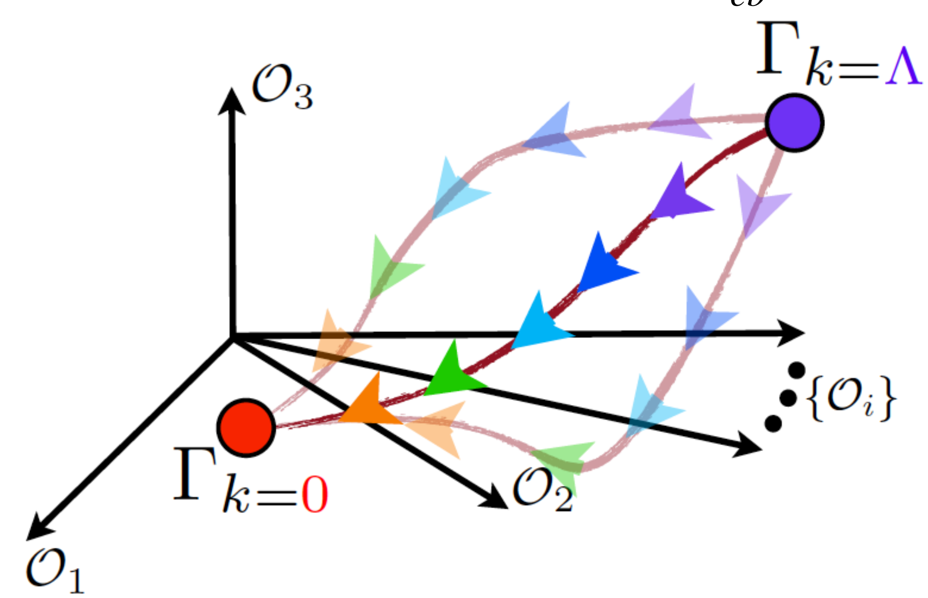

Review: WF, *CTP* 74 (2022) 097304,
arXiv: 2205.00468 [hep-ph]

Chiral symmetry breaking in RG

- β **function of 4-quark coupling:**

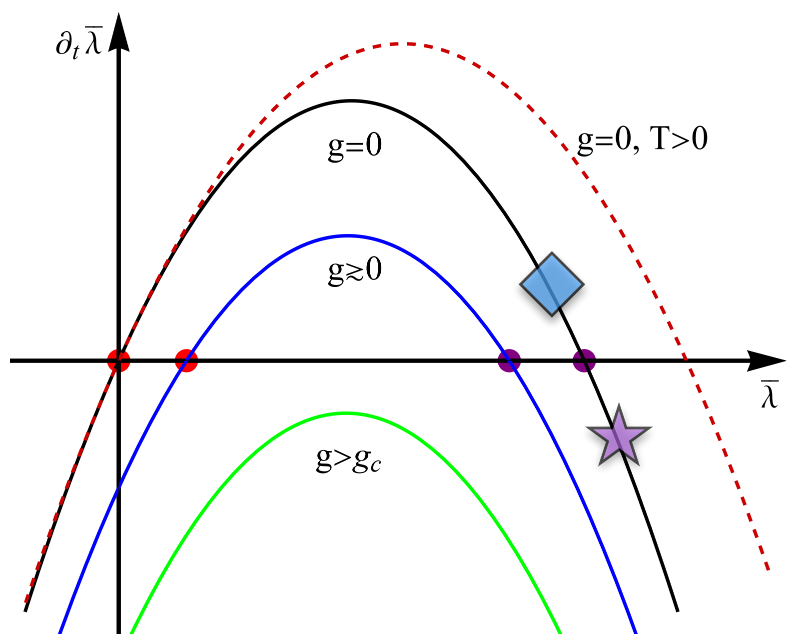

Braun, Gies, *JHEP* 06 (2006) 024.

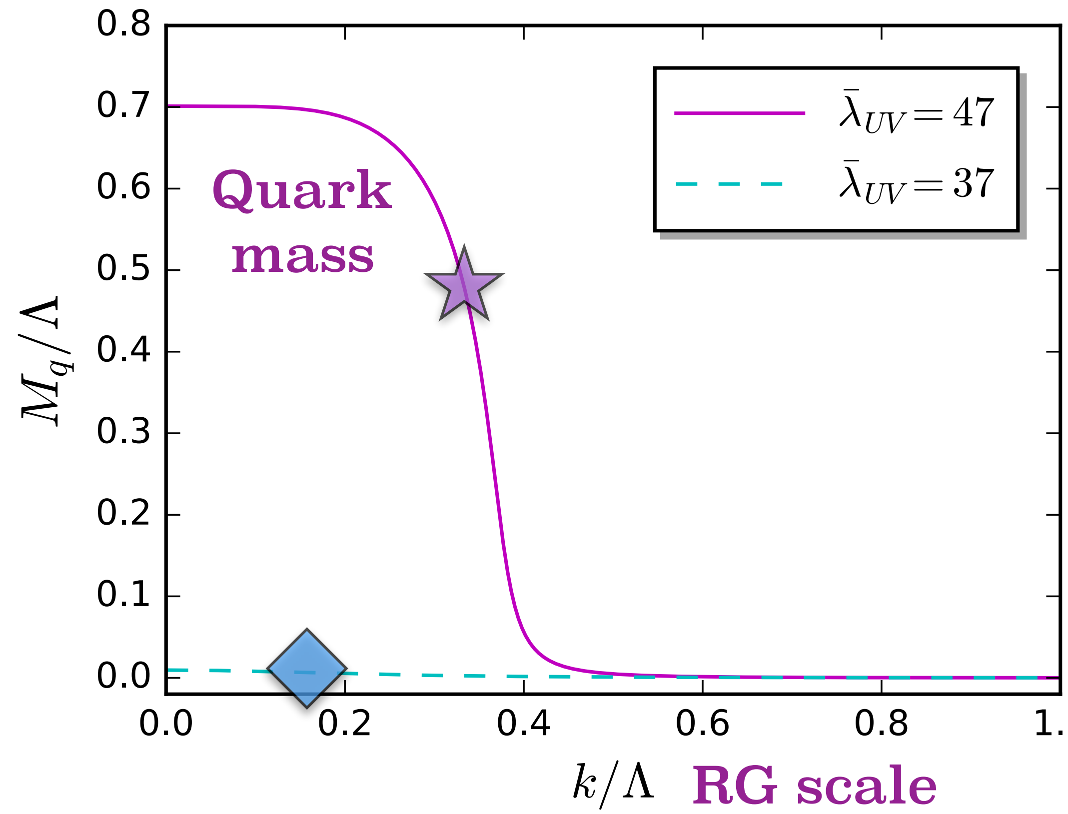

WF, Huang, Pawlowski, Tan, *SciPost Phys.* 14 (2023) 069, arXiv:2209.13120

$$\partial_t \bar{\lambda} = (d-2)\bar{\lambda} - a\bar{\lambda}^2 - b\bar{\lambda}g^2 - cg^4 \,,$$

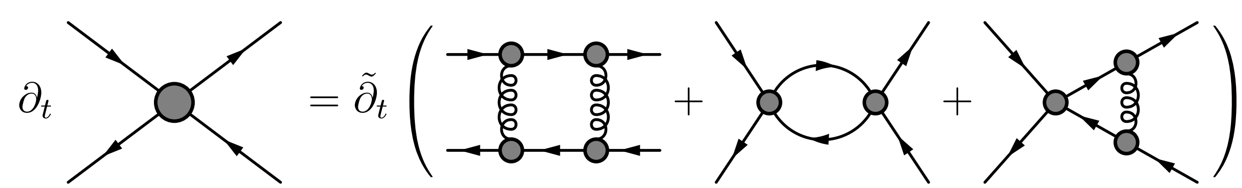

Mass production in RG

- **flow in the plane of the mass and coupling:**

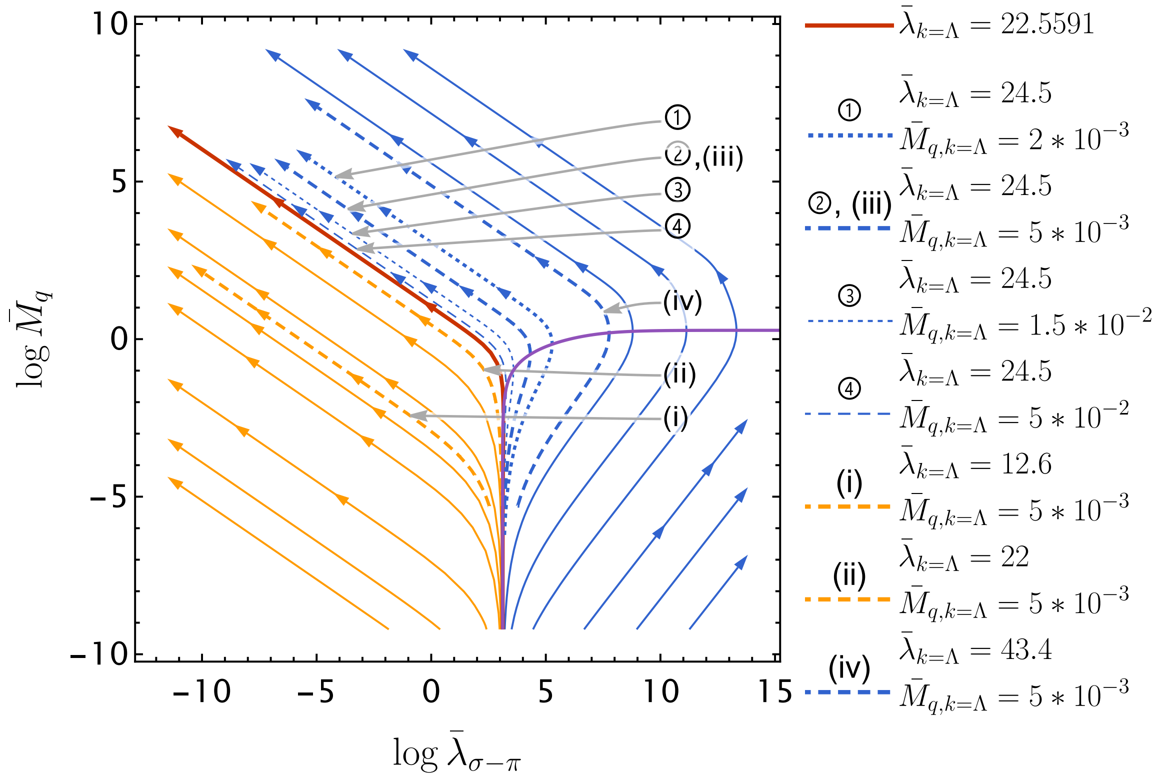

- **couplings of different channels vs RG scale:**

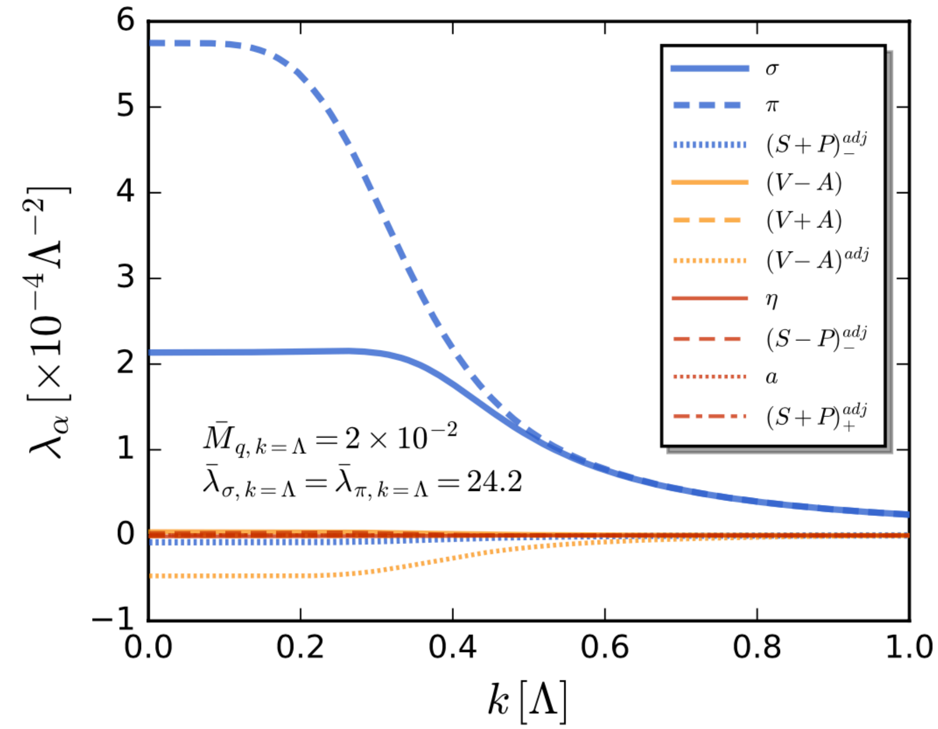

WF, Huang, Pawlowski, Tan, *SciPost Phys.* 14 (2023) 069, arXiv:2209.13120

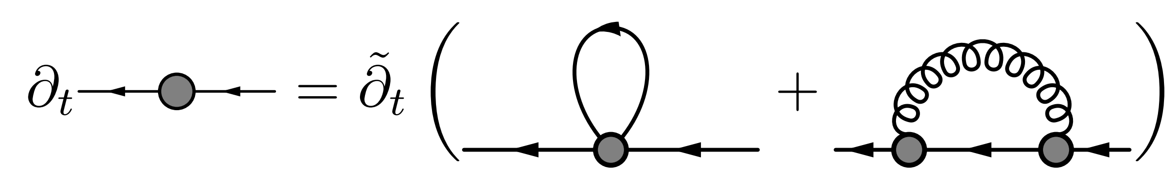

- **quark mass and couplings vs RG scale:**

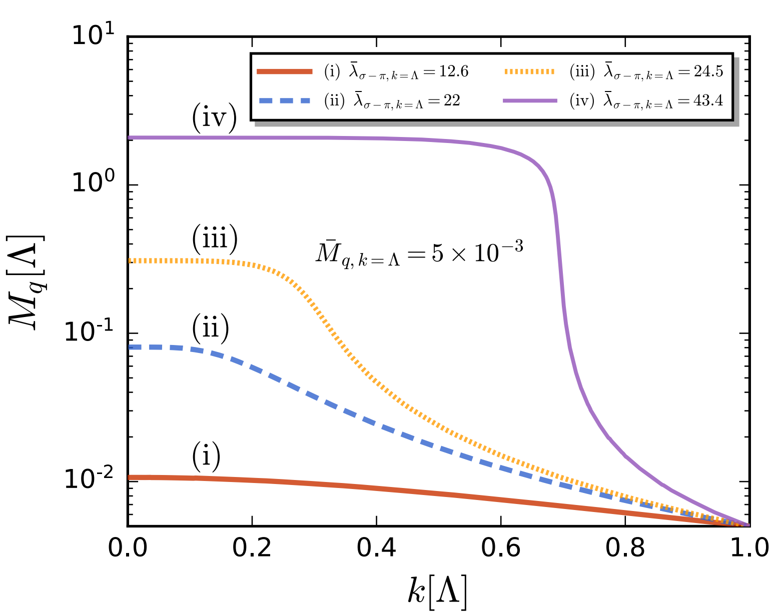

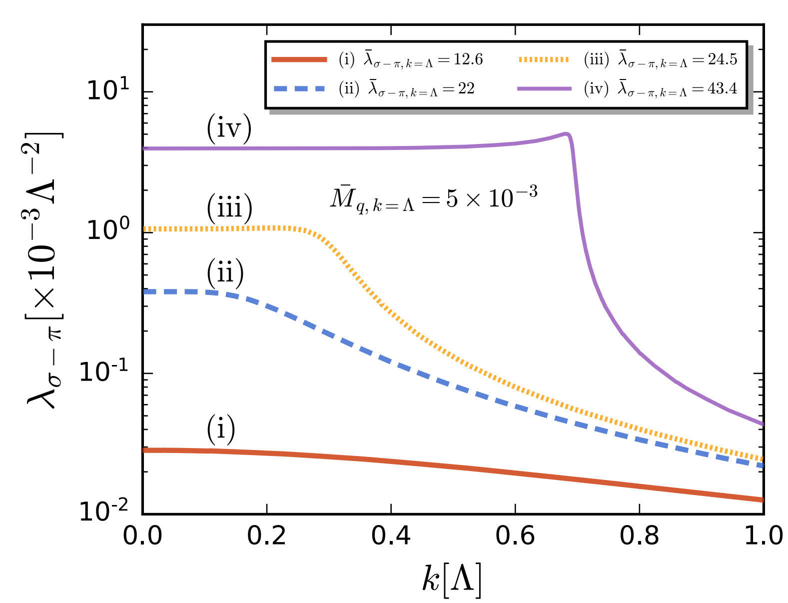

- **Understanding quark mass production from the viewpoint of phase transition.**
- **Analogue of gap equation in terms of RG flow.**

Bound states in RG

- **Bound states encoded in n-point correlation functions:**

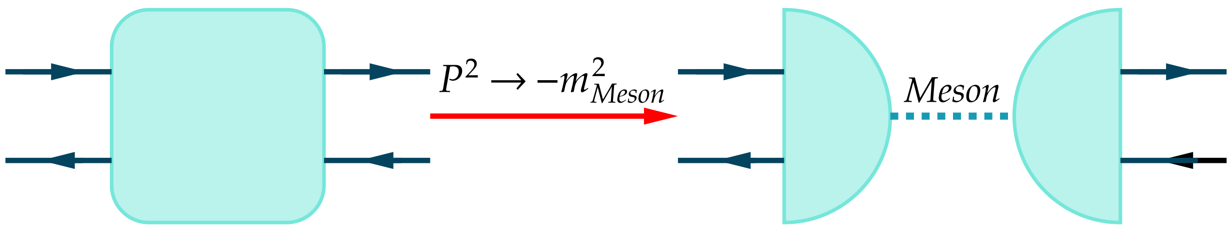

$$\partial_t \lambda_{\pi,k}(P^2) = C_k(P^2)\lambda^2_{\pi,k}(P^2) + A_k(P^2),$$

$$\lambda_{\pi,k=0}(P^2) = \frac{\lambda_{\pi,k=\Lambda}}{1 - \lambda_{\pi,k=\Lambda}\int_\Lambda^0 C_k(P^2)\frac{dk}{k}},$$

- **Flow equation of 4-quark interaction:**

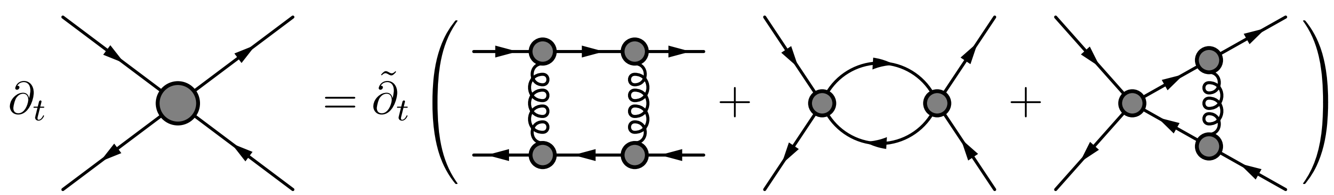

Note: playing the same role as the Bethe-Salpeter equation.

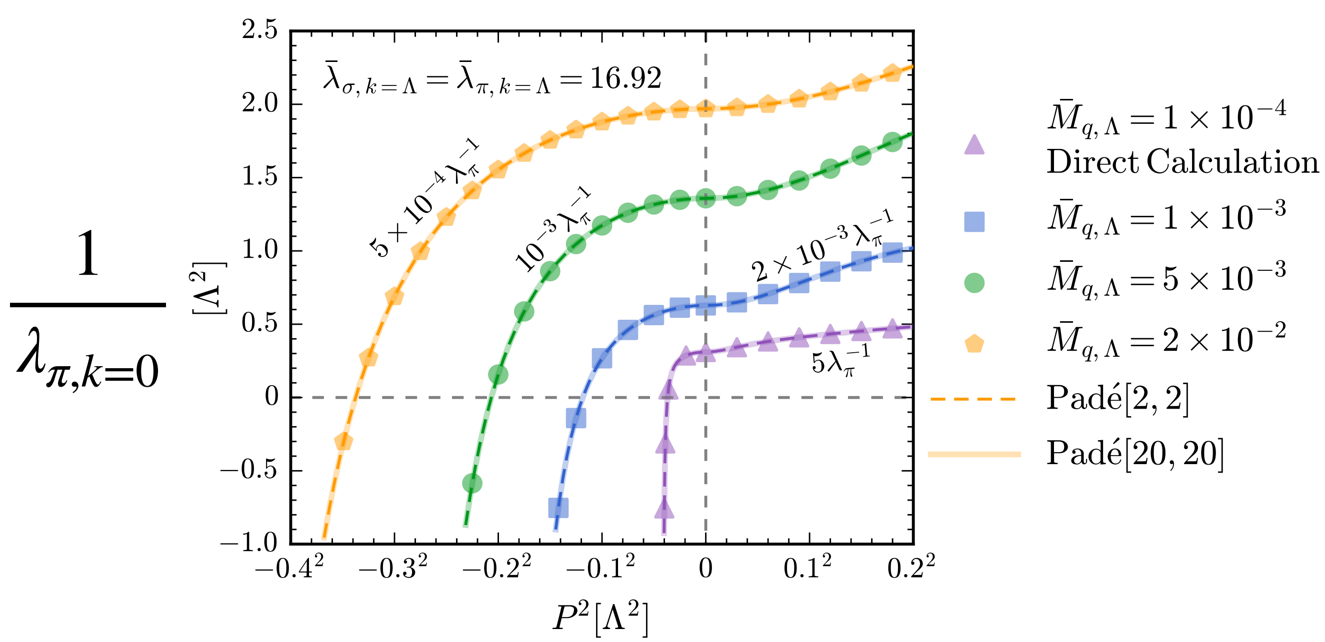

Gell-Mann--Oakes--Renner relation

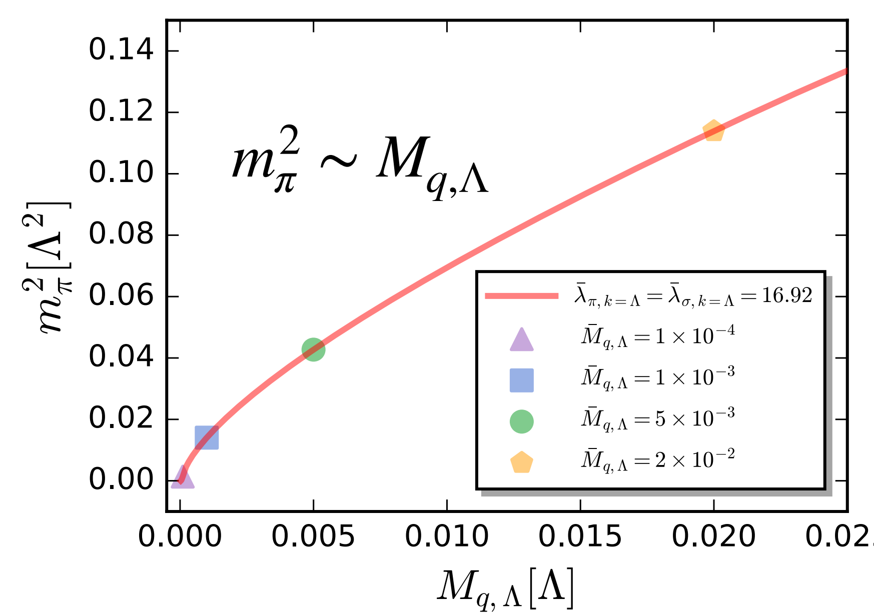

WF, Huang, Pawlowski, Tan, *SciPost Phys.* 14 (2023) 069, arXiv:2209.13120

QCD within fRG

Glue sector:

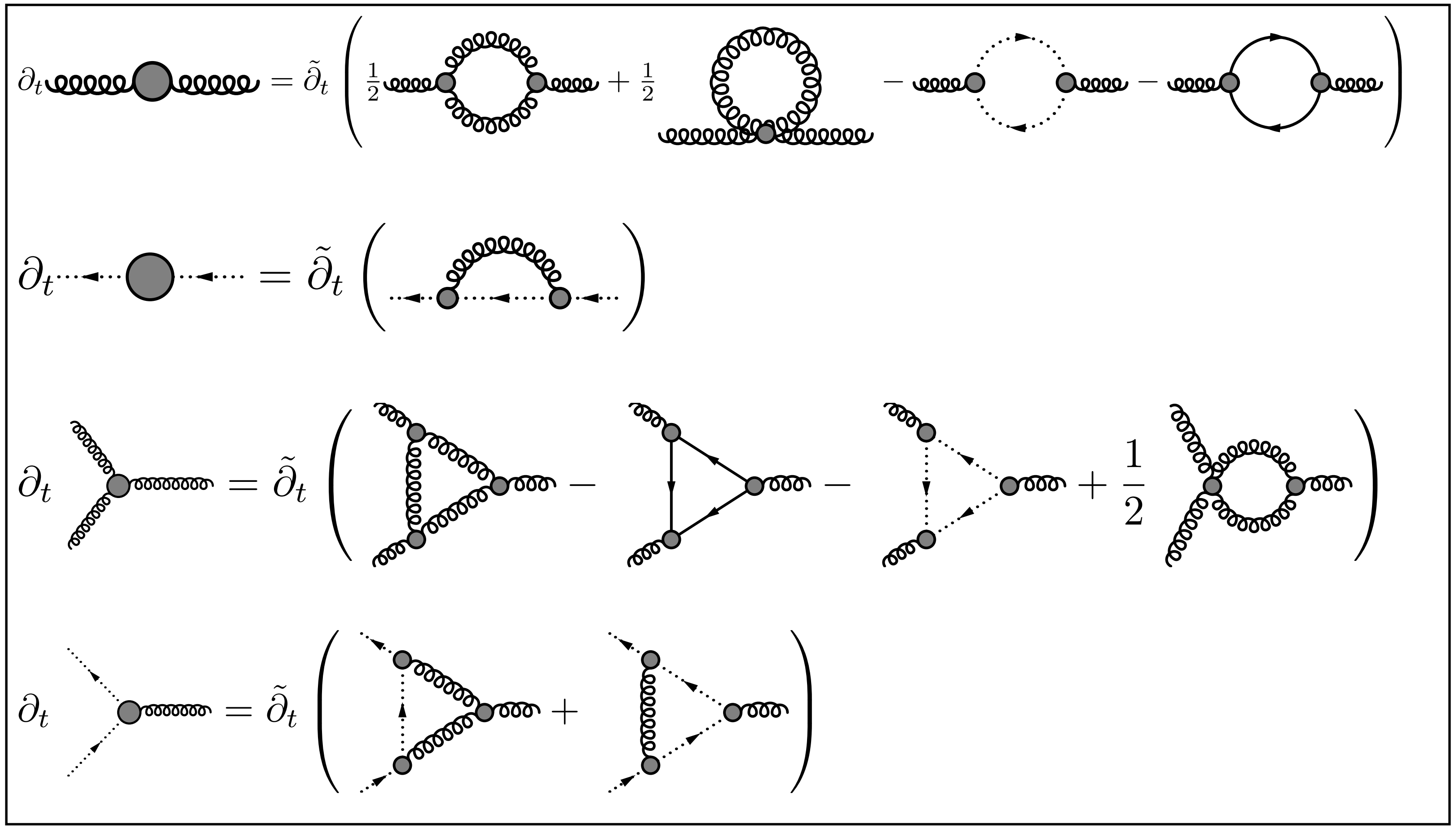

Matter sector:

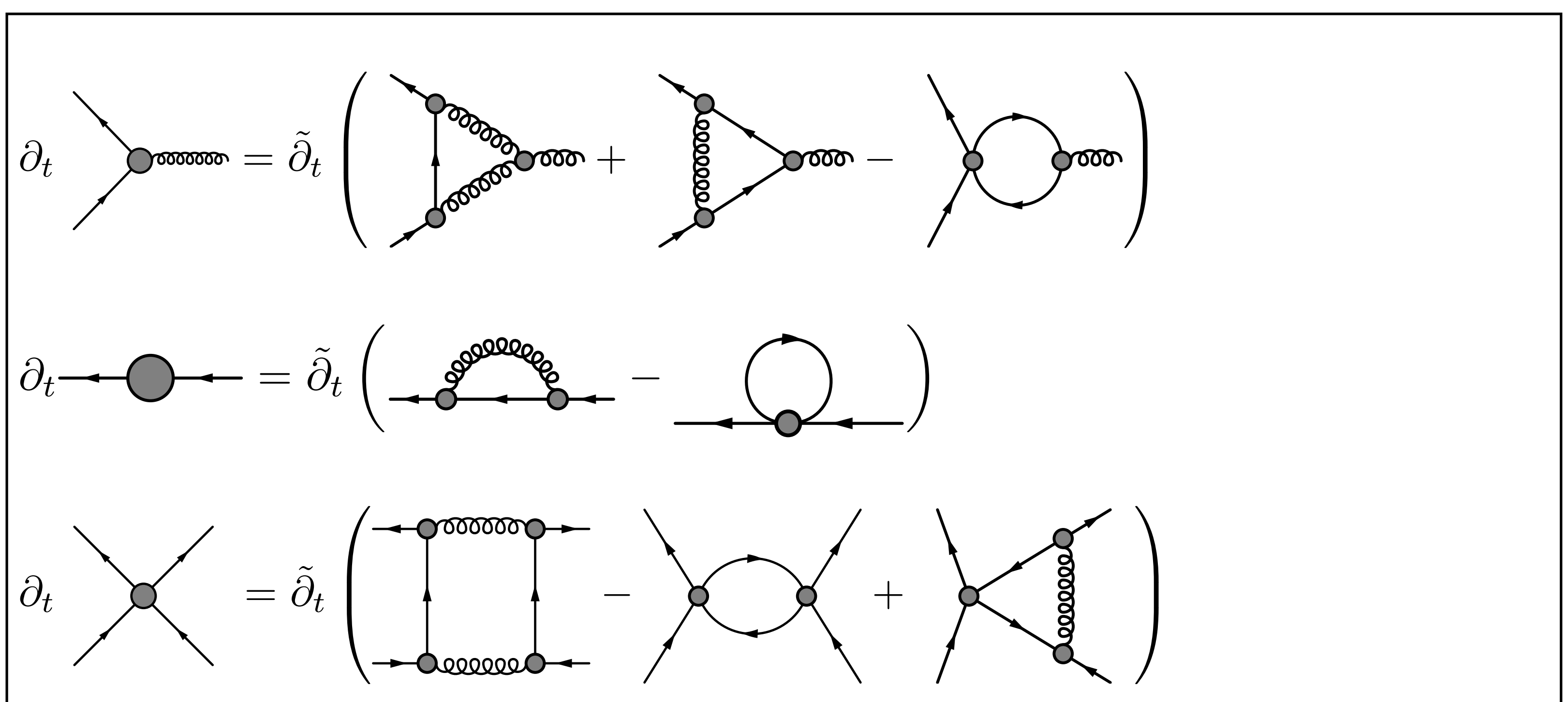

WF, Huang, Pawlowski, Tan, in preparation

QCD within fRG in vacuum

Gluon dressing:

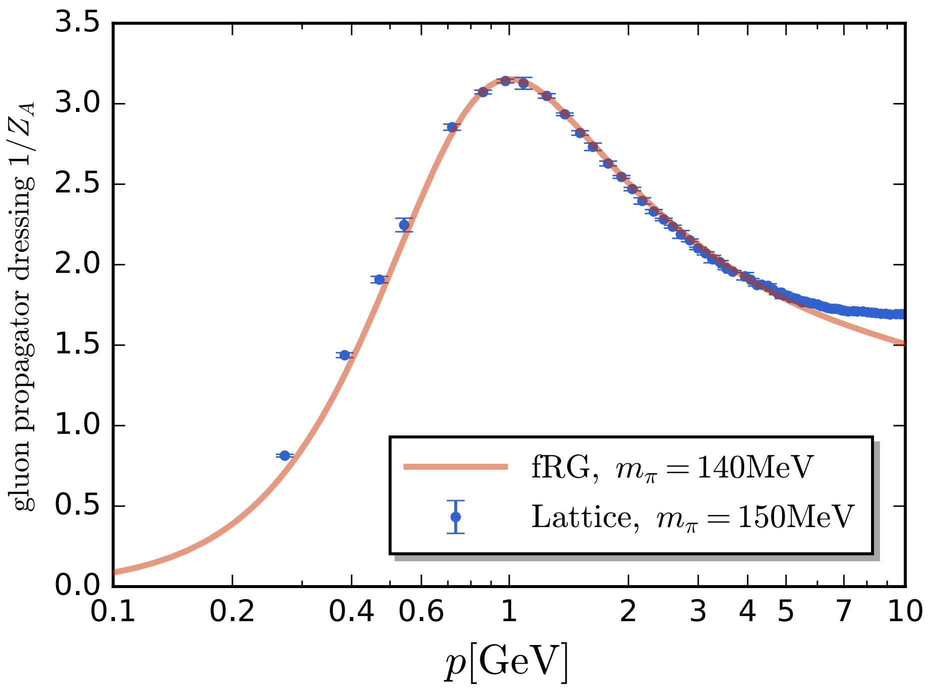

Gluon propagator:

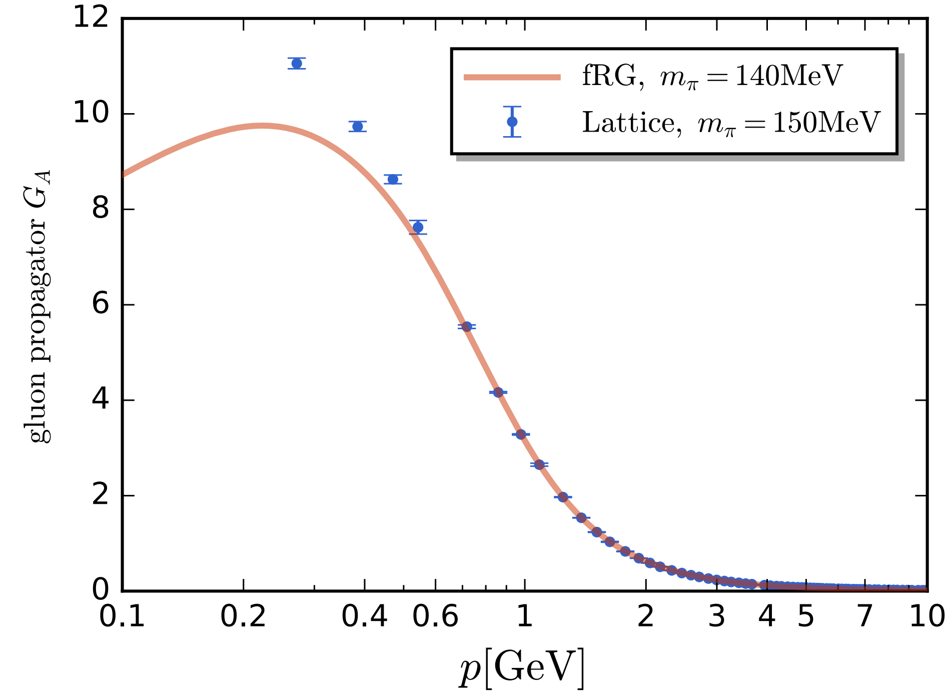

Lattice: Sternbeck *et al.*, PoS LATTICE2012 (2012) 243

fRG: WF, Huang, Pawlowski, Tan, in preparation

Ghost dressing:

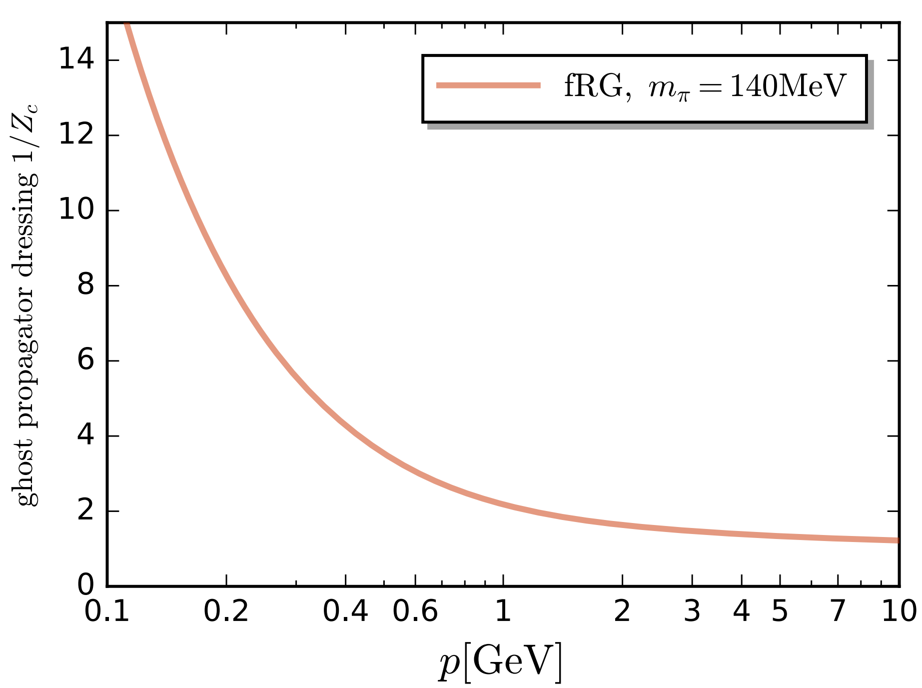

Strong couplings:

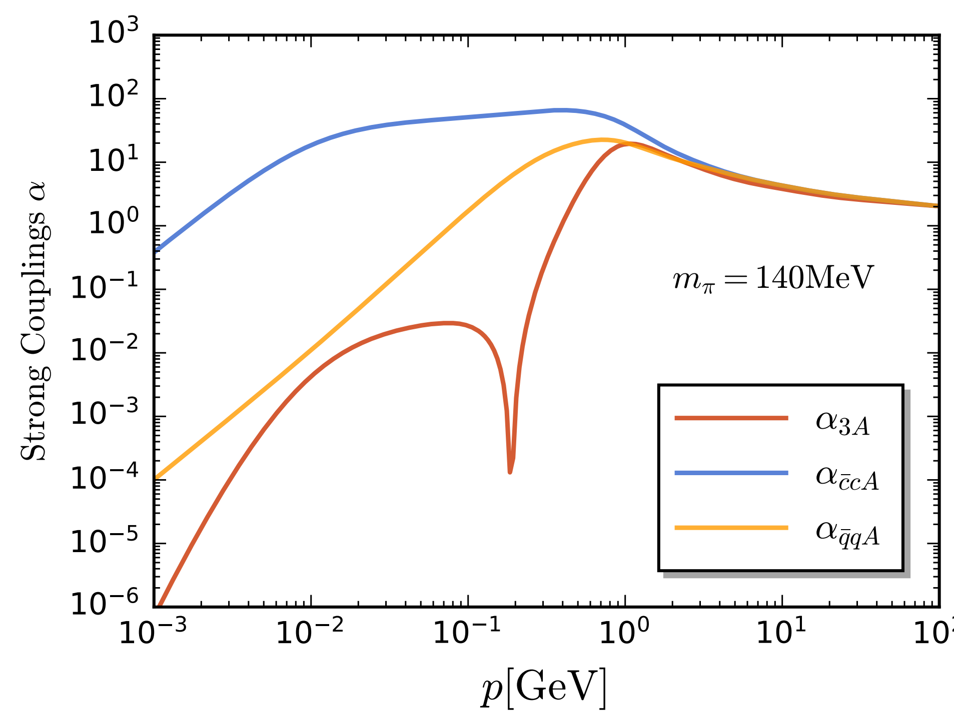

QCD within fRG in vacuum

Quark mass:

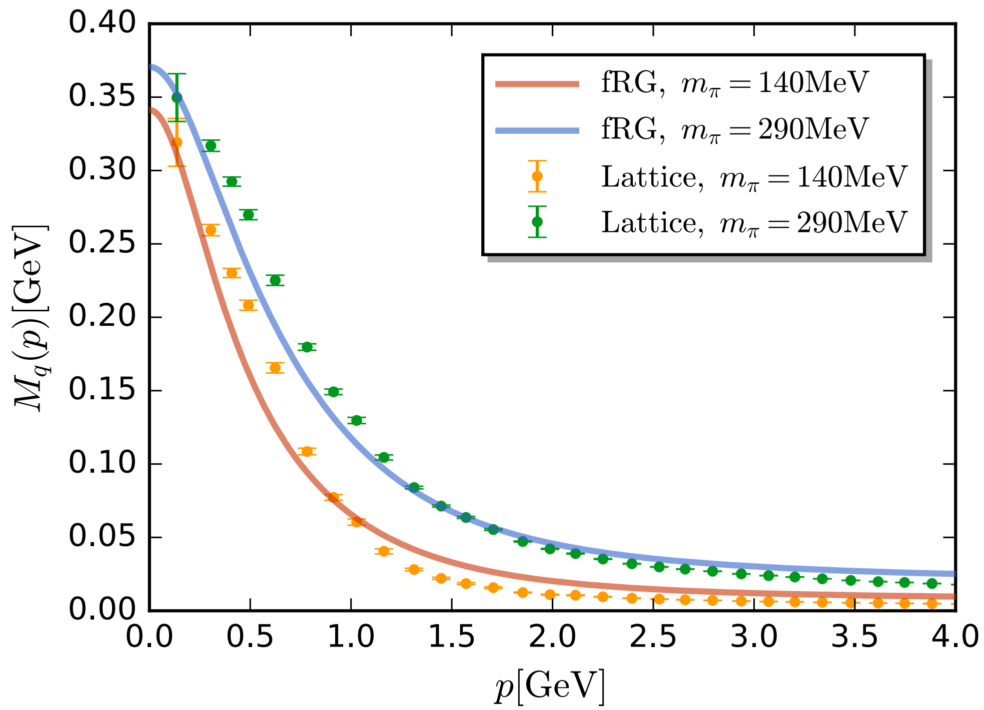

Lattice: Oliveira *et al.*, PRD 99 (2019) 094506

Quark-gluon vertex:

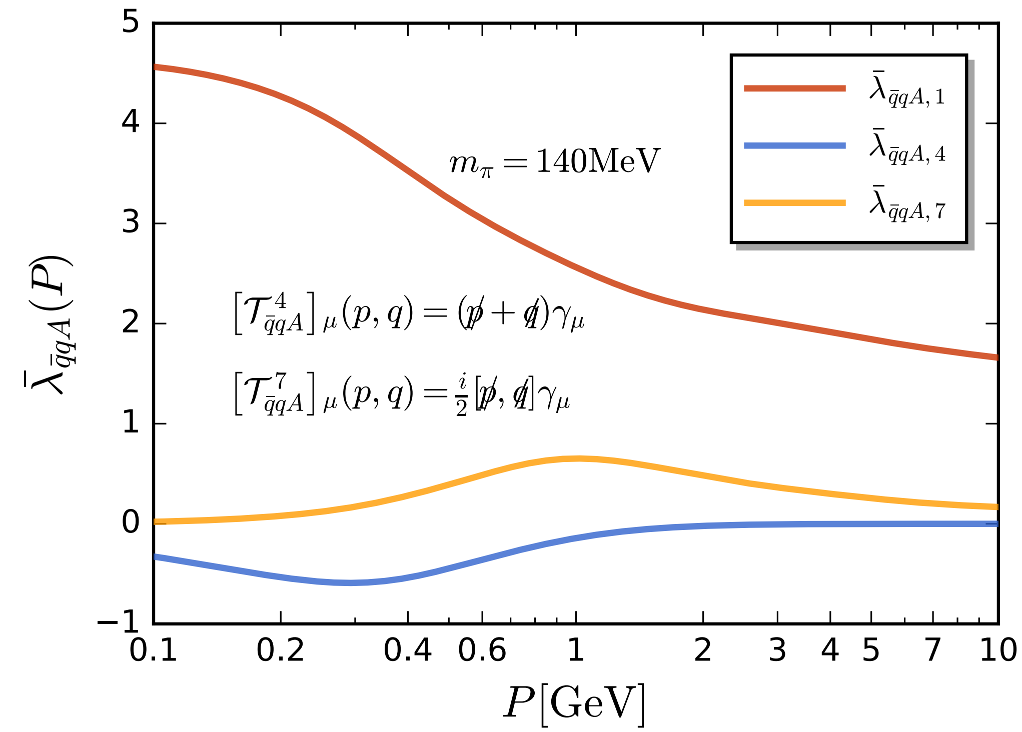

fRG: WF, Huang, Pawlowski, Tan, in preparation

Four-quark vertex (pion channel):

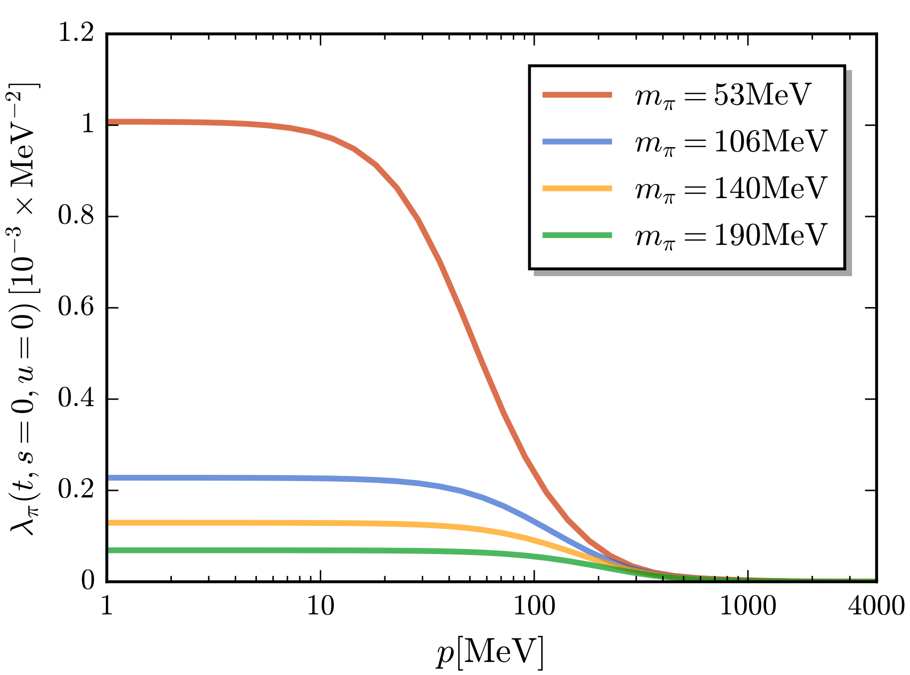

Four-quark vertex (sigma channel):

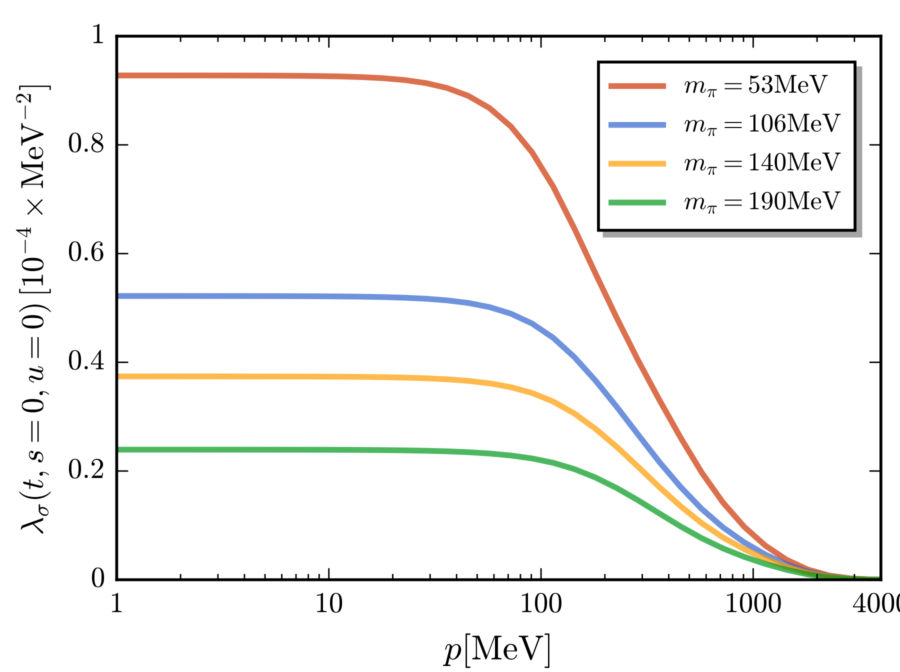

QCD with dynamical hadronization

Introducing a RG scale dependent composite field:

$$\hat{\phi}_k(\hat{\varphi}), \;\; \textbf{with } \hat{\varphi} = (\hat{A}, \hat{c}, \hat{\bar{c}}, \hat{q}, \hat{\bar{q}}),$$

$$\langle \partial_t \hat{\phi}_k \rangle = \dot{A}_k \, \bar{q}\tau q + \dot{B}_k \, \phi + \dot{C}_k \, \hat{e}_\sigma ,$$

Gies, Wetterich , *PRD* 65 (2002) 065001; 69 (2004) 025001
Pawlowski, *AP* 322 (2007) 2831
Flörchinger, Wetterich, *PLB* 680 (2009) 371

Wetterich equation is modified as

$$\partial_t \Gamma_k[\Phi] = \frac{1}{2}\mathrm{STr}\big(G_k[\Phi]\, \partial_t R_k\big) + \mathrm{Tr}\left(G_{\phi\Phi_a}[\Phi] \frac{\delta \langle \partial_t \hat{\phi}_k \rangle}{\delta \Phi_a} R_\phi\right)$$

$$- \int \langle \partial_t \hat{\phi}_{k,i} \rangle \left(\frac{\delta \Gamma_k[\Phi]}{\delta \phi_i} + c_\sigma \delta_{i\,\sigma} \right),$$

WF, Pawlowski, Rennecke, *PRD* 101 (2020) 054032

Flow of four-quark couplings:

$$\partial_t \bar{\lambda}_q - 2\left(1 + \eta_q\right) \bar{\lambda}_q - \bar{h}\, \dot{\bar{A}} = \overline{\mathbf{Flow}}^{(4)}_{(\bar{q}\tau q)(\bar{q}\tau q)} ,$$

choosing

$$\bar{\lambda}_q \equiv 0 , \qquad \forall k ,$$

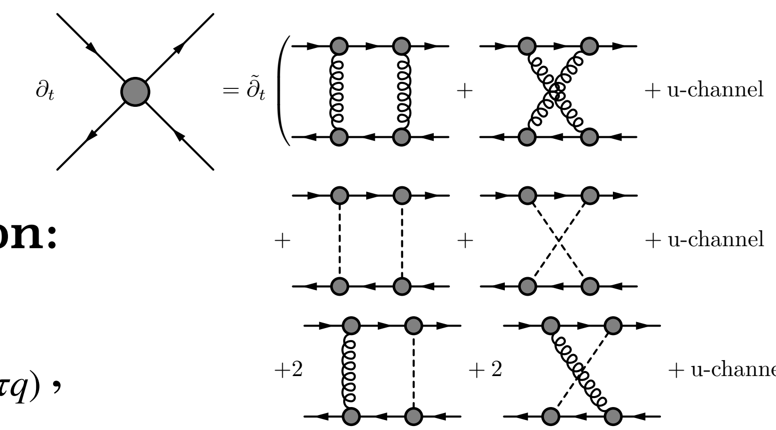

Hadronization function:

$$\dot{\bar{A}} = -\frac{1}{\bar{h}} \overline{\mathbf{Flow}}^{(4)}_{(\bar{q}\tau q)(\bar{q}\tau q)} ,$$

Flow equation:

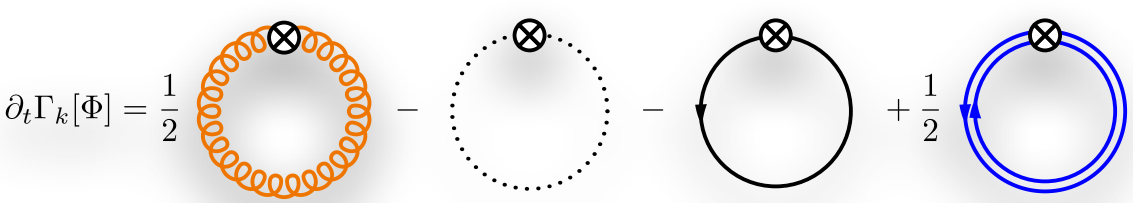

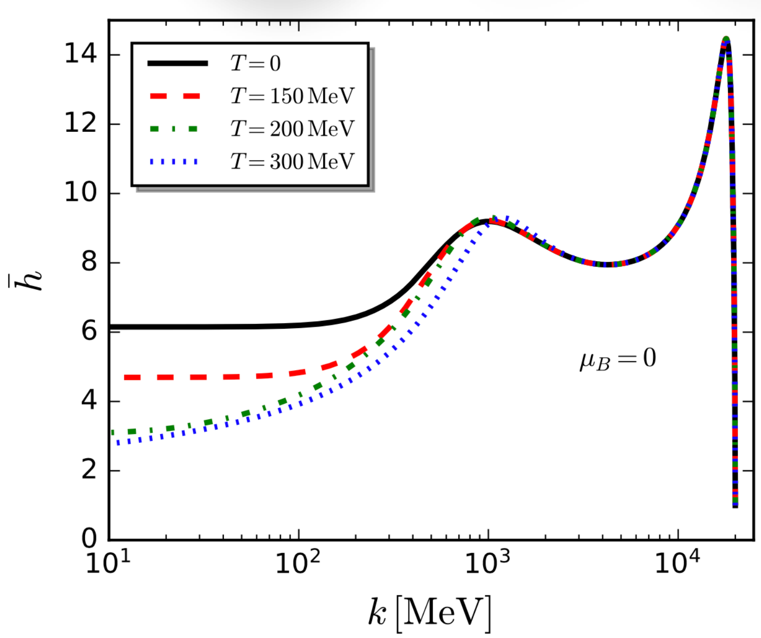

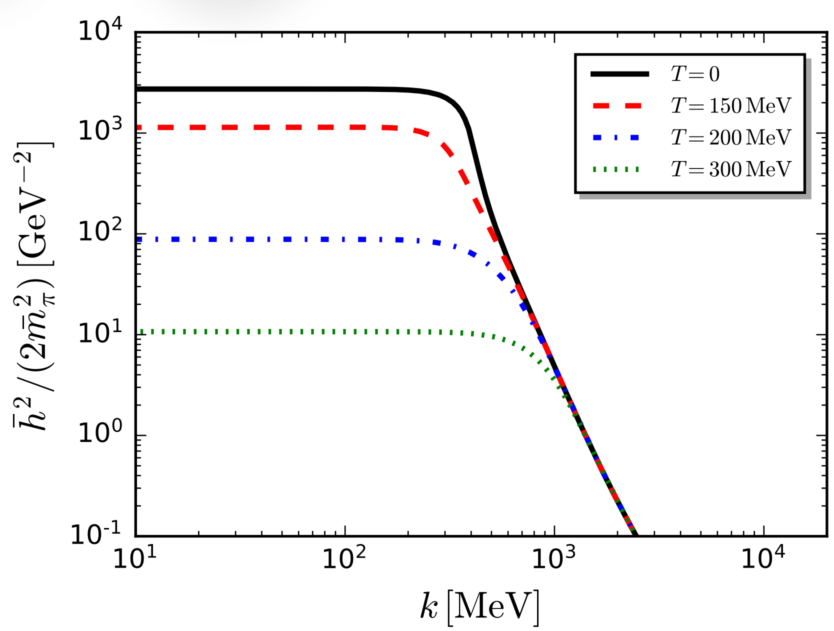

four-quark interaction encoded in Yukawa coupling:

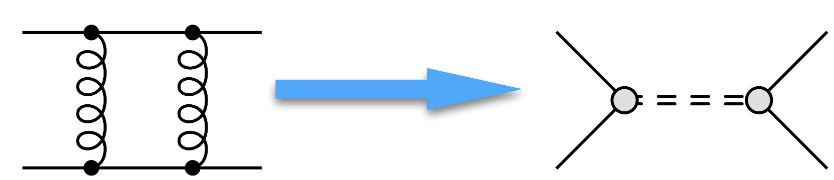

Gluon dressing functions

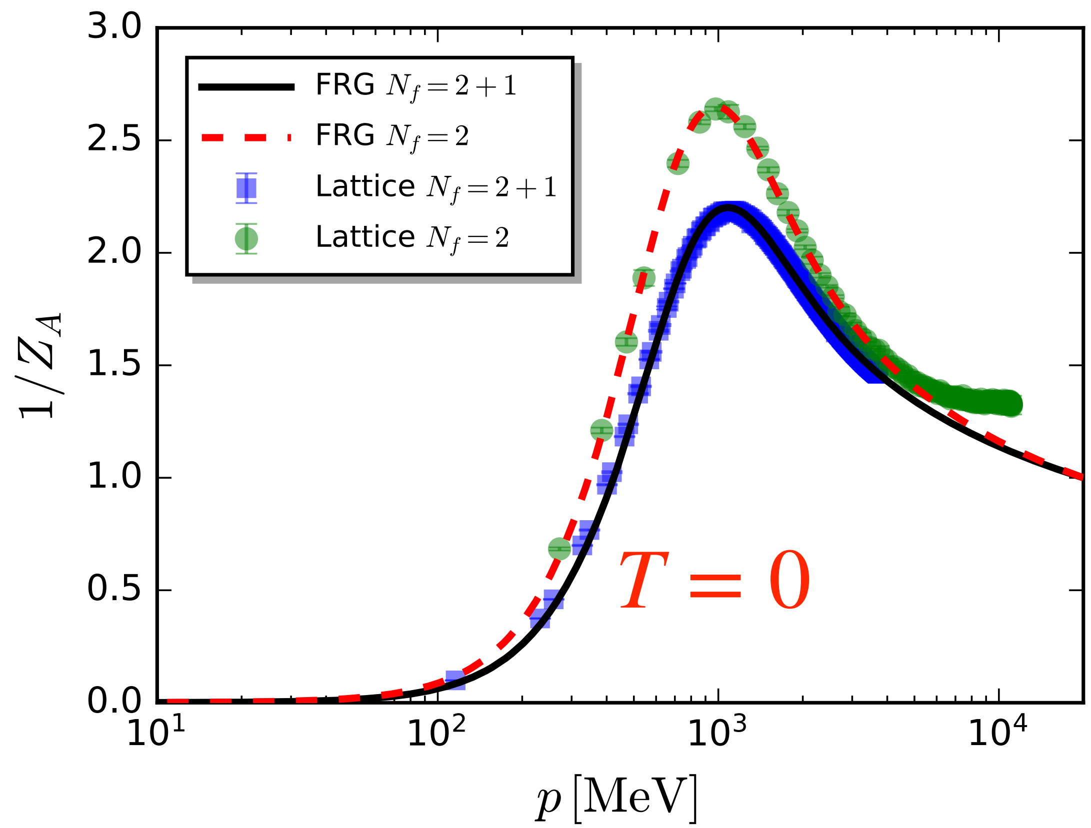

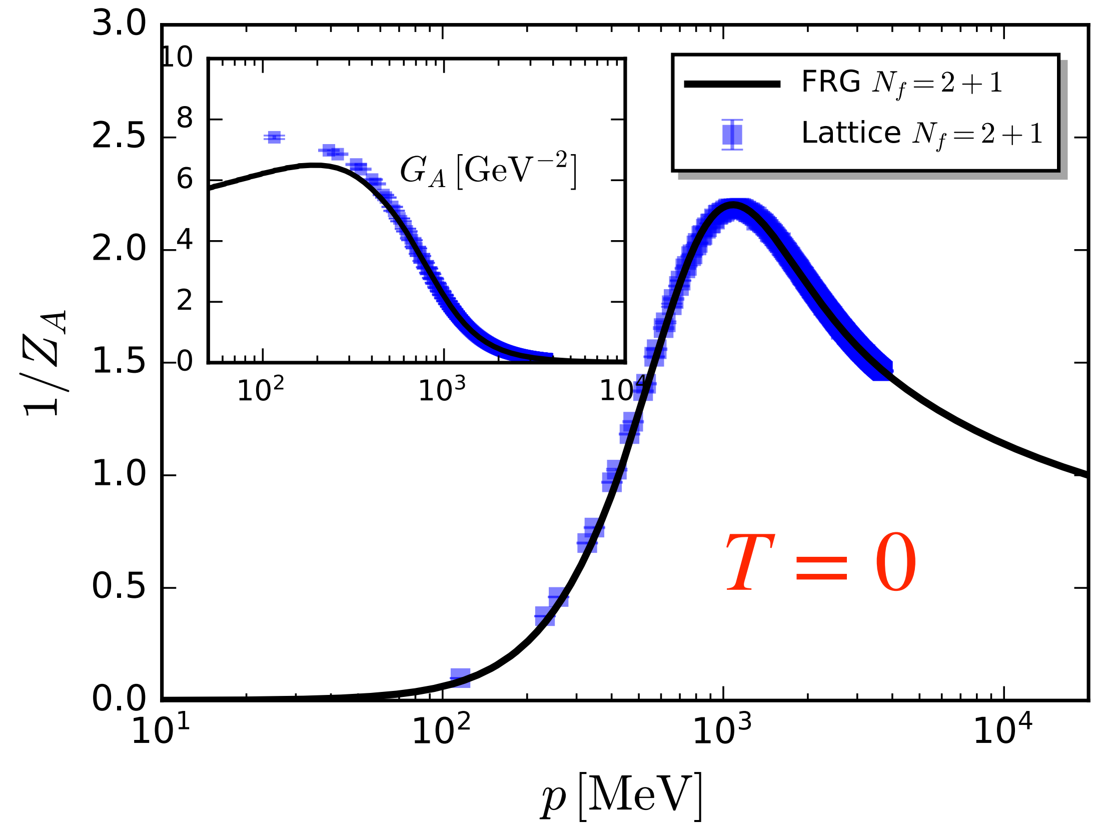

fRG $N_f = 2$: Cyrol, Mitter, Pawlowski,Strodthoff, *PRD* 97 (2018) 054006
Lattice $N_f = 2$: Sternbeck *et al.*, *PoS* (2012) LATTICE2012, 243
Lattice $N_f = 2+1$: Boucaud *et al.*, *PRD* 98 (2018) 114515

fRG: WF, Pawlowski, Rennecke, *PRD* 101 (2020) 054032

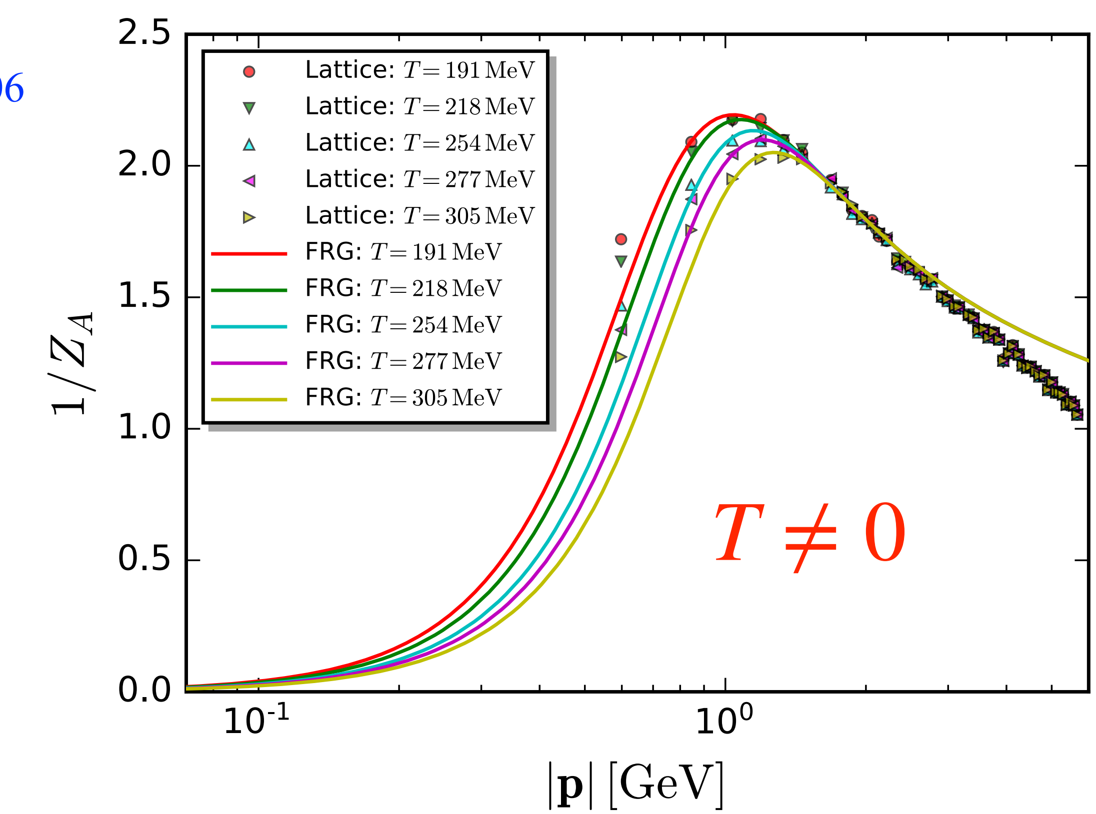

Natural emergence of LEFTs from QCD

- **Exchange couplings**

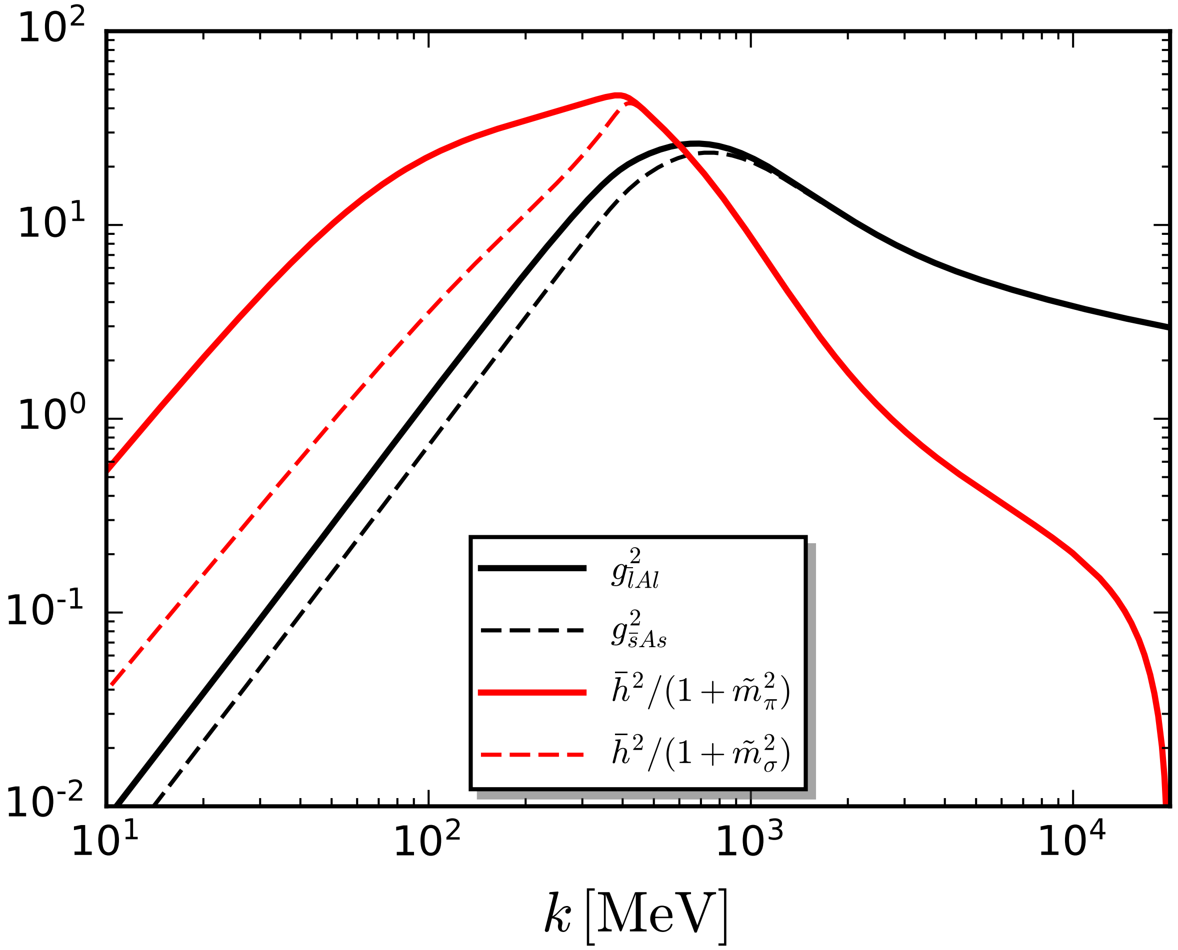

- **Propagator gapping**

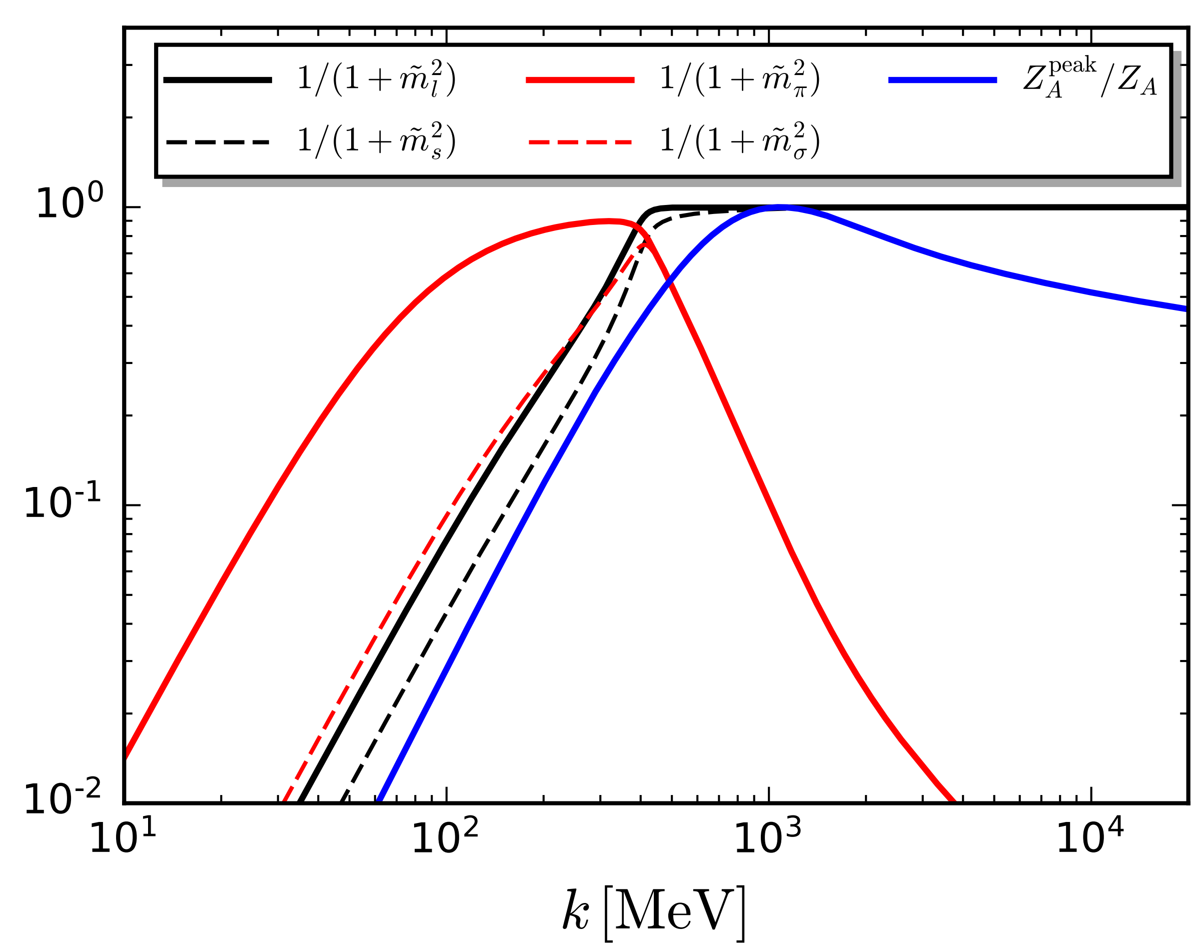

- Composite (mesonic) degrees of freedom take over active dynamics from partonic ones when the RG scale is lowered down $k \lesssim 600 \sim 800$ MeV.
- LEFTs emerge naturally from fundamental theory in the regime of low energy, in agreement with the viewpoint of RG.

WF, Pawlowski, Rennecke, *PRD* 101 (2020) 054032

Renormalized light quark condensate

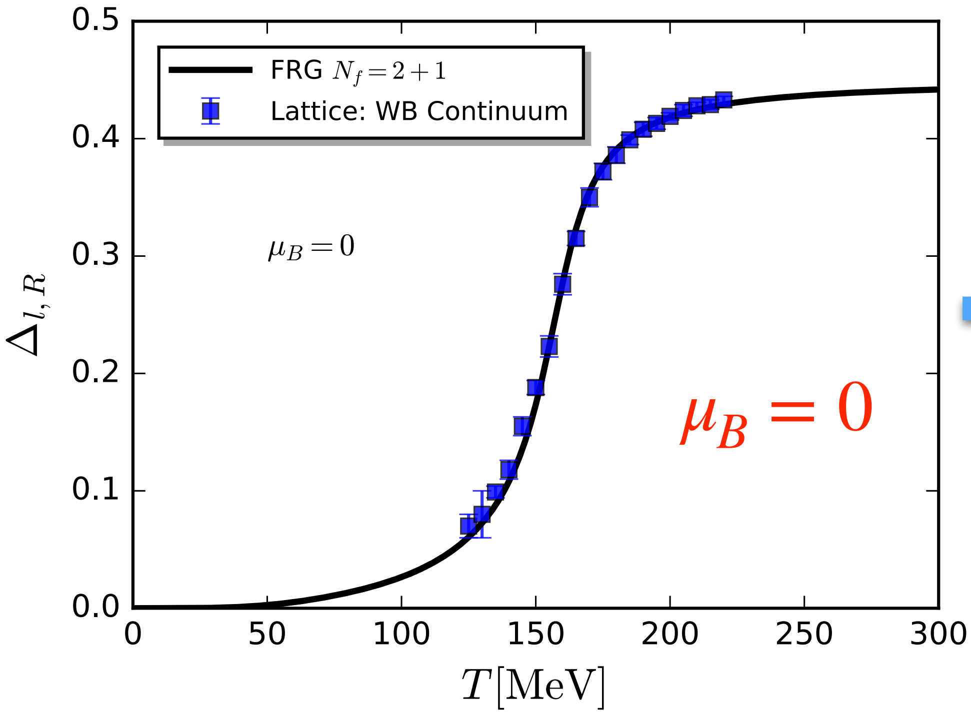

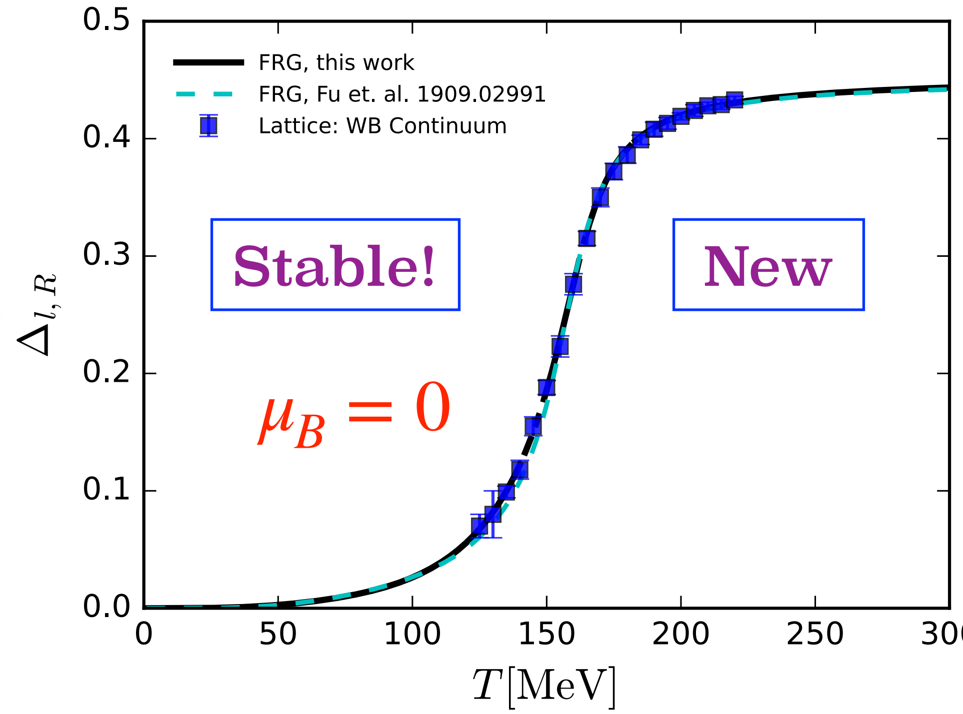

improved truncations for the sector of s quark and the full mesonic potential of $N_f = 2+1$.

Lattice: Borsanyi *et al.* (WB), *JHEP* 09 (2010) 073

fRG: WF, Pawlowski, Rennecke, *PRD* 101 (2020) 054032

fRG: WF, Pawlowski, Rennecke, Wen, Yin, in preparation

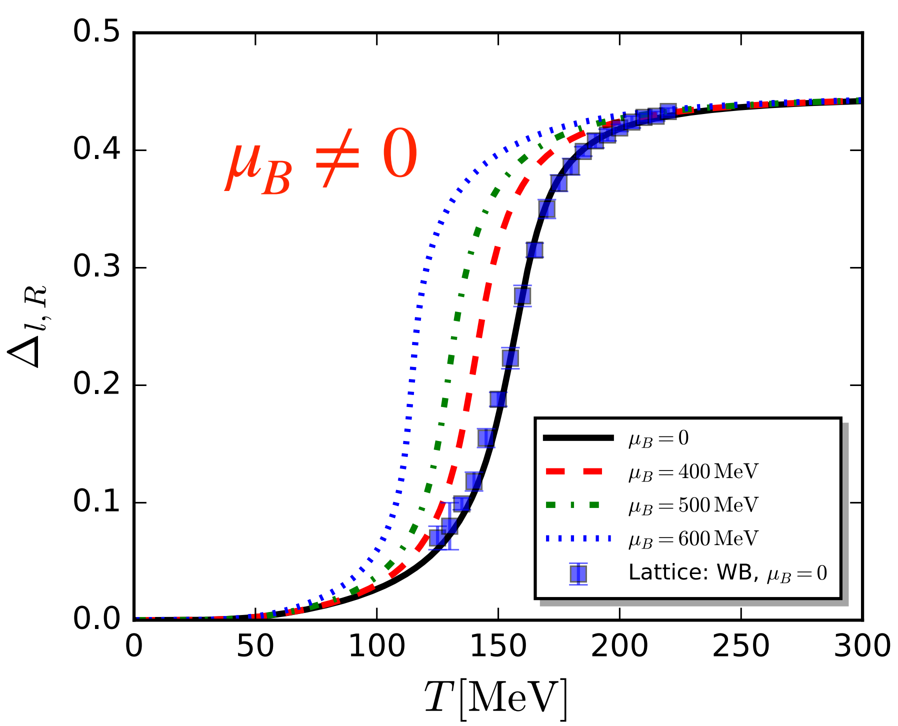

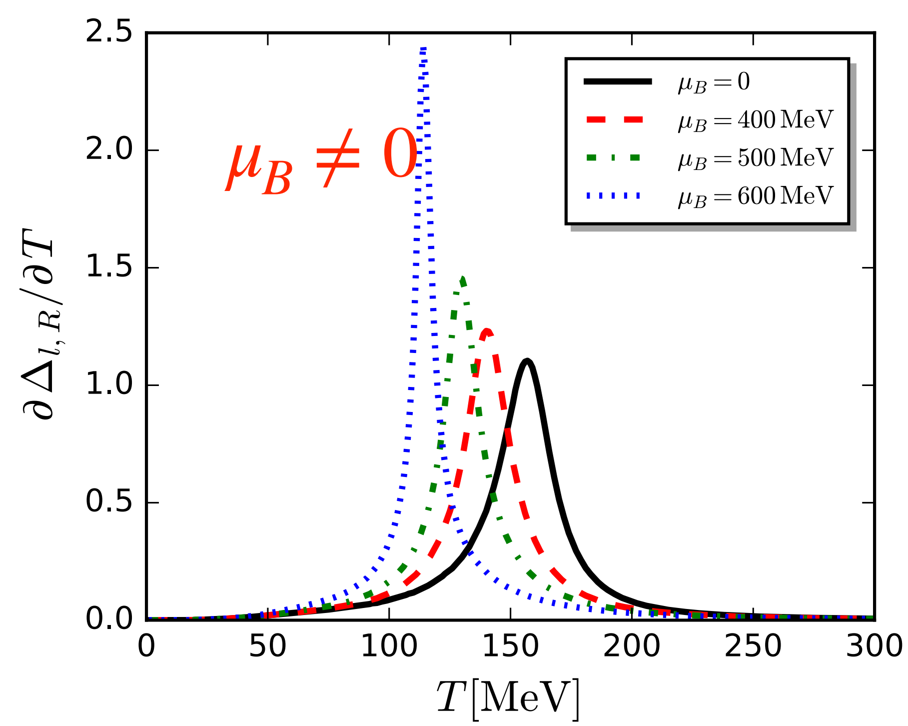

quark condensate:

$$\Delta_{q_i} \simeq -m_{q_i}^0 T \sum_{n\in\mathbb{Z}} \int \frac{d^3q}{(2\pi)^3} \mathrm{tr}\, G_{q_i\bar{q}_i}(q)\,,$$

$$\Delta_{q_i,R} = \frac{1}{\mathcal{N}_R}\left[\Delta_{q_i}(T,\mu_q) - \Delta_{q_i}(0,0)\right]\,.$$

Other fermionic observables

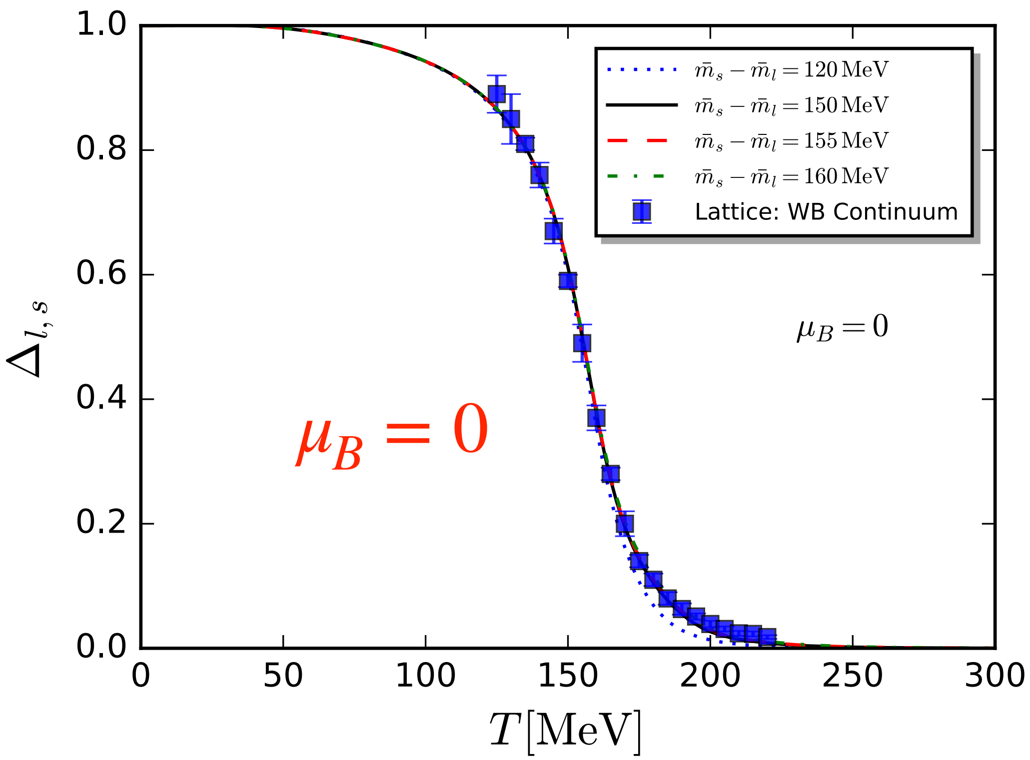

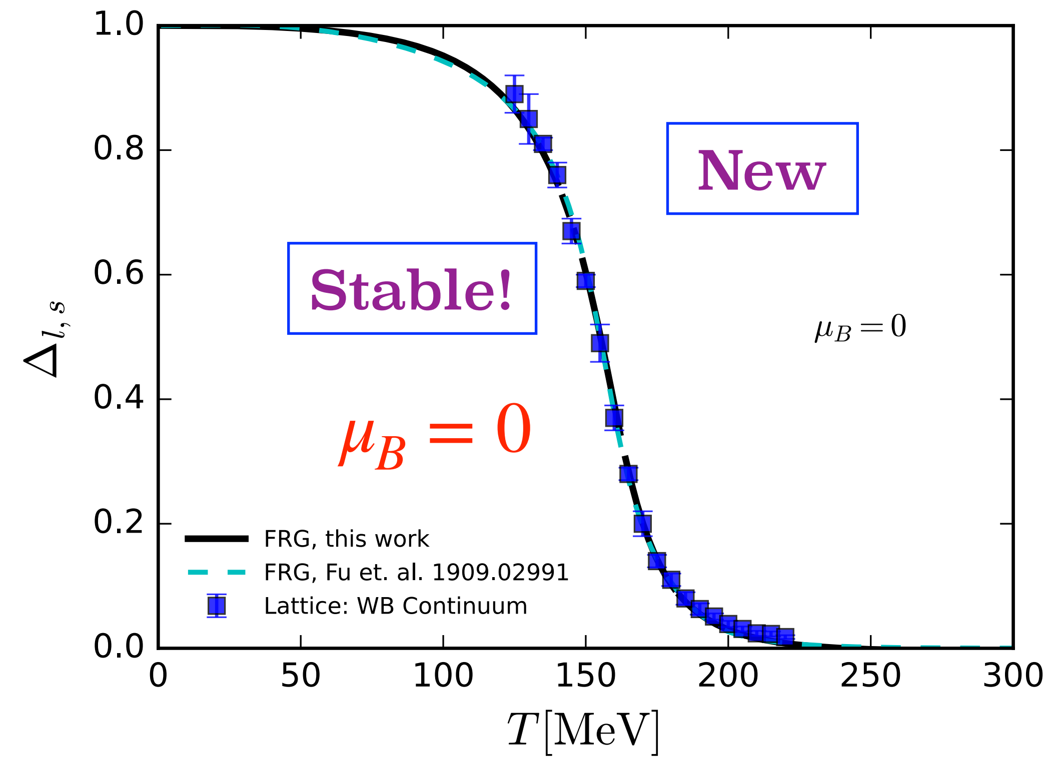

improved truncations for the sector of s quark and the full mesonic potential of $N_f = 2+1$.

Lattice: Borsanyi *et al.* (WB), *JHEP* 09 (2010) 073

fRG: WF, Pawlowski, Rennecke, *PRD* 101 (2020) 054032

fRG: WF, Pawlowski, Rennecke, Wen, Yin, in preparation

Reduced condensate:

$$\Delta_{l,s}(T,\mu_q) = \frac{\Delta_l(T,\mu_q) - \left(\frac{m_l^0}{m_s^0}\right)^2 \Delta_s(T,\mu_q)}{\Delta_l(0,0) - \left(\frac{m_l^0}{m_s^0}\right)^2 \Delta_s(0,0)}$$

Effective four-quark coupling:

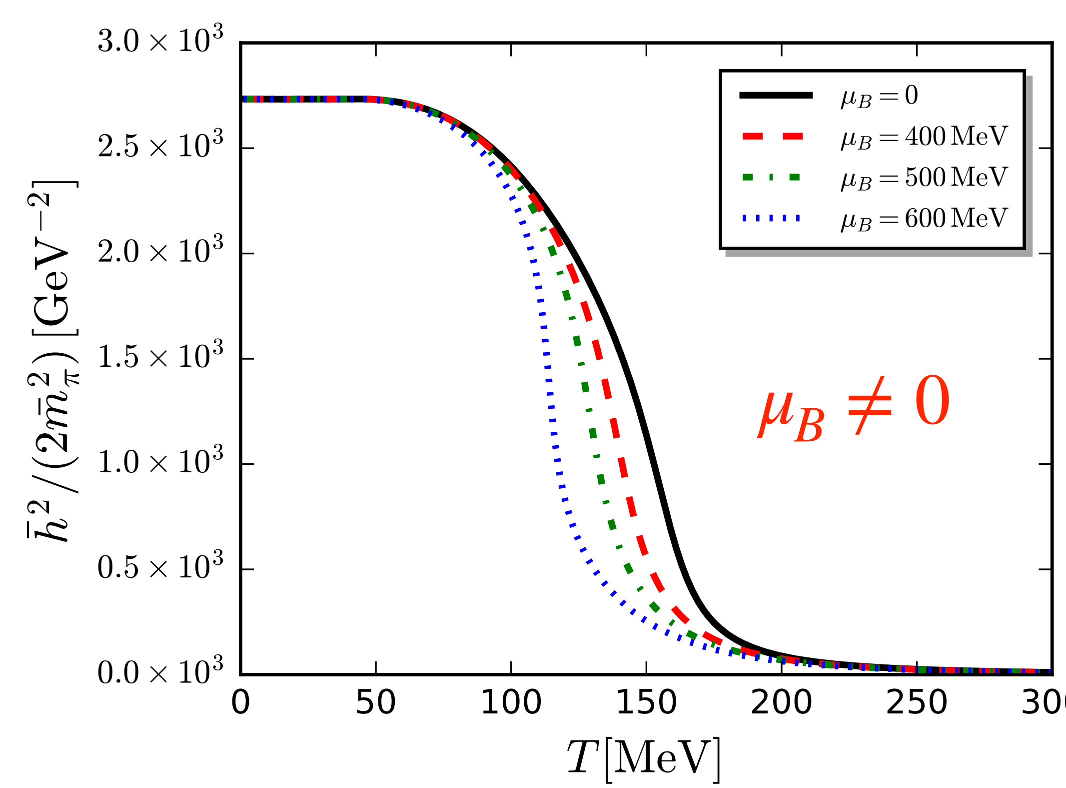

Phase boundary and curvature

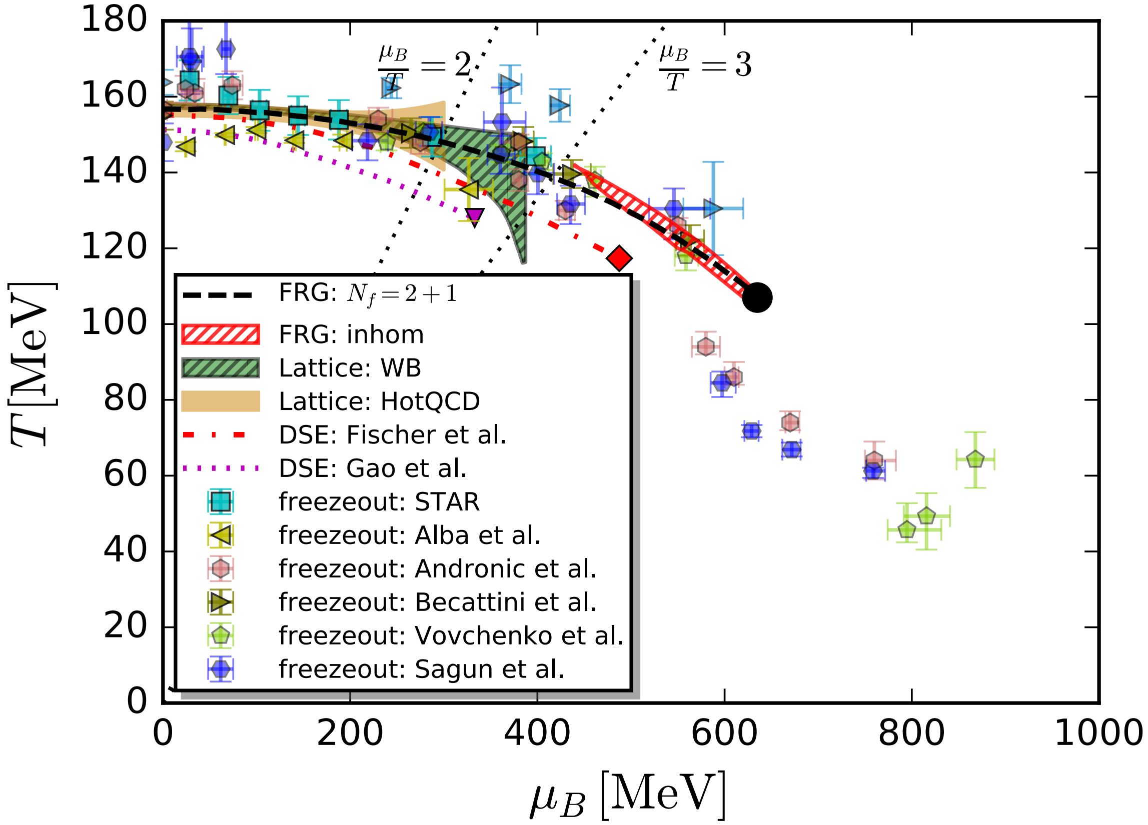

fRG: WF, Pawlowski, Rennecke, *PRD* 101 (2020) 054032

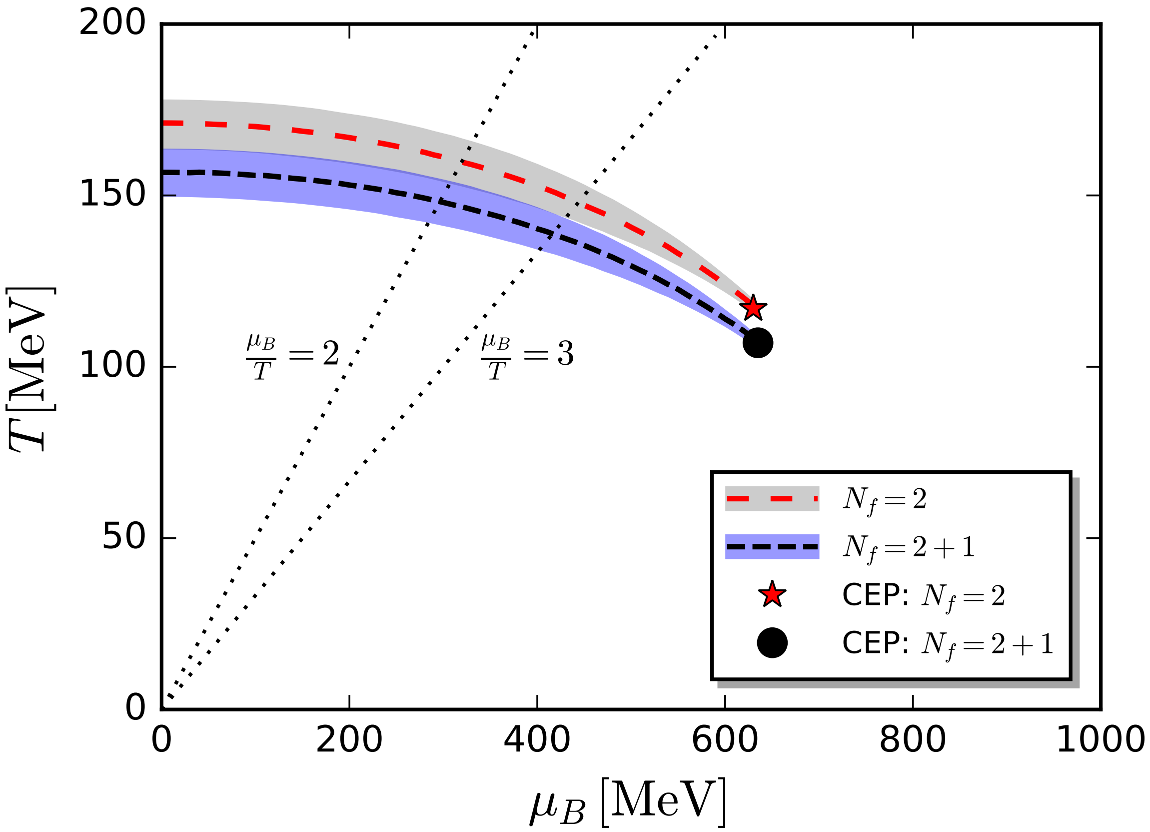

CEP:

$$(T_{\mathrm{CEP}}, {\mu_B}_{\mathrm{CEP}})_{N_f=2+1} = (107\,\mathrm{MeV}, 635\,\mathrm{MeV})\,,$$

$$(T_{\mathrm{CEP}}, {\mu_B}_{\mathrm{CEP}})_{N_f=2} = (117\,\mathrm{MeV}, 630\,\mathrm{MeV})\,,$$

FRG curvature of the phase boundary:

$$\frac{T_c(\mu_B)}{T_c} = 1 - \kappa\left(\frac{\mu_B}{T_c}\right)^2 + \lambda\left(\frac{\mu_B}{T_c}\right)^4 + \cdots\,,$$

$$\kappa_{N_f=2+1} = 0.0142(2)$$

$$\kappa_{N_f=2} = 0.0176(1)$$

Lattice result:

$$\kappa = 0.0149 \pm 0.0021$$

Lattice: Bellwied *et al.* (WB), *PLB* 751 (2015) 559

$$\kappa = 0.015 \pm 0.004$$

Lattice: Bazavov *et al.* (HotQCD), *PLB* 795 (2019) 15

CEP from functional QCD

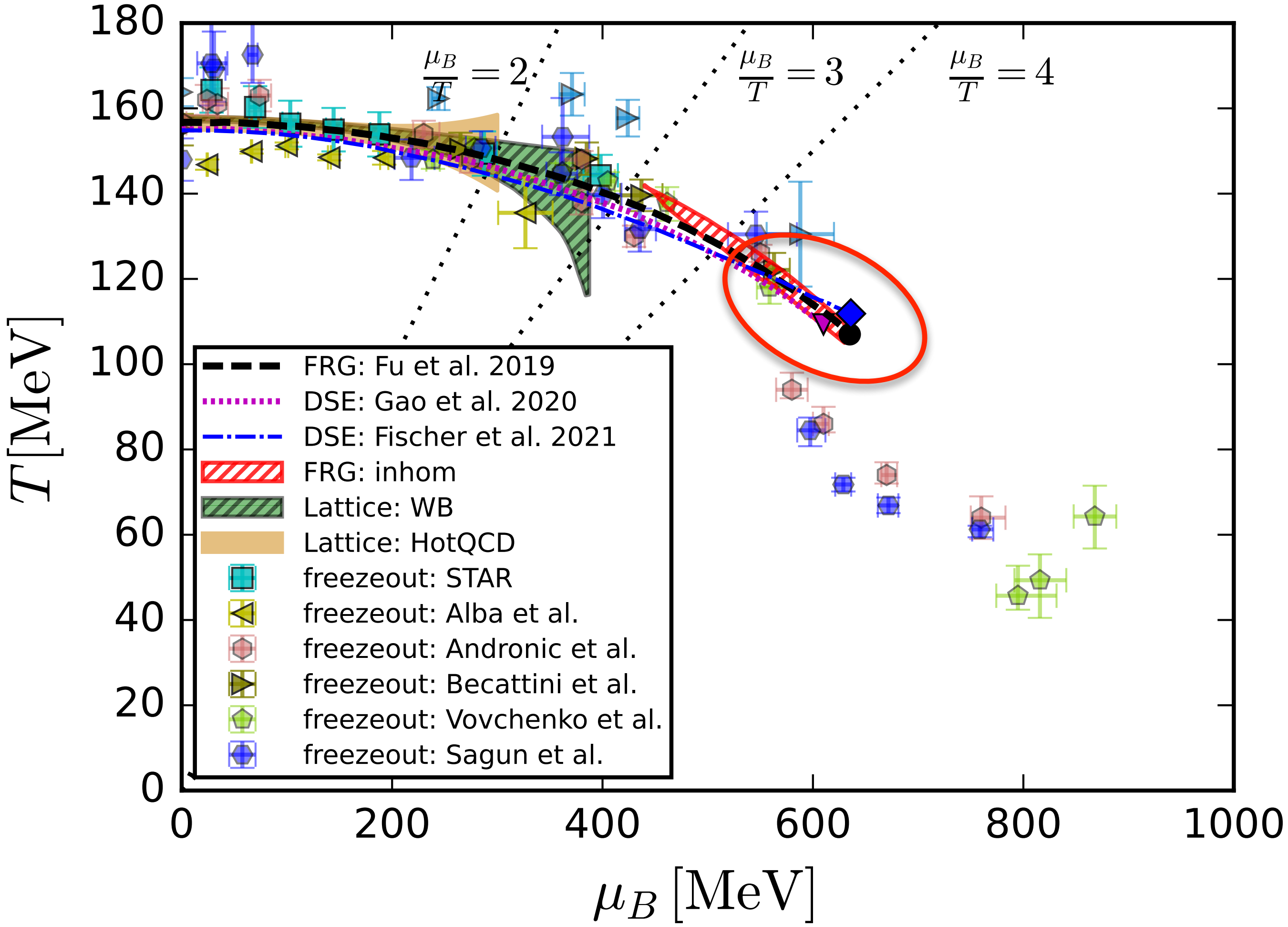

- No CEP observed in $\mu_B/T \lesssim 2 \sim 3$ from lattice QCD. Karsch, *PoS* CORFU2018 (2019)163
- Recent studies of QCD phase structure from both fRG and DSE have shown convergent estimate for the location of CEP.
- Considering relatively larger errors when $\mu_B/T \gtrsim 4$, one arrives at a reasonable estimation : $450\ \mathrm{MeV} \lesssim \mu_{B_{\mathrm{CEP}}} \lesssim 650\ \mathrm{MeV}$.

Prediction of location of CEP from functional QCD in literature

fRG:

● $(T,\mu_B)_{\mathrm{CEP}} = (107, 635)\mathbf{MeV}$

fRG: WF, Pawlowski, Rennecke, *PRD* 101 (2020), 054032

DSE:

▼ $(T,\mu_B)_{\mathrm{CEP}} = (109, 610)\mathbf{MeV}$

DSE (fRG): Gao, Pawlowski, *PLB* 820 (2021) 136584

◆ $(T,\mu_B)_{\mathrm{CEP}} = (112, 636)\mathbf{MeV}$

DSE: Gunkel, Fischer, *PRD* 104 (2021) 5, 054022

Update: CEP from functional QCD

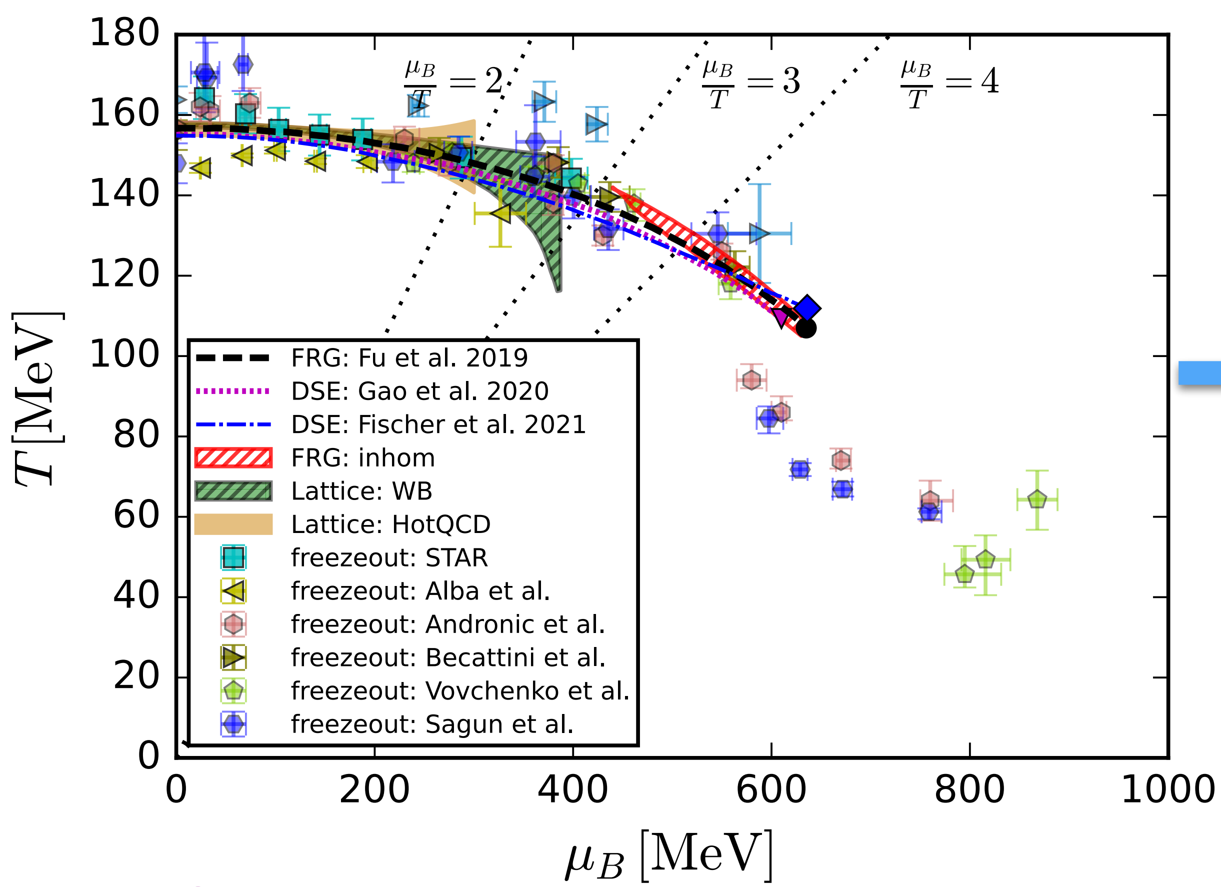

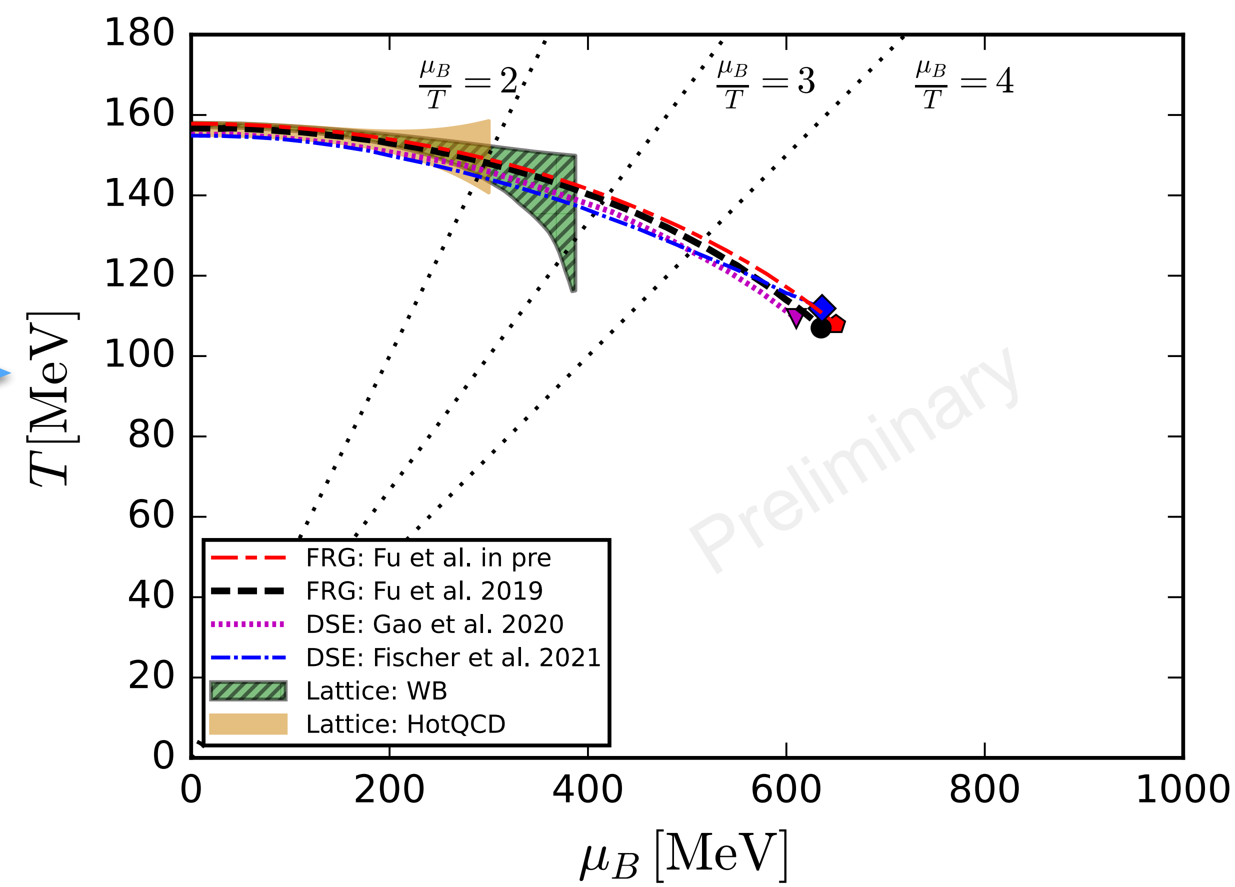

fRG:

⬟ $(T, \mu_B)_{\mathrm{CEP}} = (108, 650)\,\mathbf{MeV}$

improved truncations for the sector of *s* quark and the full mesonic potential of $N_f = 2+1$.

fRG: WF, Pawlowski, Rennecke, Wen, Yin, in preparation

DSE:

$(T, \mu_B)_{\mathrm{CEP}} = (110, 610)\,\mathbf{MeV}$ **(preliminary)**

Effects of thermal splitting on the location of CEP is small.

DSE: Gao, Schneider, Pawlowski, private communications.

Update: CEP from functional QCD

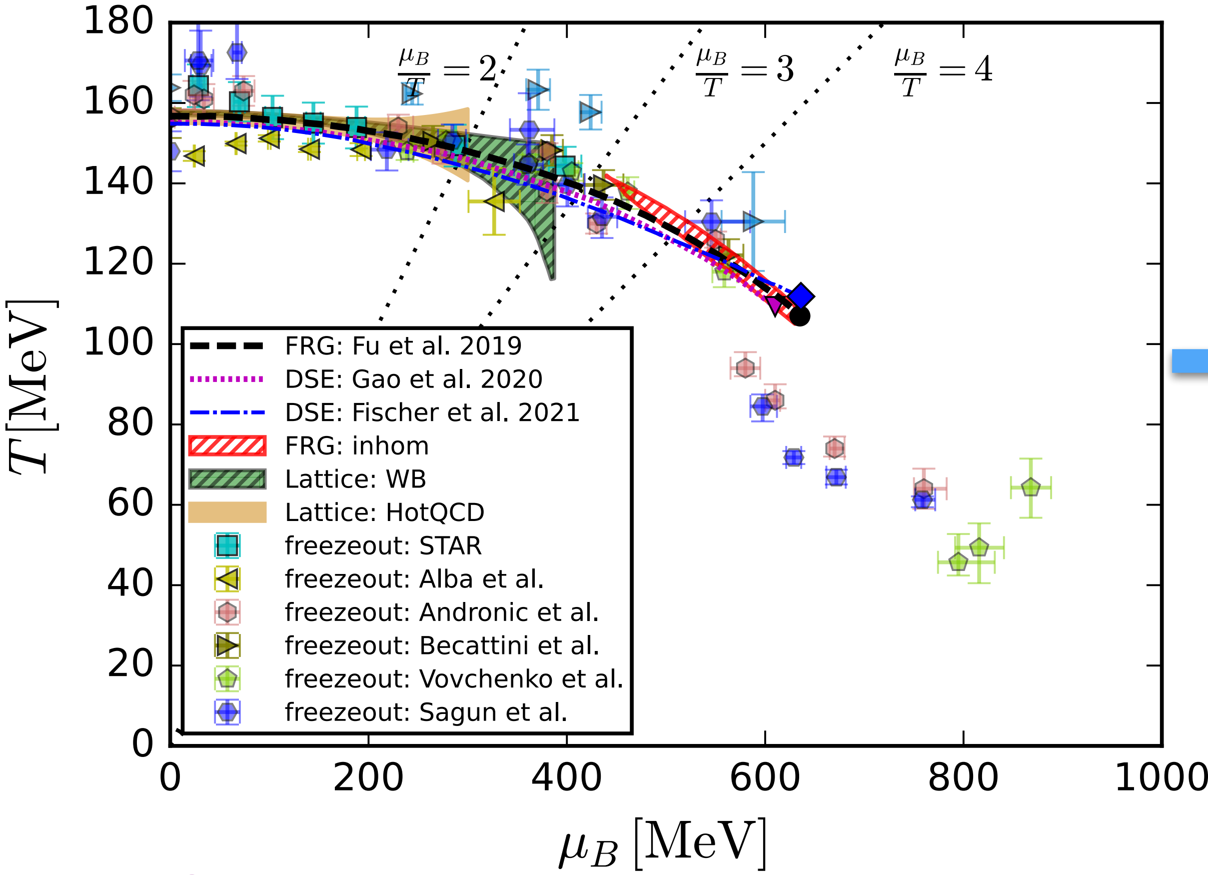

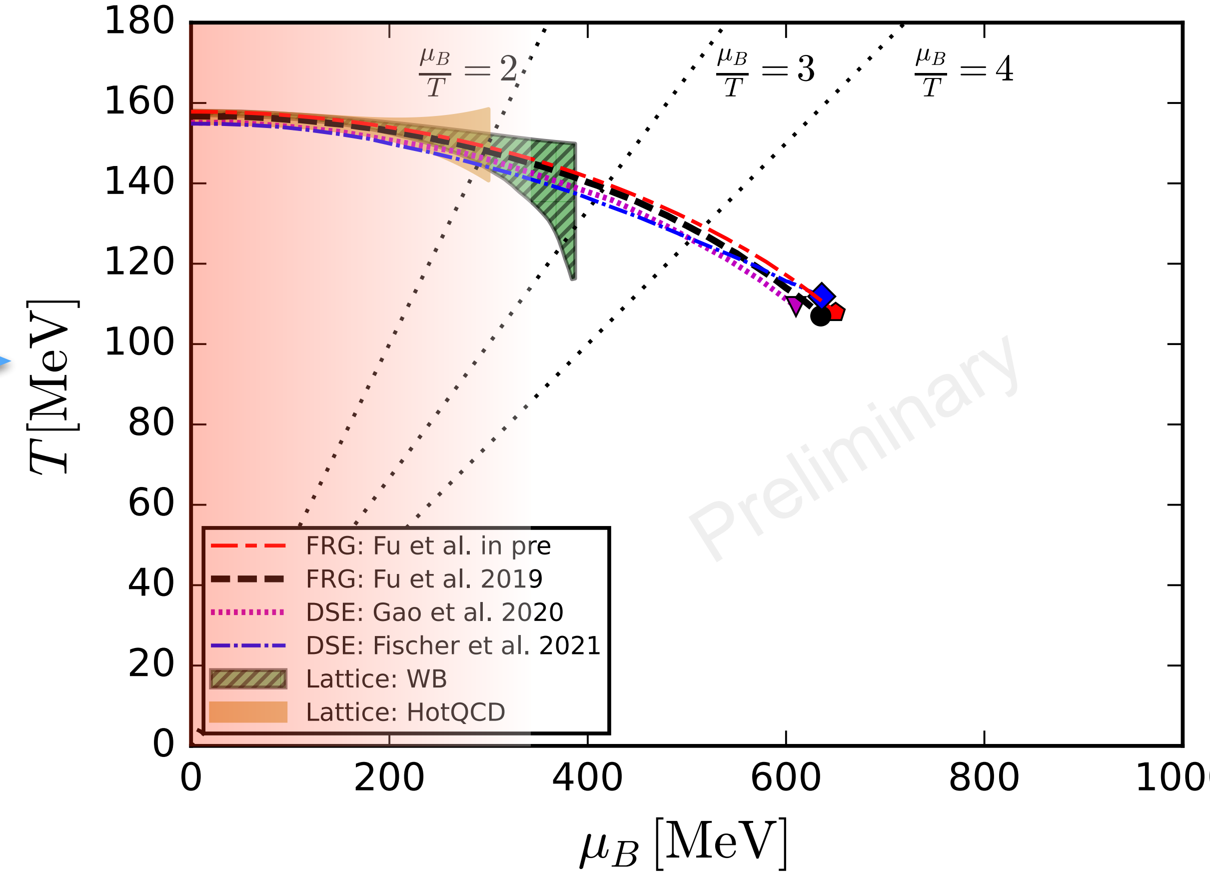

fRG:

⬟ $(T, \mu_B)_{\mathrm{CEP}} = (108, 650)\,\mathbf{MeV}$

improved truncations for the sector of *s* quark and the full mesonic potential of N_f = 2+1.

fRG: WF, Pawlowski, Rennecke, Wen, Yin, in preparation

Passing lattice benchmark tests at vanishing μ_B.

DSE:

$(T, \mu_B)_{\mathrm{CEP}} = (110, 610)\,\mathbf{MeV}$ **(preliminary)**

Effects of thermal splitting on the location of CEP is small.

DSE: Gao, Schneider, Pawlowski, private communications.

Update: CEP from functional QCD

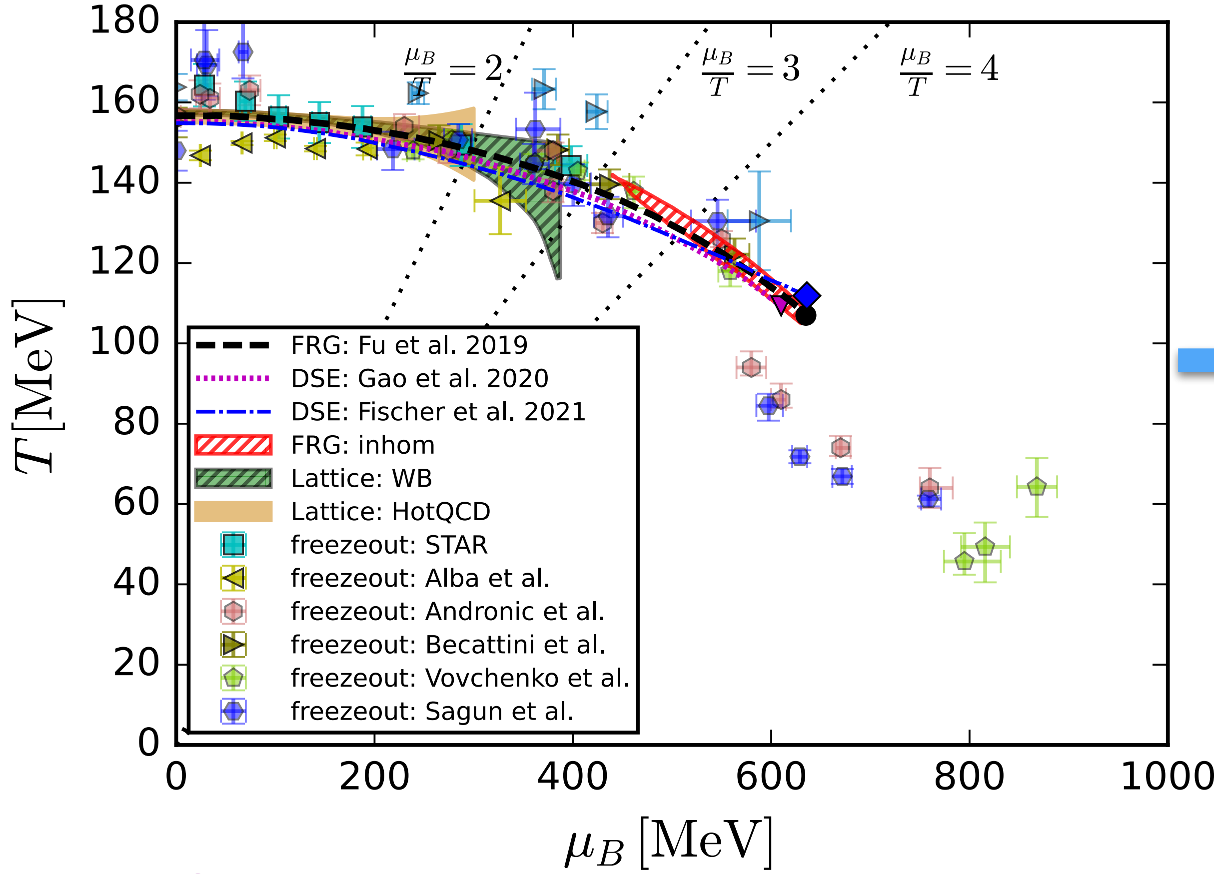

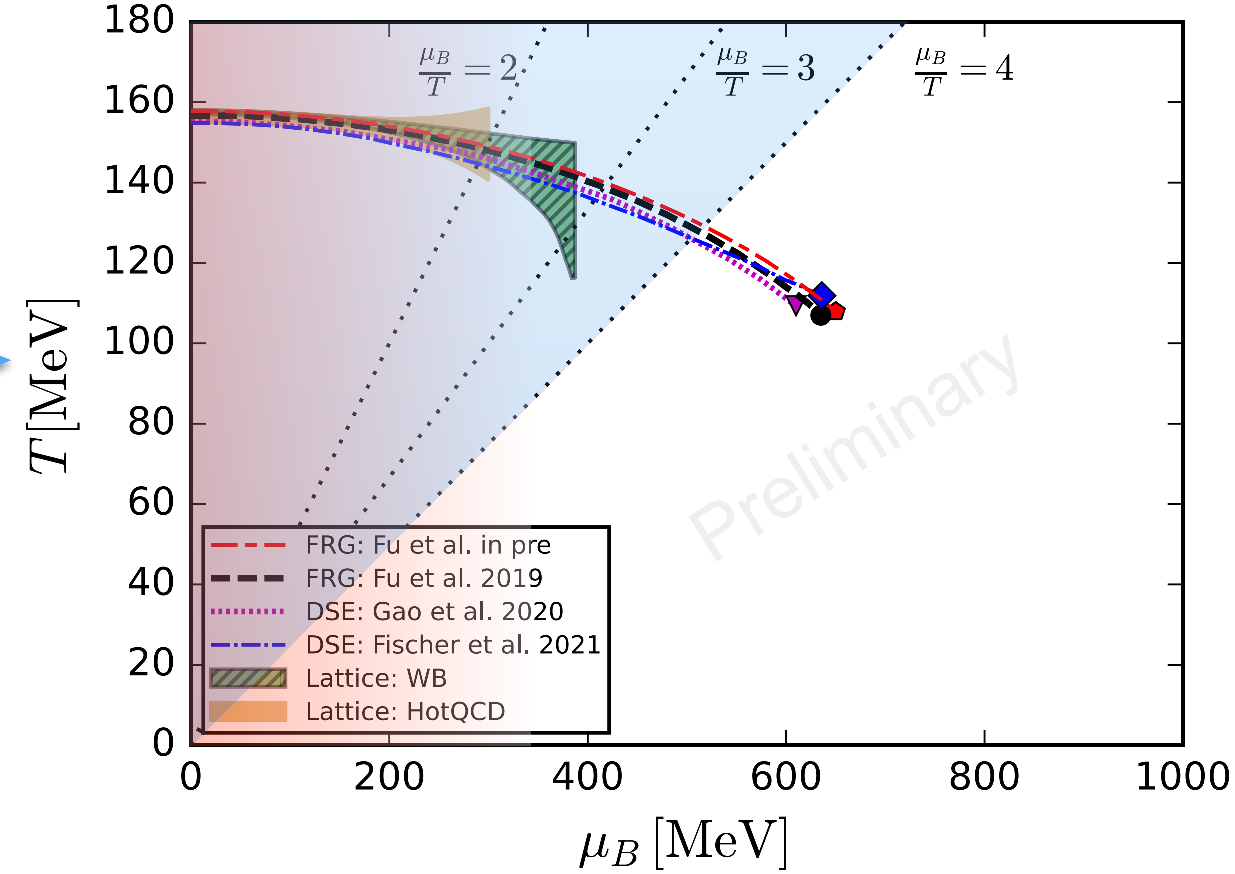

fRG:

$$(T,\mu_B)_{\rm CEP} = (108, 650)\,\mathbf{MeV}$$

improved truncations for the sector of *s* quark and the full mesonic potential of $N_f = 2+1$.

fRG: WF, Pawlowski, Rennecke, Wen, Yin, in preparation

DSE:

$$(T,\mu_B)_{\rm CEP} = (110, 610)\,\mathbf{MeV}\ \textbf{(preliminary)}$$

Effects of thermal splitting on the location of CEP is small.

DSE: Gao, Schneider, Pawlowski, private communications.

Passing lattice benchmark tests at vanishing μ_B.

Regime of reliability of current best truncation.

Inhomogeneous instabilities in QCD phase diagam

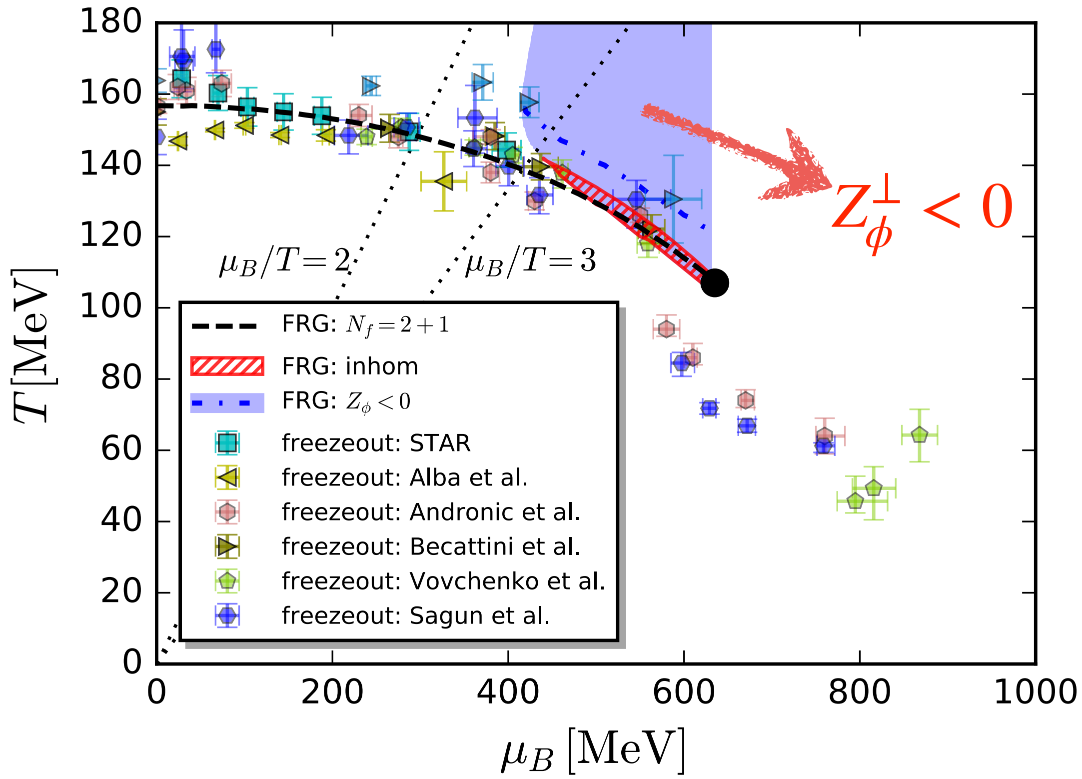

Mesonic two-point correlation function:

$$\Gamma^{(2)}_{\phi\phi}(p) = \left[Z^{\parallel}_\phi(p_0,\mathbf{p})\,p_0^2 + Z^{\perp}_\phi(p_0,\mathbf{p})\,\mathbf{p}^2\right] + m_\phi^2$$

with

$$\Gamma^{(2)}_{\phi\phi,k} = \left.\frac{\delta^2\Gamma_k[\Phi]}{\delta\phi\delta\phi}\right|_{\Phi=\Phi_{\mathrm{EoM}}}$$

WF, Pawlowski, Rennecke, *PRD* 101 (2020) 054032

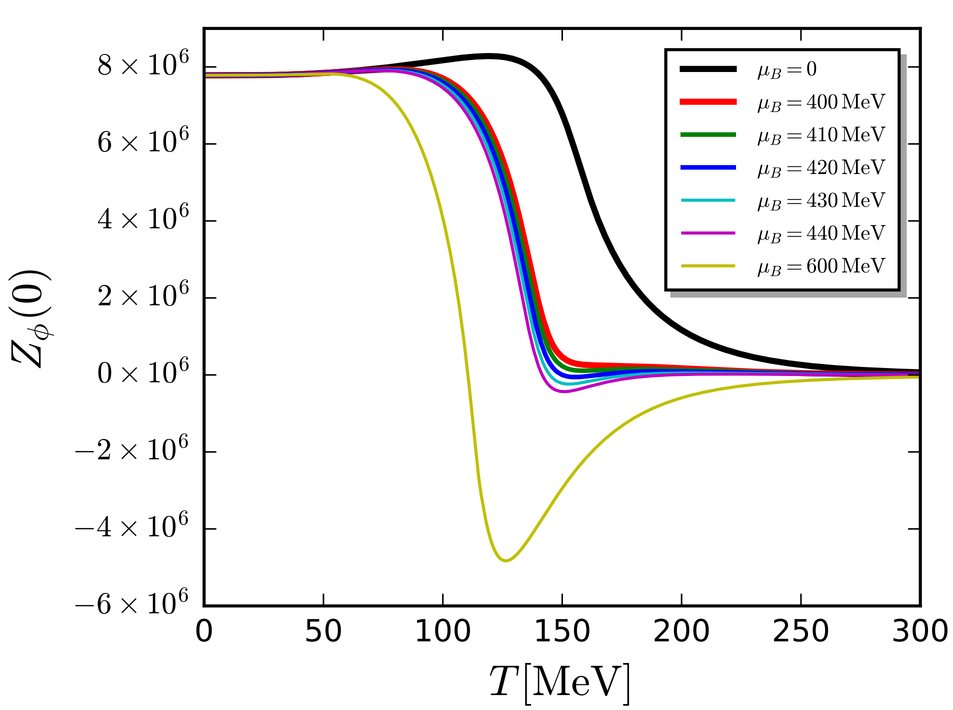

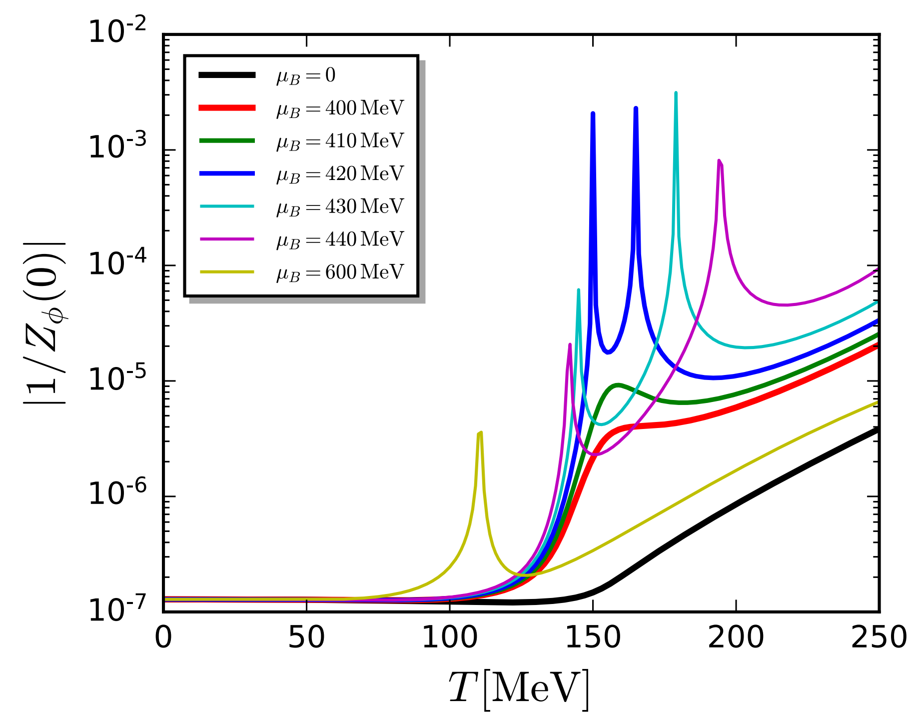

Signature of inhomogeneous instability in heavy-ion collisions—-"moat" spectrum

- **transverse momentum spectrum of one particle:**

moat behavior

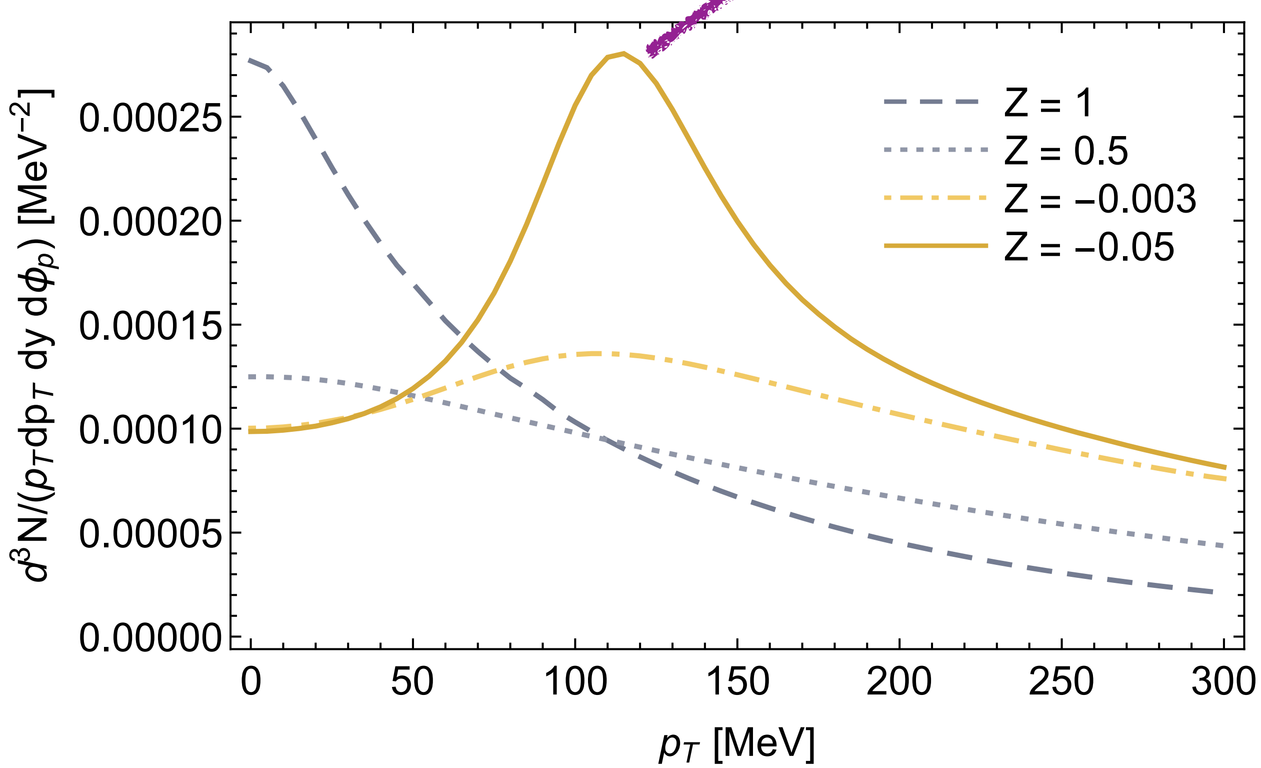

Pisarski, Rennecke, *PRL* 127 (2021) 152302;
Rennecke, Pisarski, arXiv:2110.02625

- **two-particle correlation:**

normal phase

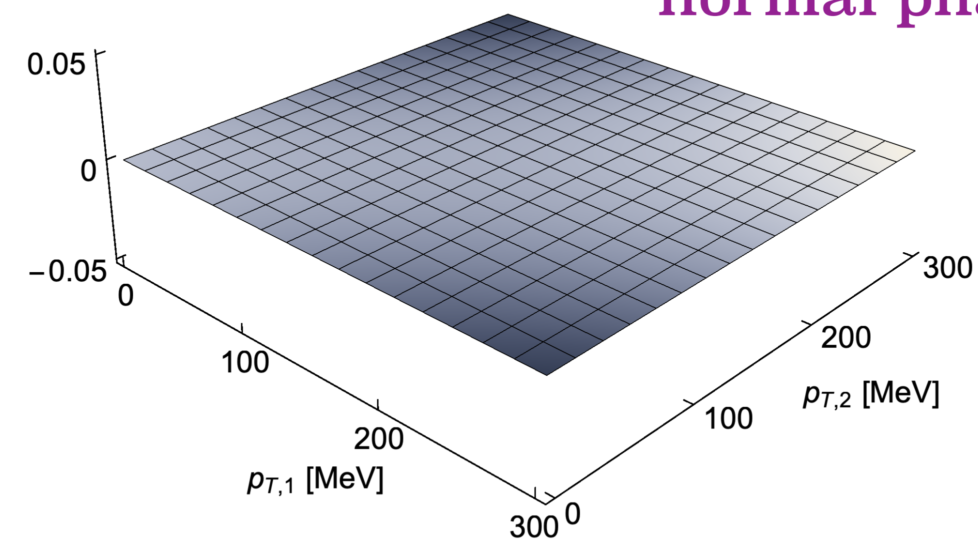

moat regime

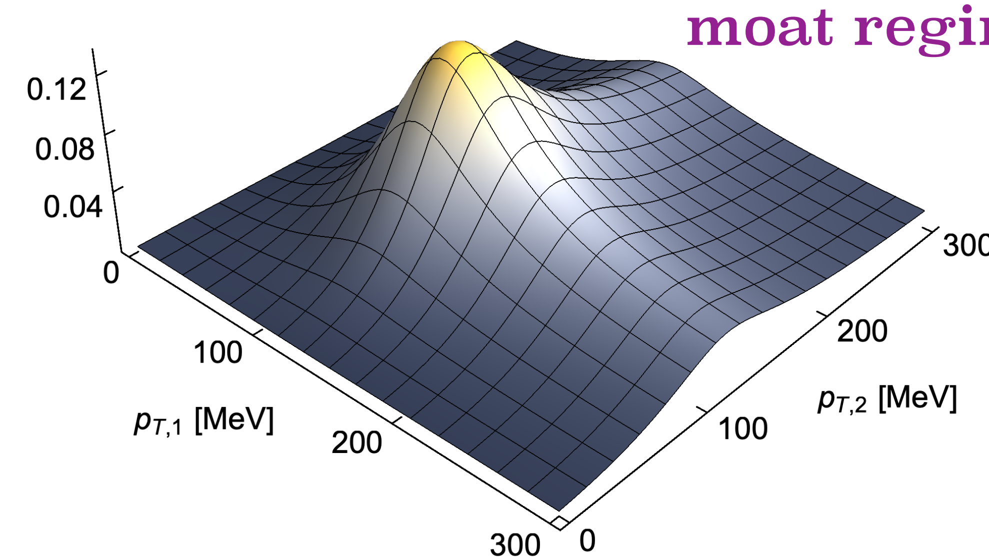

$$\Delta n_{12} = \left\langle \left(\frac{d^3N}{d\mathbf{p}^3}\right)^2 \right\rangle_c \Big/ \left\langle \frac{d^3N}{d\mathbf{p}^3} \right\rangle^2$$

Momentum-dependent mesonic wave function

Flow equation for mesonic two-point functions:

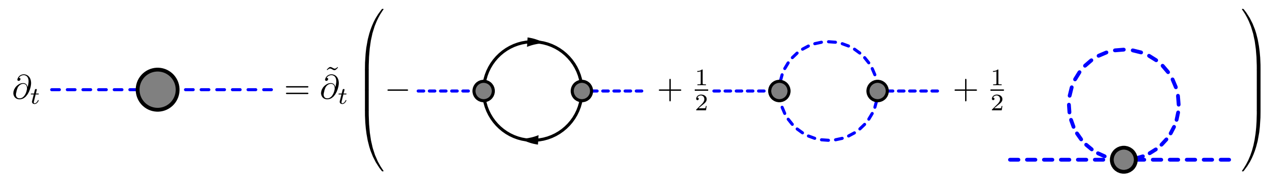

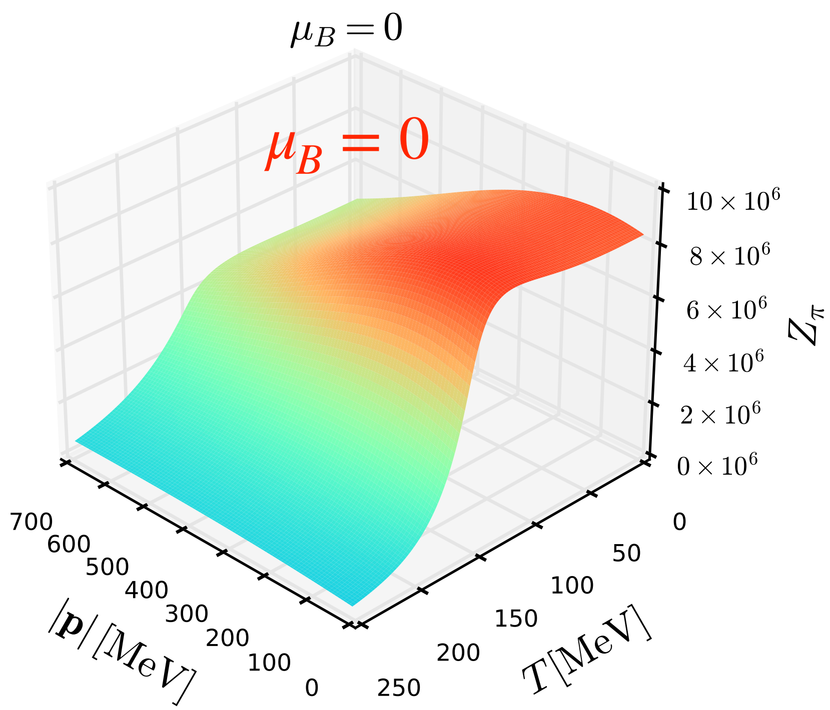

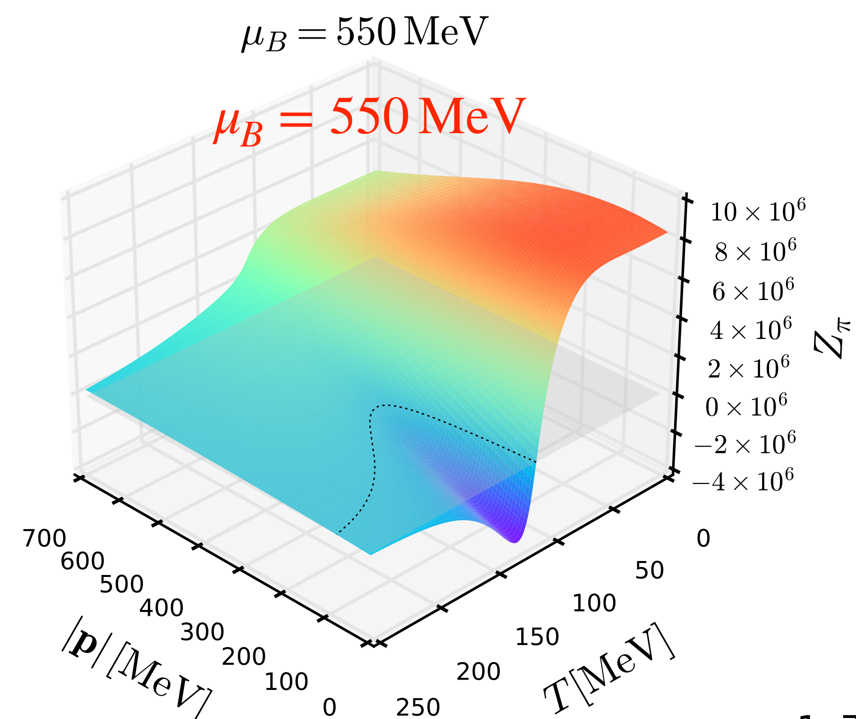

- Inhomogeneous instability is resulted from Landau damping of two quarks in thermal bath in the regime of large baryon chemical potential.

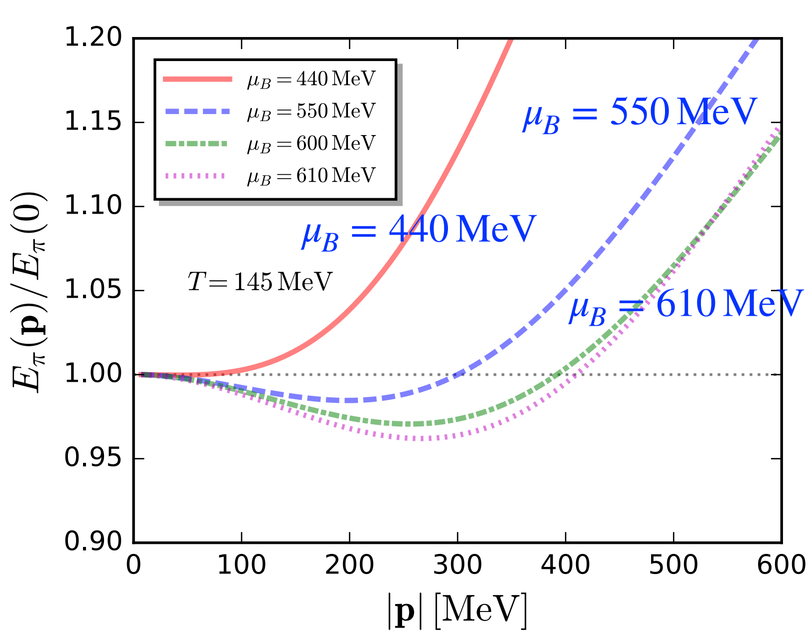

Dispersion relation:

$$E_\phi(\mathbf{p}) = \left[Z_\phi^\perp(\mathbf{p})\,\mathbf{p}^2 + m_\phi^2\right]^{1/2}$$

WF, Pawlowski, Rennecke, Wen, Yin, in preparation.

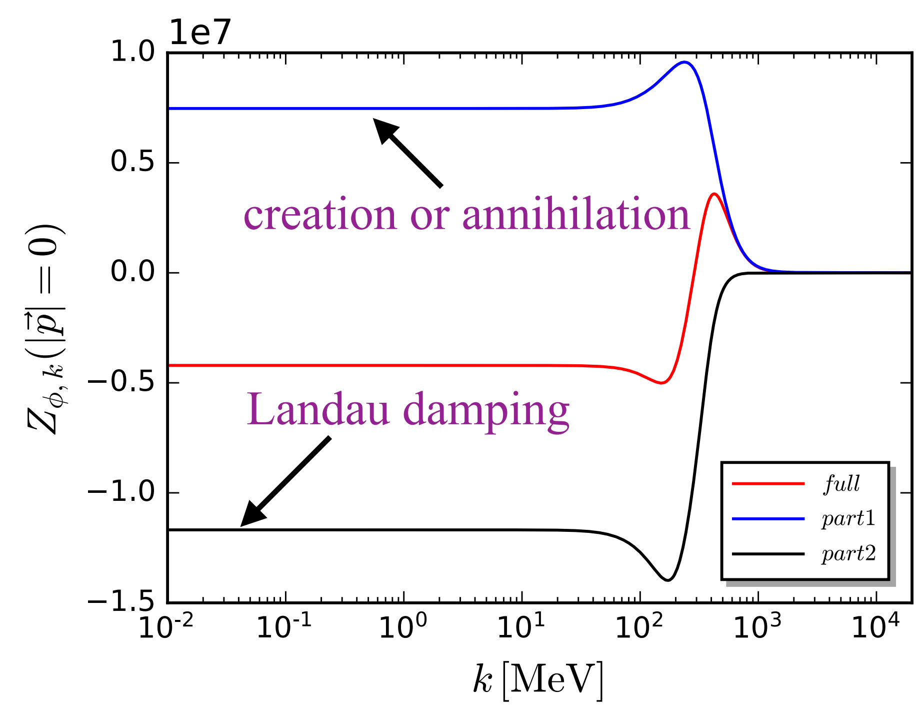

Real-time mesonic two-point functions

Analytic continuation on the flow equation:

$$\Gamma^{(2)}_{\phi\phi,\mathrm{R}}(\omega,\mathbf{p}) = \lim_{\epsilon\to 0^+} \Gamma^{(2)}_{\phi\phi}\big(-\mathrm{i}(\omega+\mathrm{i}\epsilon),\mathbf{p}\big)$$

Note: not on data!

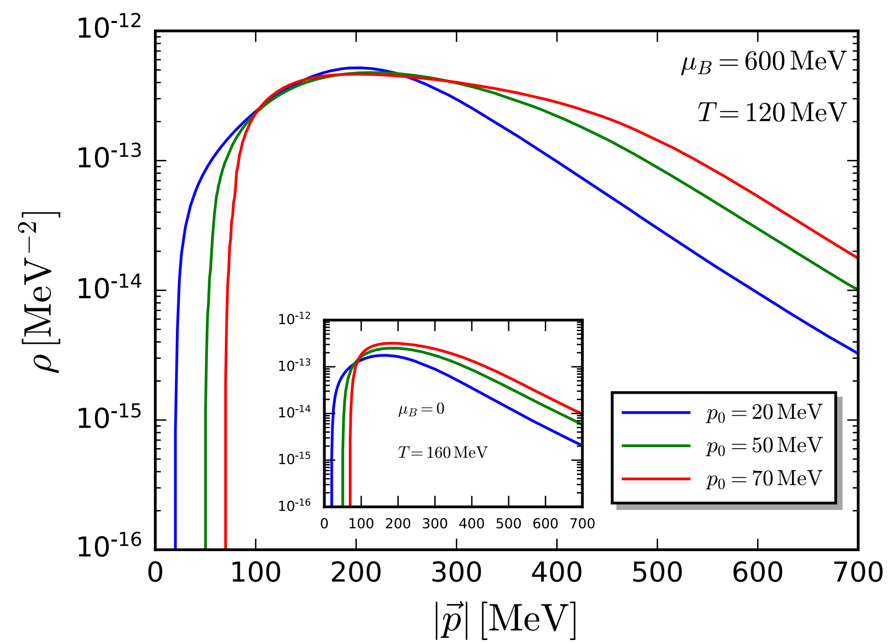

Spectral function

Real part of $\Gamma^{(2)}_{\phi\phi,\mathrm{R}}(p_0,\mathbf{p})$:

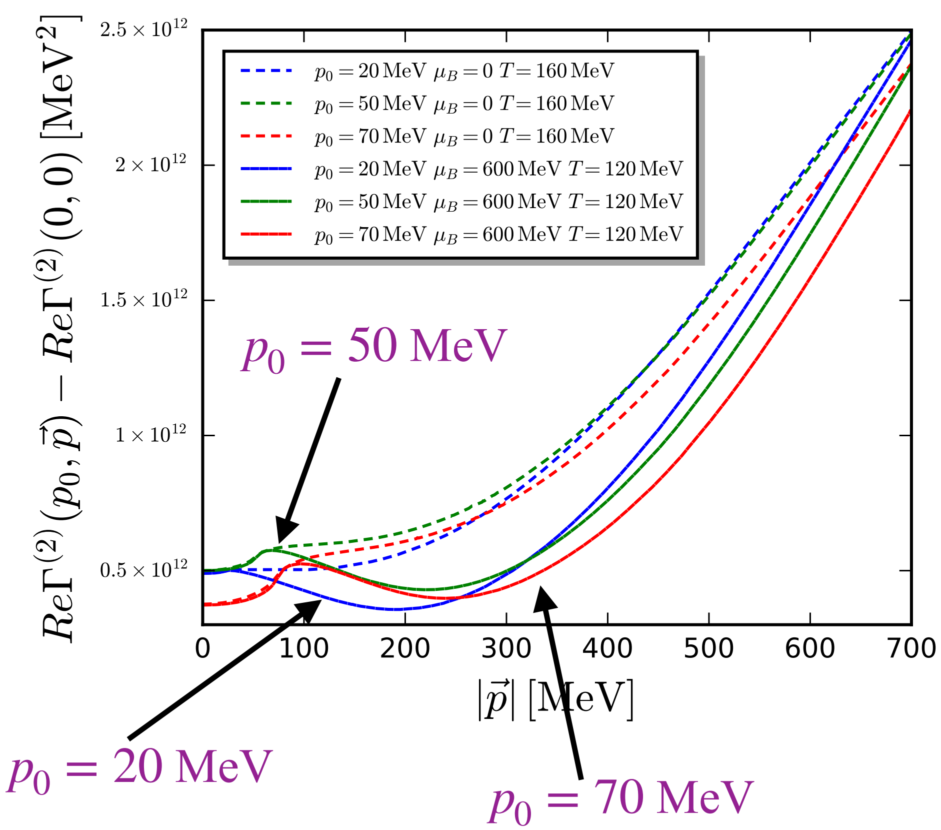

Imaginary part of $\Gamma^{(2)}_{\phi\phi,\mathrm{R}}(p_0,\mathbf{p})$:

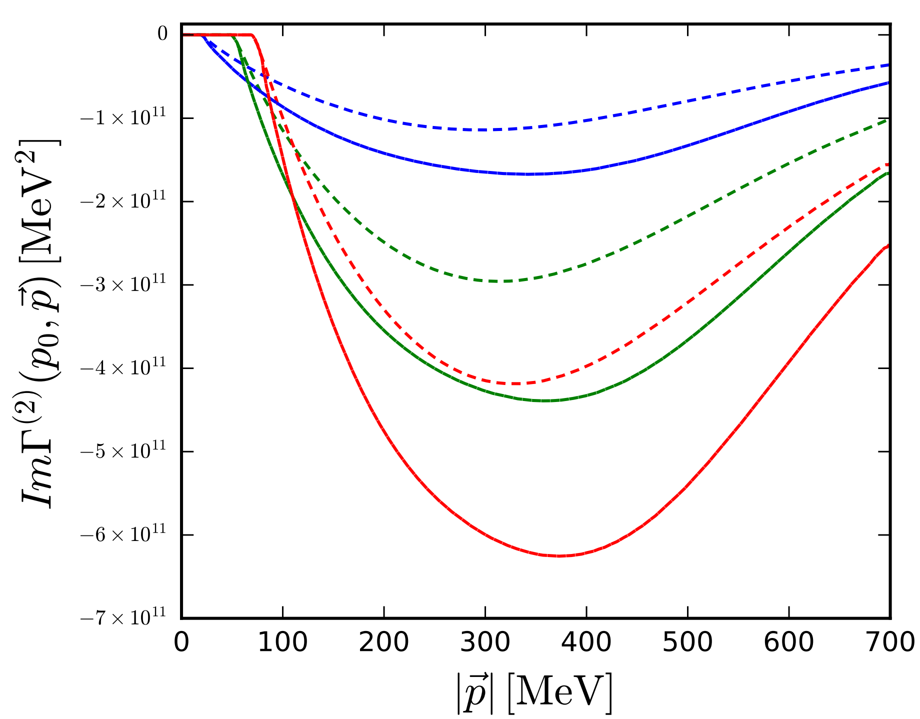

- Imaginary part of the mesonic two-point functions and spectral function are enhanced by the Landau damping effect

WF, Pawlowski, Rennecke, Wen, Yin, in preparation.

Real-time mesonic two-point functions

Real part:

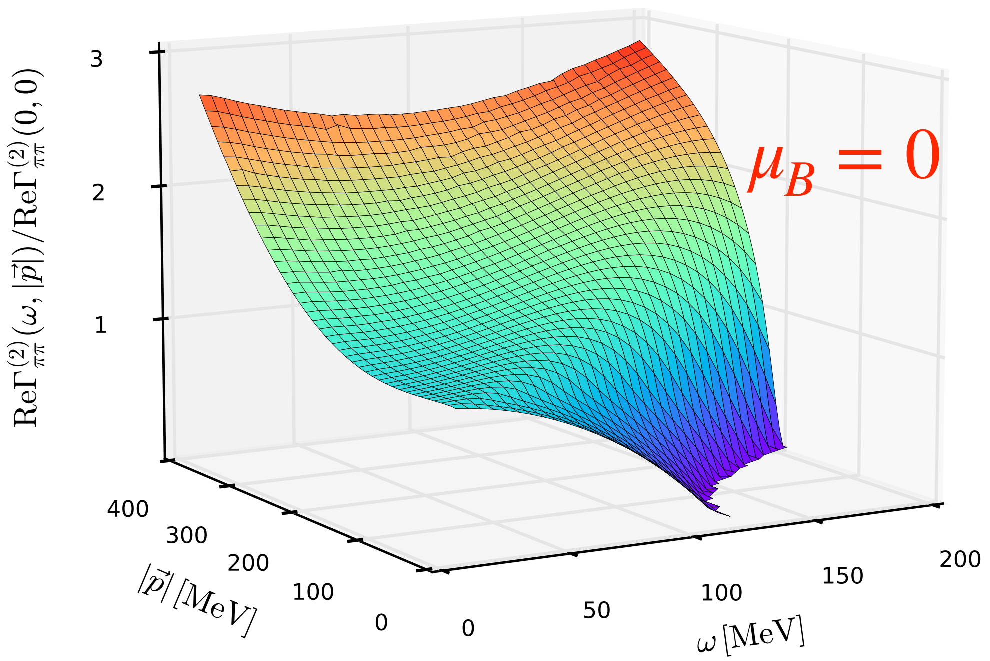

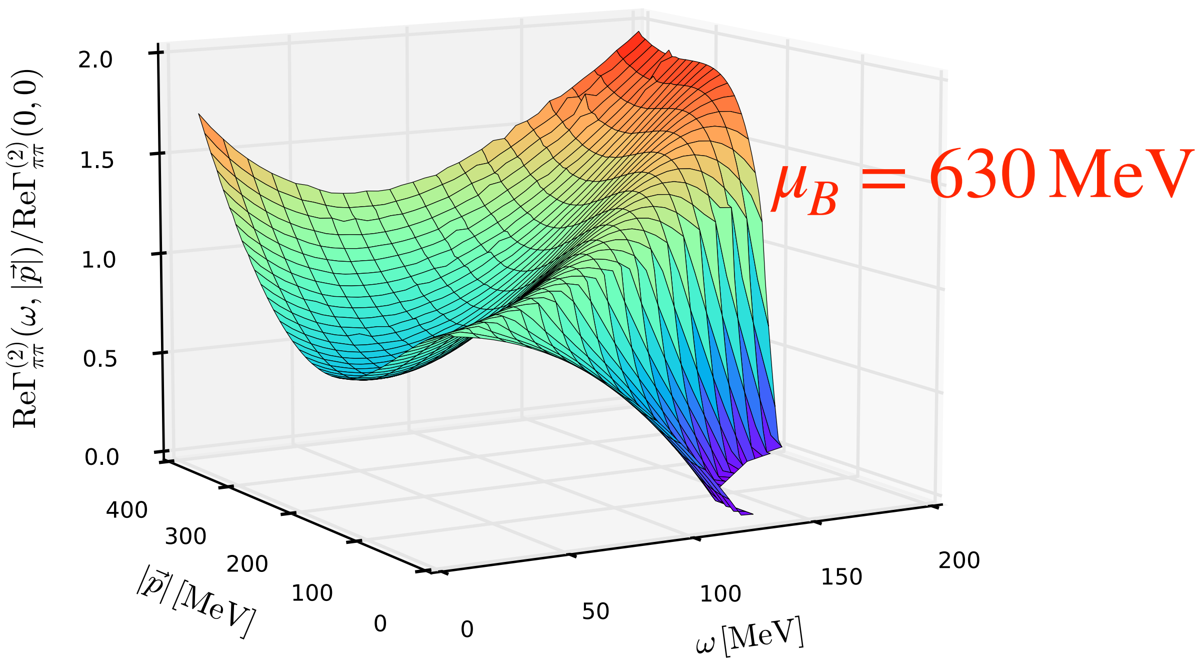

Spectral function:

WF, Pawlowski, Rennecke, Wen, Yin, in preparation

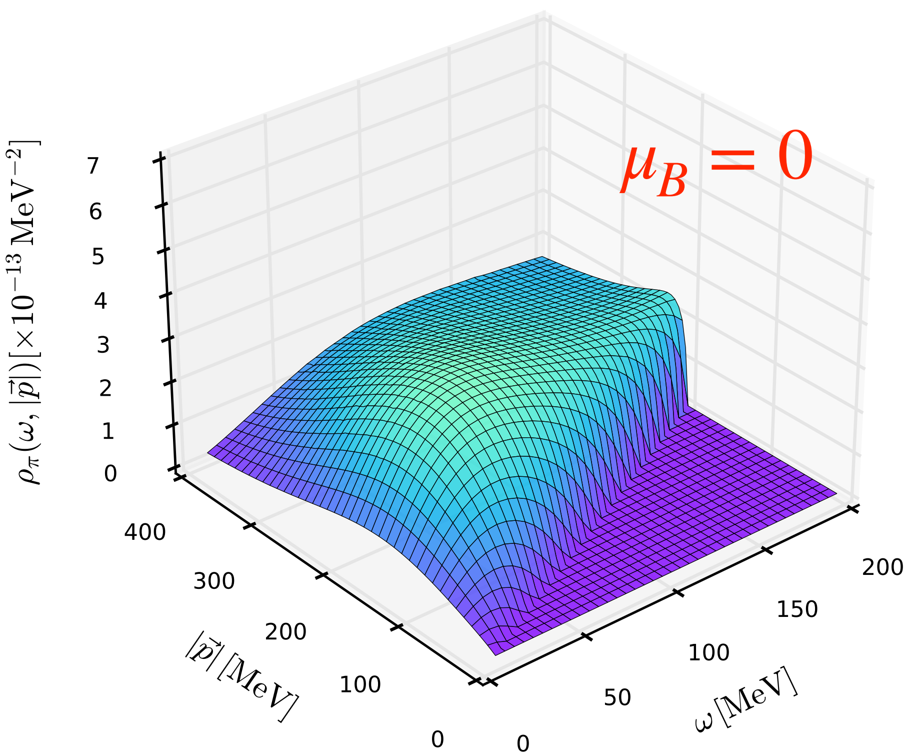

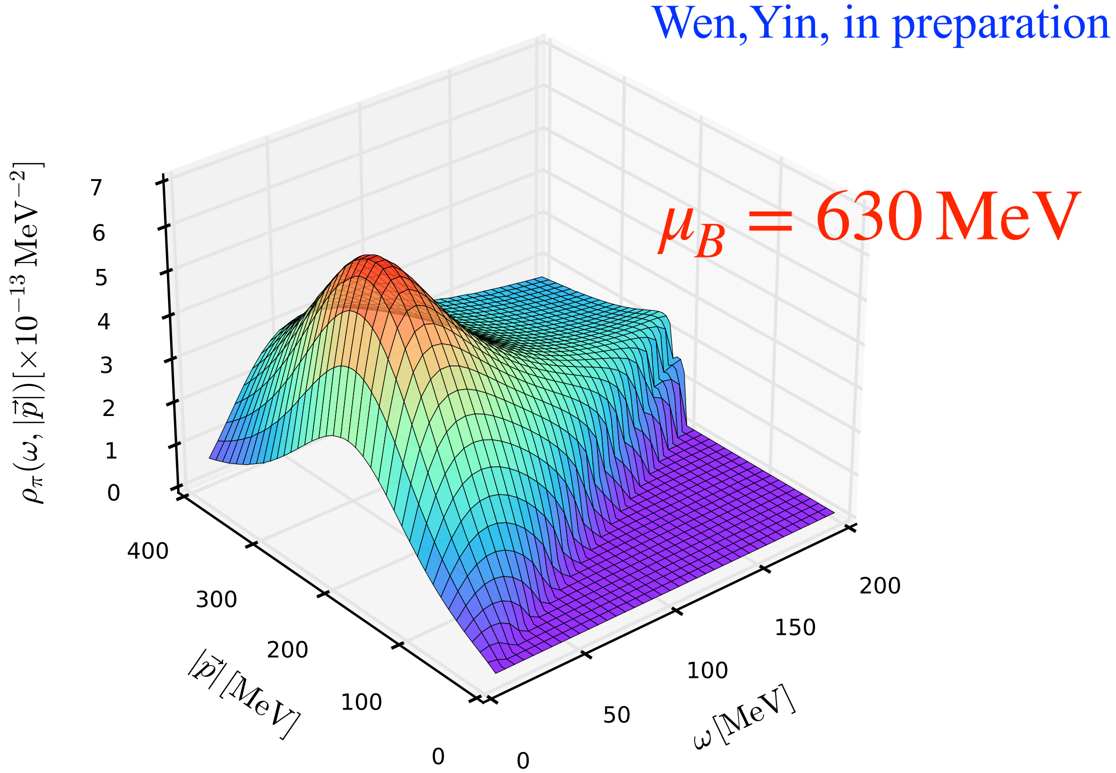

Spectral functions for mesons

- **spectral function:**

$$\rho(\omega,\vec{p}) = -\frac{1}{\pi}\frac{\mathrm{Im}\Gamma^{(2),R}(\omega,\vec{p})}{(\mathrm{Re}\Gamma^{(2),R}(\omega,\vec{p}))^2 + (\mathrm{Im}\Gamma^{(2),R}(\omega,\vec{p}))^2}$$

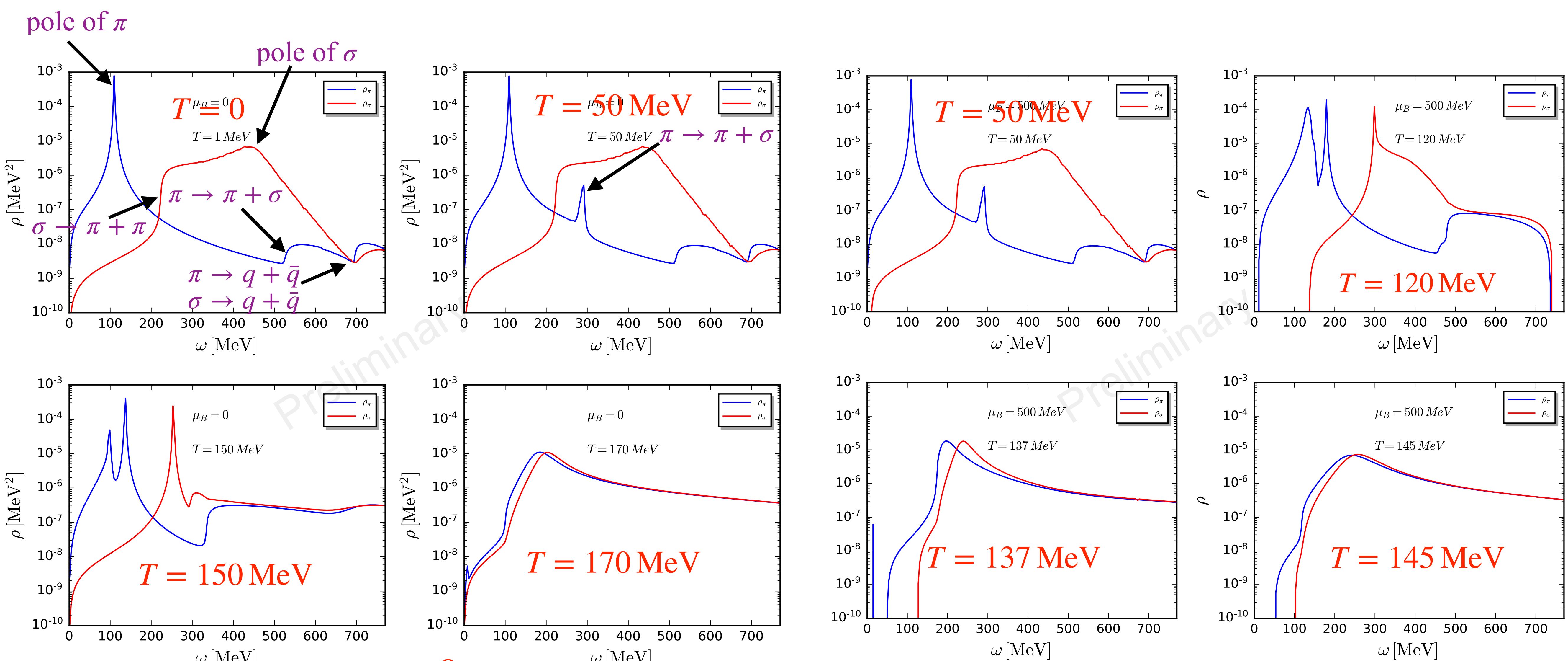

$\mu_B = 0$ $\mu_B = 500$ MeV

WF, Pawlowski, Rennecke, Wen, Yin, in preparation

Baryon number fluctuations

fRG in comparison to lattice results and HRG

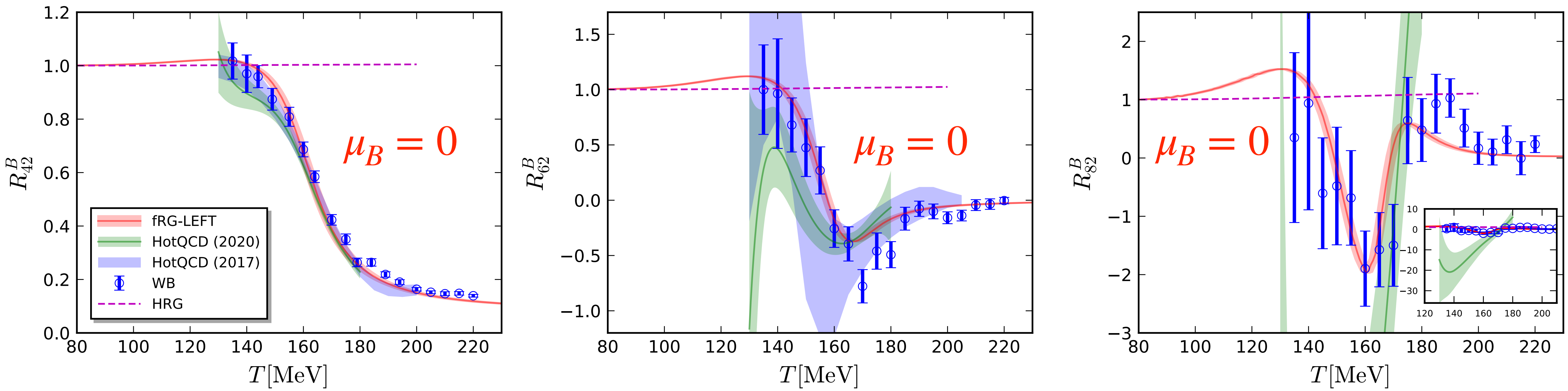

HotQCD: A. Bazavov *et al.*, *PRD* 95 (2017) 054504; *PRD* 101 (2020) 074502

fRG: WF, Luo, Pawlowski, Rennecke, Wen, Yin, *PRD* 104 (2021) 094047

WB: S. Borsanyi *et al.*, *JHEP* 10 (2018) 205

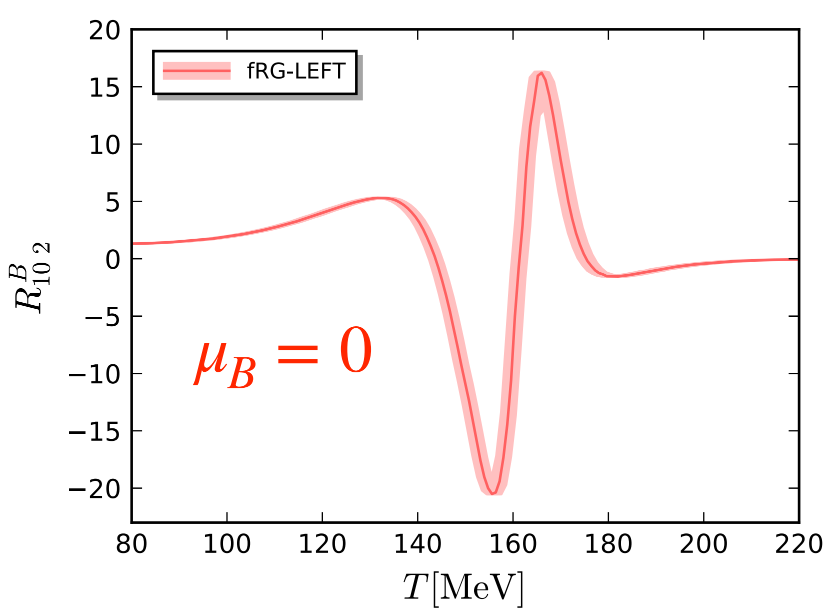

baryon number fluctuations:

$$\chi_n^B = \frac{\partial^n}{\partial(\mu_B/T)^n}\frac{p}{T^4}\,, \qquad R_{nm}^B = \frac{\chi_n^B}{\chi_m^B}$$

relation to the cumulants:

$$M = VT^3\chi_1^B\,, \qquad \sigma^2 = VT^3\chi_2^B$$

$$S = \chi_3^B/(\chi_2^B\sigma)\,, \qquad \kappa = \chi_4^B/(\chi_2^B\sigma^2)$$

Convergence radius of Taylor expansion?

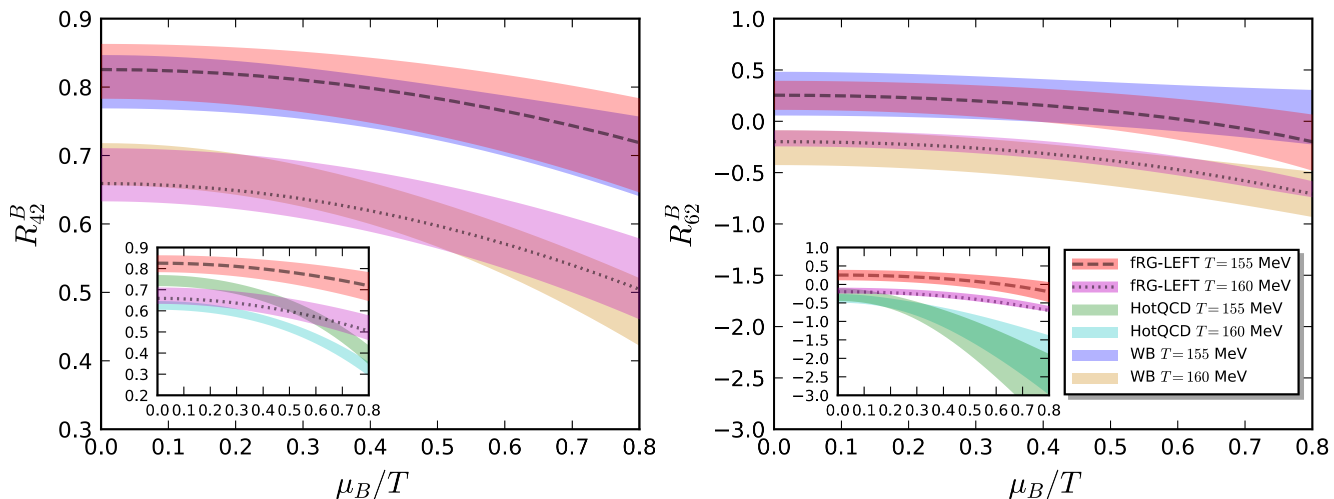

$\mu_B \neq 0$ **fRG vs Lattice**

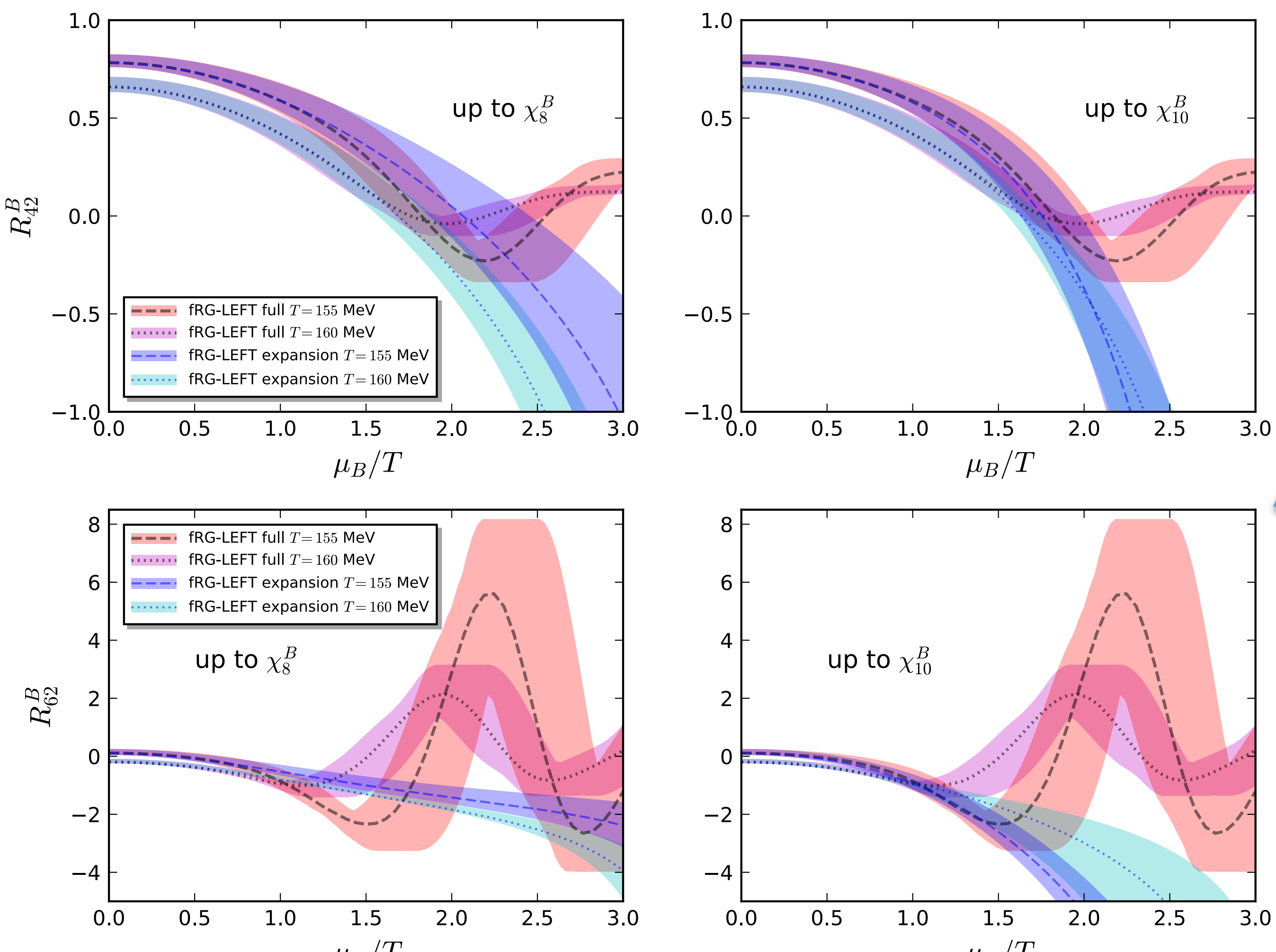

full vs expanded

expanding the pressure at $\mu_B = 0$

$$\frac{p(\mu_B)}{T^4} = \frac{p(0)}{T^4} + \sum_{i=1}^{\infty} \frac{\chi^B_{2i}(0)}{(2i)!}\,\hat{\mu}_B^{2i}\,,$$

expanded fluctuations

$$\chi^B_2(\mu_B) \simeq \chi^B_2(0) + \frac{\chi^B_4(0)}{2!}\hat{\mu}_B^2 + \frac{\chi^B_6(0)}{4!}\hat{\mu}_B^4 + \frac{\chi^B_8(0)}{6!}\hat{\mu}_B^6\,,$$

$$\chi^B_4(\mu_B) \simeq \chi^B_4(0) + \frac{\chi^B_6(0)}{2!}\hat{\mu}_B^2 + \frac{\chi^B_8(0)}{4!}\hat{\mu}_B^4\,,$$

$$\chi^B_6(\mu_B) \simeq \chi^B_6(0) + \frac{\chi^B_8(0)}{2!}\hat{\mu}_B^2$$

$$T = 155\,\text{MeV}: \quad [\mu_B/T]_{\text{Max}} \approx 1.5\,,$$

$$T = 160\,\text{MeV}: \quad [\mu_B/T]_{\text{Max}} \approx 1.2$$

Yang-Lee edge singularity?

Fluctuations on the freeze-out curve

R^B_{42} on the phase diagram

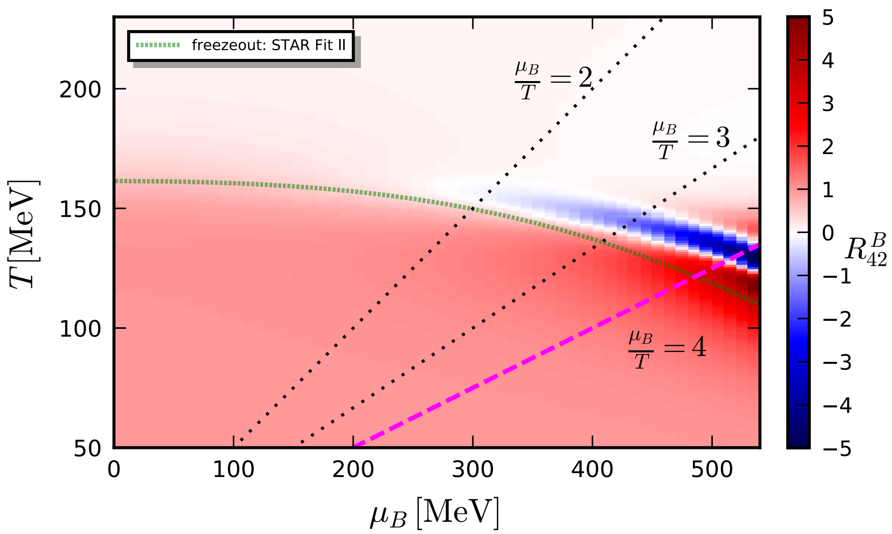

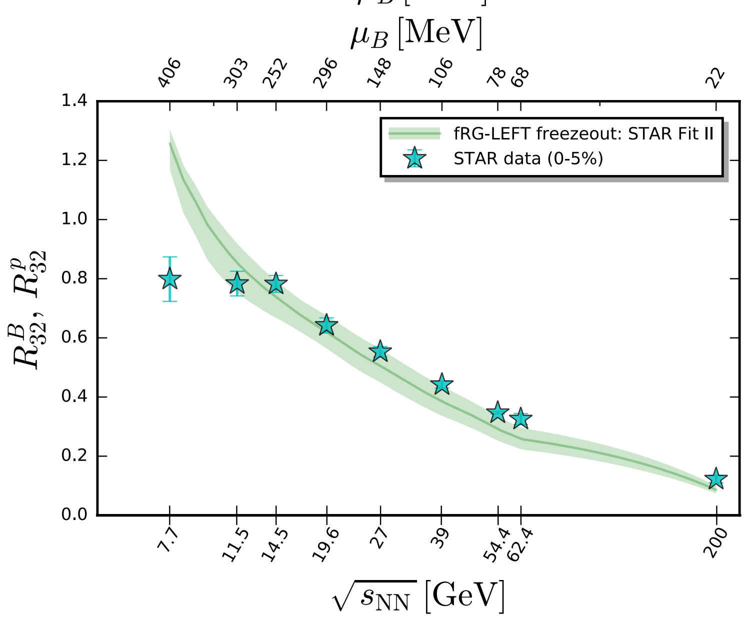

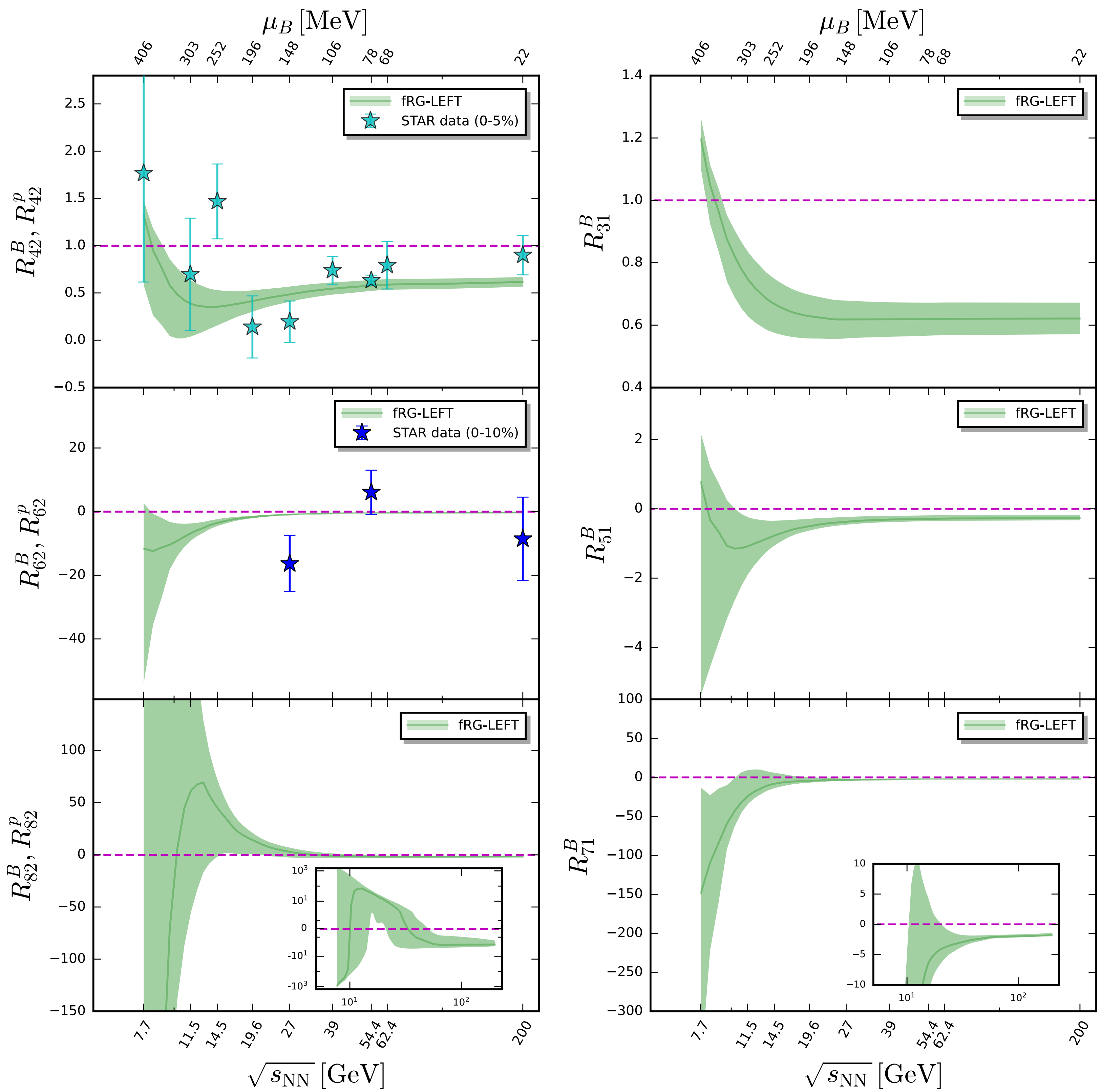

STAR (R^p_{32}, R^p_{42}):

J. Adam *et al.* (STAR), *PRL* 126 (2021) 092301

STAR (R^p_{62}):

M. Abdallah *et al.* (STAR), arXiv:2105.14698

fRG:

WF, Luo, Pawlowski, Rennecke, Wen, Yin, *PRD* 104 (2021) 094047

Update: Fluctuations at large μ_B

R_{42}^B on the phase diagram

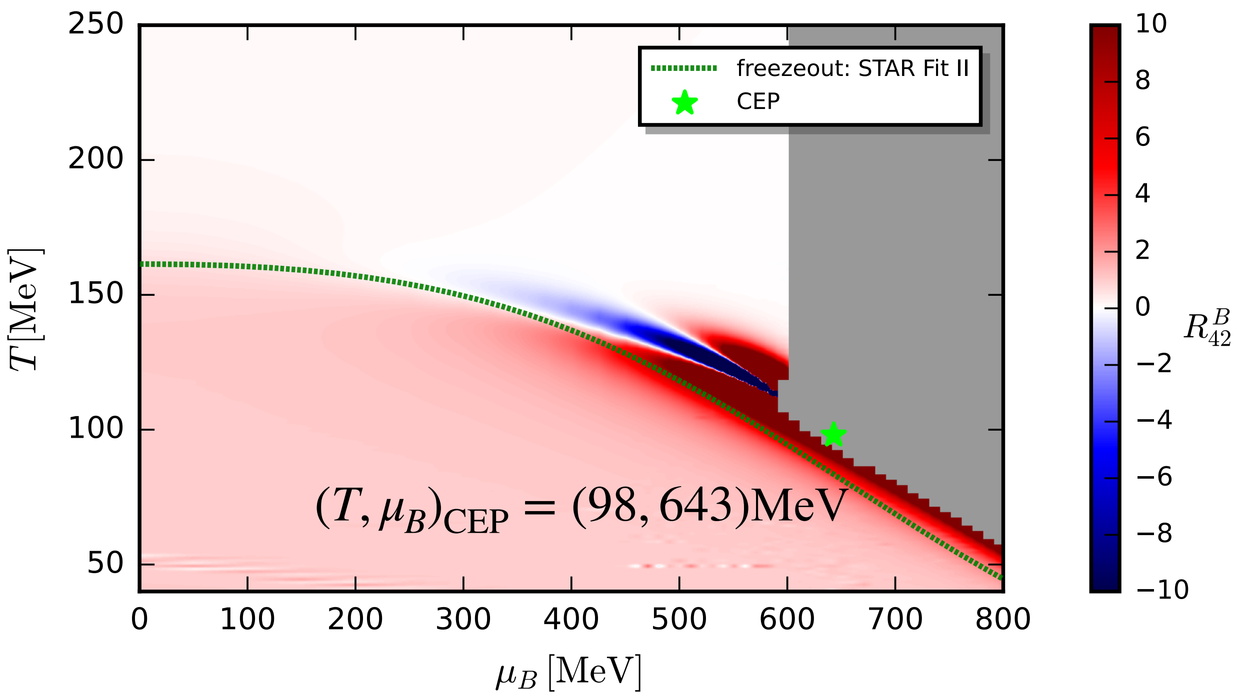

$\sqrt{S_{NN}} \simeq 5.4$ GeV, $\mu_B \simeq 510$ MeV

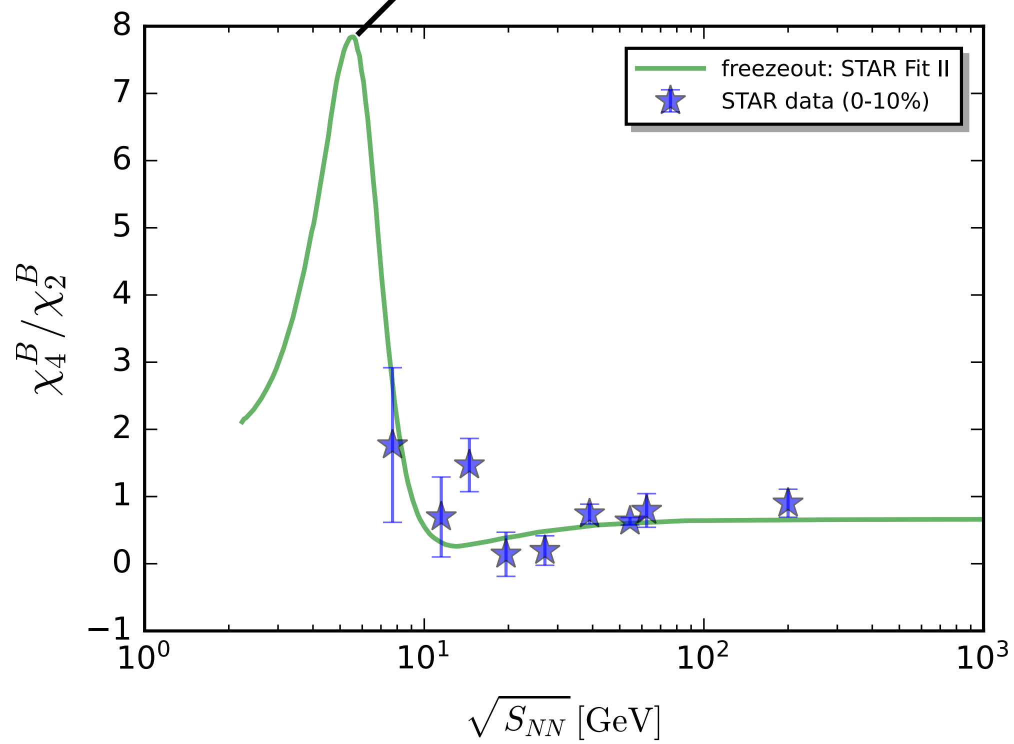

fRG:

WF, Luo, Pawlowski, Rennecke, Yin, in preparation

STAR:

J. Adam *et al.* (STAR), *PRL* 126 (2021) 092301

- Calculations have been extended from $\mu_B \sim$ 500 to 800 MeV in the improved fRG-LEFT.
- A "peak" structure is found in the regime of low collision energy.

Error estimate: Location of CEP

R_{42}^B on the phase diagram

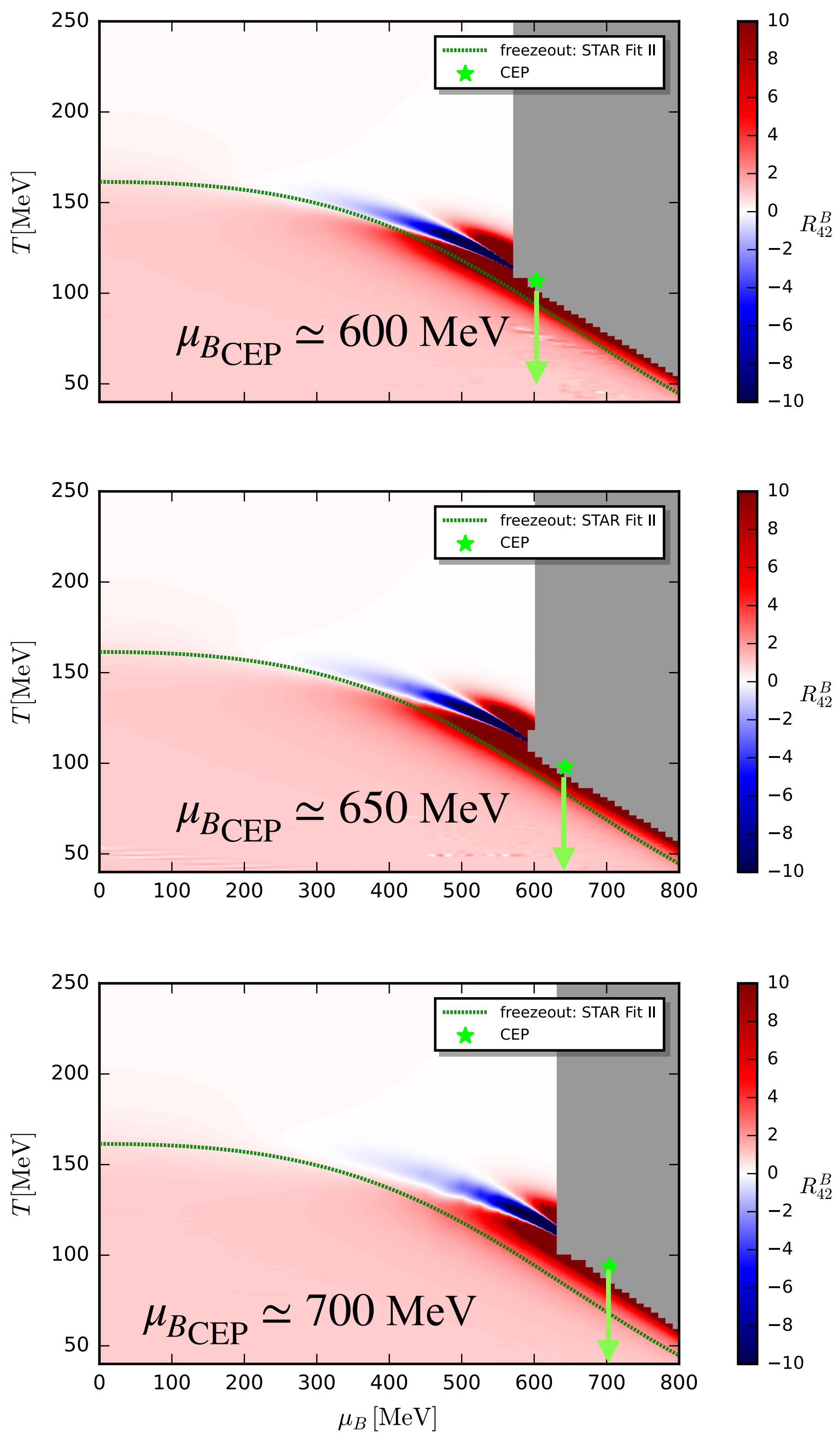

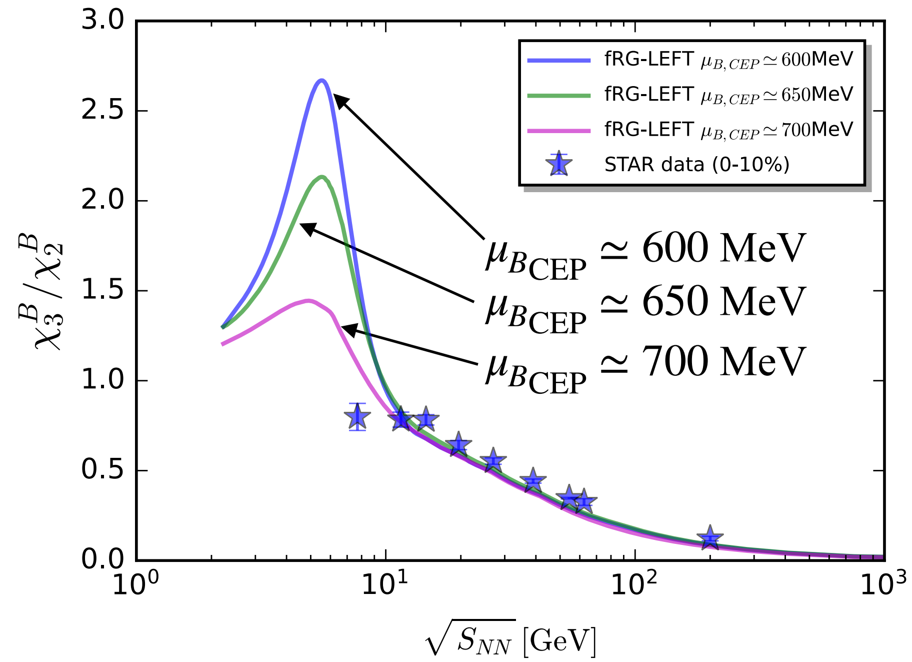

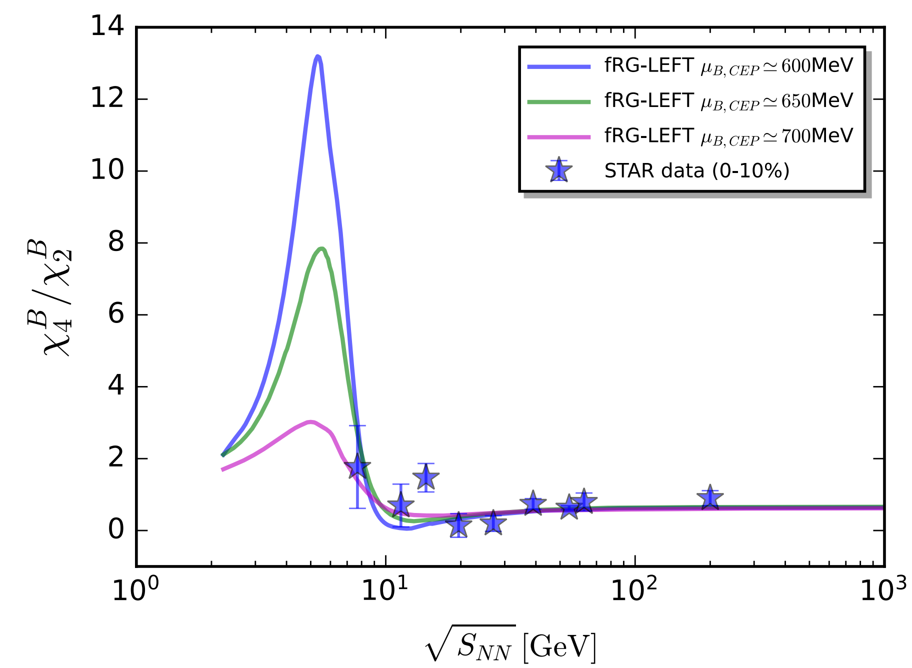

STAR:

J. Adam *et al.* (STAR), *PRL* 126 (2021) 092301

fRG:

WF, Luo, Pawlowski, Rennecke, Yin, in preparation

- Location of the peak, i.e., the corresponding collision energy shows very mild dependence on the location of CEP in the range $\mu_{B_{\rm CEP}} \simeq (600 \sim 700)$ MeV.
- While the height of the peak shows significant dependence.

Error estimate: Different freeze-out curves

R^B_{42} on the phase diagram

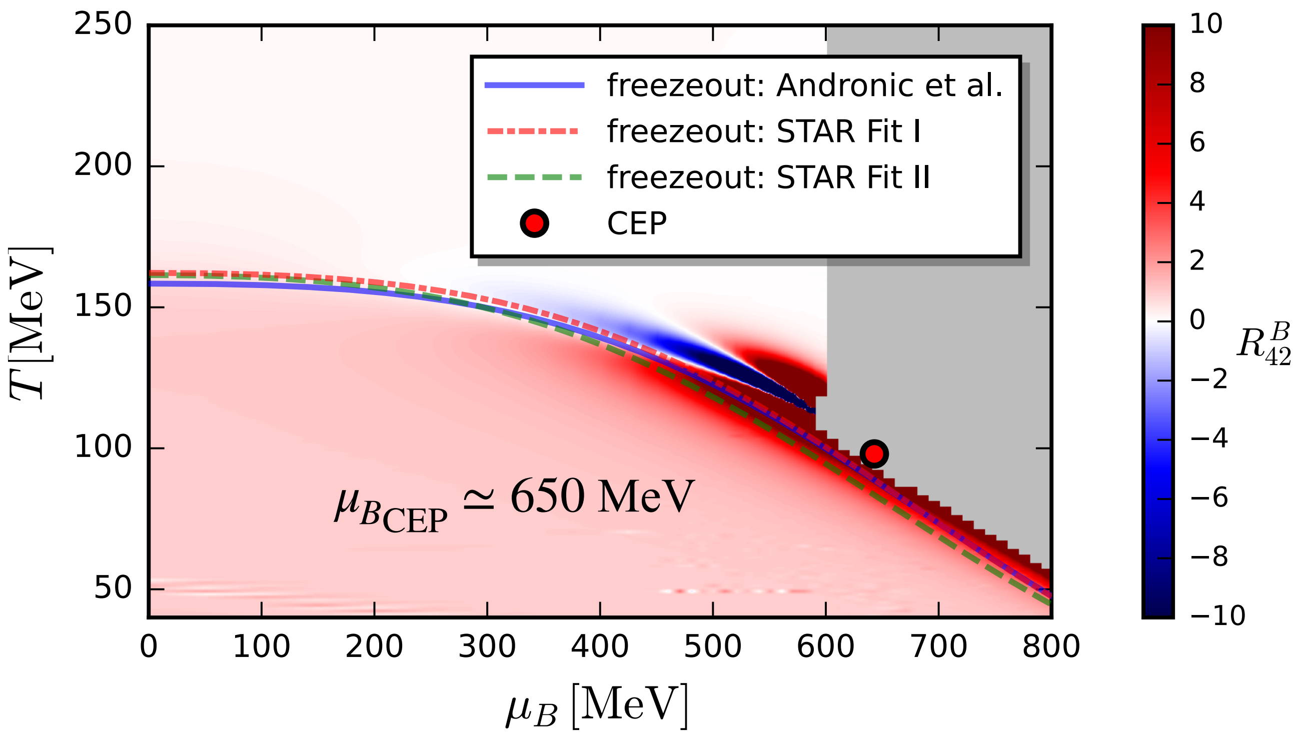

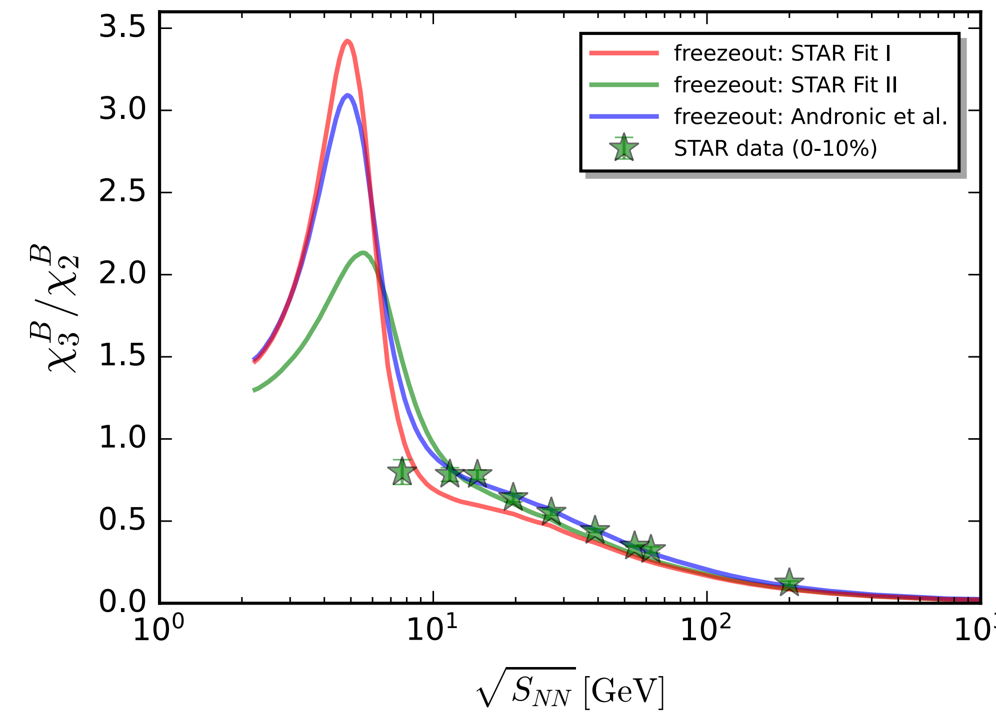

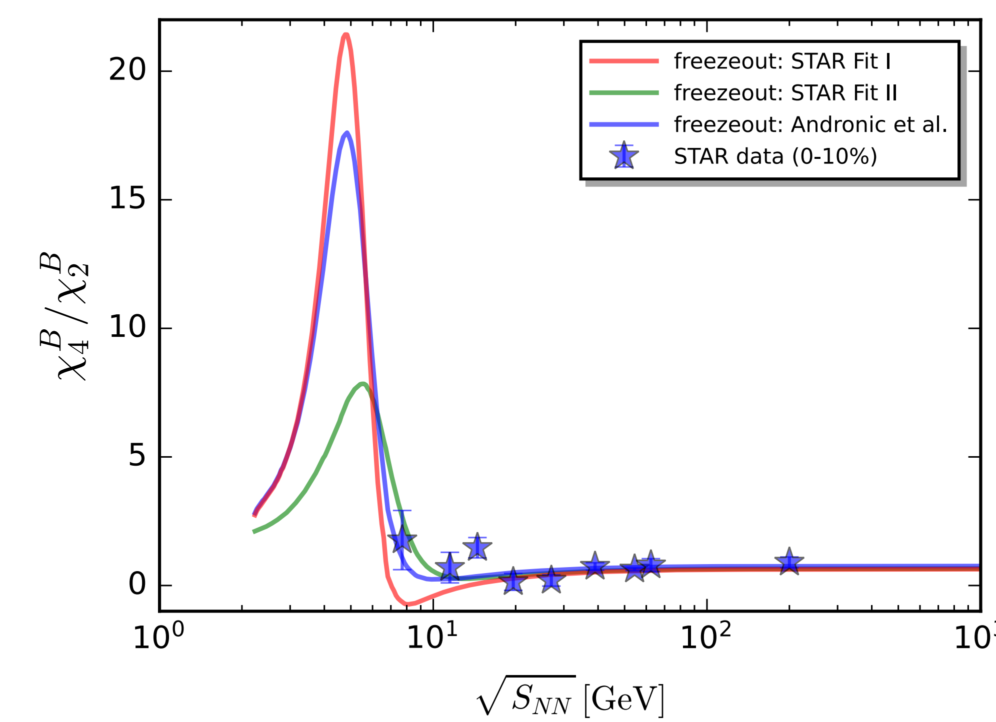

STAR:

J. Adam *et al.* (STAR), *PRL* 126 (2021) 092301

fRG:

WF, Luo, Pawlowski, Rennecke, Yin, in preparation

- The height of peak is significantly influenced by different freeze-out curves.
- The location of peak shows weak dependence on freeze-out curves.

Fluctuations: grand canonical ensemble

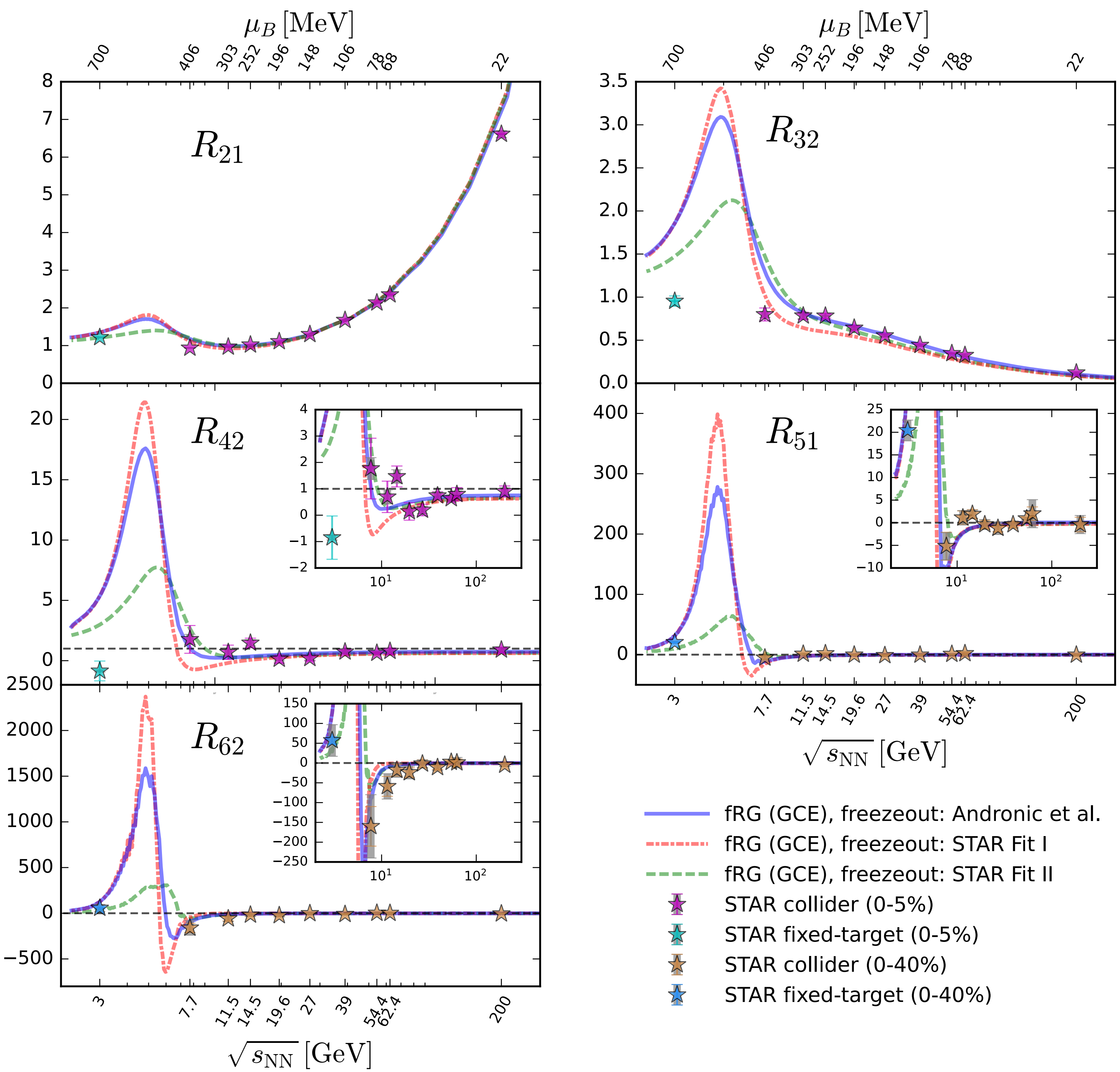

STAR:

J. Adam *et al.* (STAR), *PRL* 126 (2021) 092301

fRG:

WF, Luo, Pawlowski, Rennecke, Yin, in preparation

Fluctuations: canonical ensemble

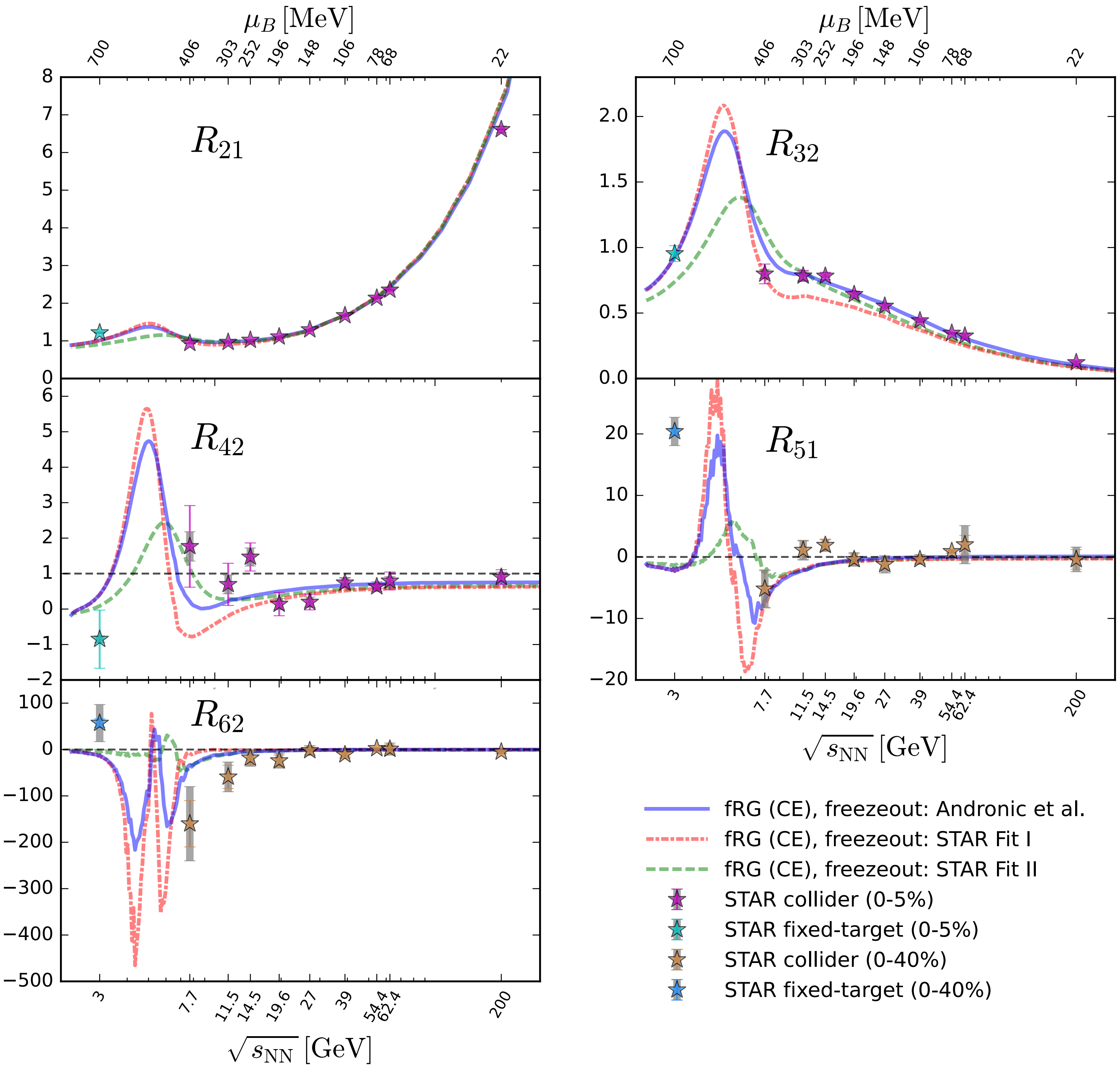

STAR:

J. Adam *et al.* (STAR), *PRL* 126 (2021) 092301

fRG:

WF, Luo, Pawlowski, Rennecke, Yin, in preparation

Summary

- ★ Recent years have seen significant progresses in studies of QCD in vacuum, QCD phase structure, phase transitions and properties of QCD matter in heavy-ion collisions within the fRG approach.

- ★ Estimates for the location of the CEP from fRG and Dyson-Schwinger Equations converge in a rather small region at baryon chemical potentials of around 600 MeV.

- ★ Theoretical calculations in fRG indicate that there would be a peak structure in the kurtosis of the baryon number fluctuations as a function of the collision energy in the regime of low collision energy, which would provide us a promising probe to pin down the location of CEP.

Summary

- ★ Recent years have seen significant progresses in studies of QCD in vacuum, QCD phase structure, phase transitions and properties of QCD matter in heavy-ion collisions within the fRG approach.
- ★ Estimates for the location of the CEP from fRG and Dyson-Schwinger Equations converge in a rather small region at baryon chemical potentials of around 600 MeV.
- ★ Theoretical calculations in fRG indicate that there would be a peak structure in the kurtosis of the baryon number fluctuations as a function of the collision energy in the regime of low collision energy, which would provide us a promising probe to pin down the location of CEP.

Thank you very much for your attentions!

Backup

Flow of 4-quark coupling—gluon versus meson

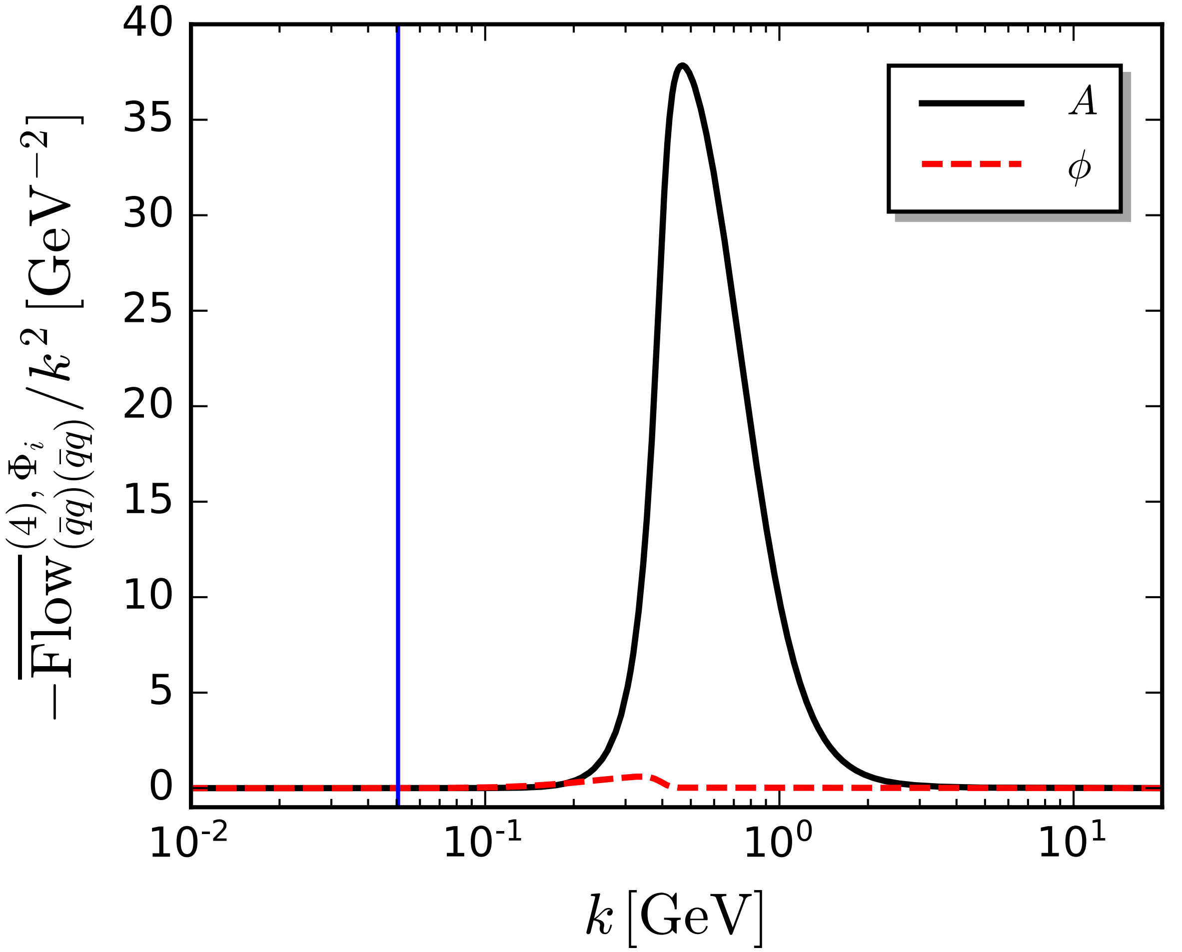

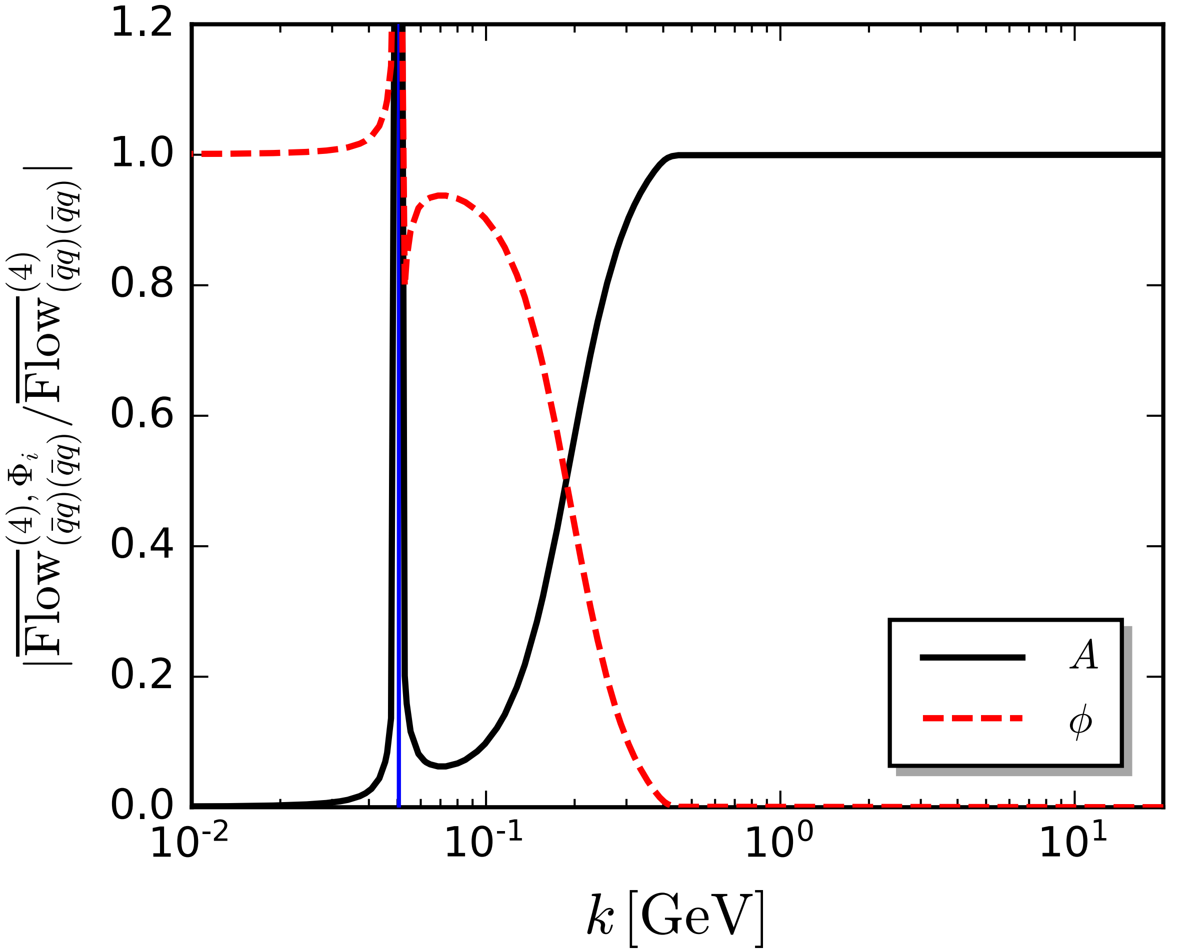

WF, Pawlowski, Rennecke, *PRD* 101 (2020), 054032

Vacuum QCD within fRG

Input: fundamental parameters of QCD at a large momentum scale: $\Lambda = 20$ GeV

2-flavor QCD

- $\alpha_{s,k=\Lambda}$
- $m_{u,k=\Lambda} = m_{d,k=\Lambda} = m_{l,k=\Lambda}(m_\pi)$ $\qquad m_\pi = 138$ **MeV**

2+1-flavor QCD

- $\alpha_{s,k=\Lambda}$
- $m_{u,k=\Lambda} = m_{d,k=\Lambda} = m_{l,k=\Lambda}(m_\pi)$ $\qquad m_\pi = 138$ **MeV**
- $\dfrac{m_{s,k=\Lambda}}{m_{l,k=\Lambda}} = 27$ $\qquad m_K = 498$ **MeV**

QCD strong couplings among quarks and gluons

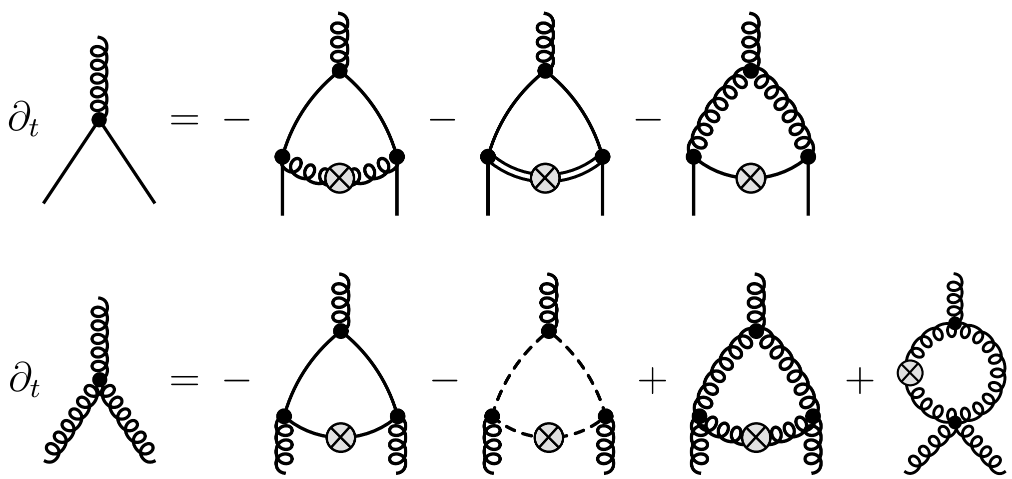

+ (permutations of the regulator insertions)

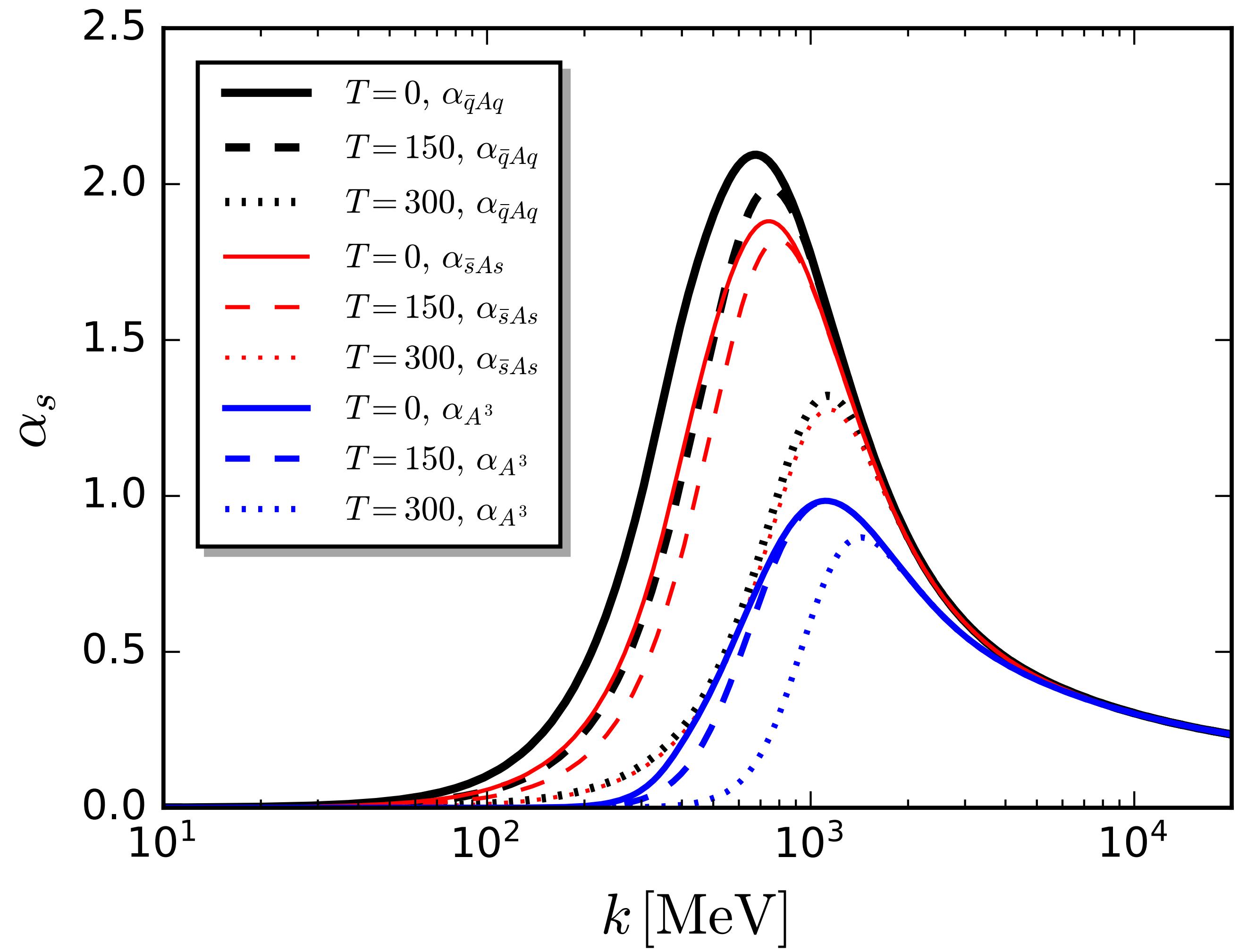

WF, Pawlowski, Rennecke, *PRD* 101 (2020), 054032